AD

USAAVLABS TECHNICAL REPORT 67-21

XV-11A
DESCRIPTION AND PRELIMINARY FLIGHT TEST

By

S. C. Roberts
D. Stewart
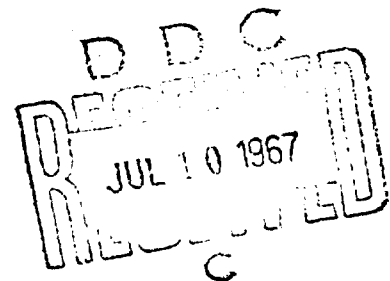V. Boaz
G. Bryant
L. Mertaugh
G. Wells
M. Gaddis

May 1967

U. S. ARMY AVIATION MATERIEL LABORATORIES
FORT EUSTIS, VIRGINIA

CONTRACT DA 44-177-AMC-266(T)
MISSISSIPPI STATE UNIVERSITY
STATE COLLEGE, MISSISSIPPI

D D C

JUL 10 1967

Disclaimers

The findings in this report are not to be construed as an official Department of the Army position unless so designated by other authorized documents.

When Government drawings, specifications, or other data are used for any purpose other than in connection with a definitely related Government procurement operation, the United States Government thereby incurs no responsibility nor any obligation whatsoever; and the fact that the Government may have formulated, furnished, or in any way supplied the said drawings, specifications, or other data is not to be regarded by implication or otherwise as in any manner licensing the holder or any other person or corporation, or conveying any rights or permission, to manufacture, use, or sell any patented invention that may in any way be related thereto.

Trade names cited in this report do not constitute an official endorsement or approval of the use of such commercial hardware or software.

Disposition Instructions

Destroy this report when no longer needed. Do not return it to originator.

DEPARTMENT OF THE ARMY
U. S. ARMY AVIATION MATERIEL LABORATORIES
FORT EUSTIS. VIRGINIA 23604

This report is a presentation of a research project currently
being undertaken at Mississippi State University, in which an
aerodynamic research aircraft, the XV-11A, is being used to
explore the problem areas associated with STOL fixed-wing aircraft.

This report presents the background history of the XV-11A and
test results for the first 35 hours of flight.

Task 1F125901A14203
Contract DA 44-177-AMC-266(T)
USAAVLABS Technical Report 67-21
May 1967

XV-11A
DESCRIPTION AND PRELIMINARY FLIGHT TEST

Aerophysics Research Report No. 75

by

S. C. Roberts
D. Stewart   L. Mertaugh
V. Boaz   G. Wells
G. Bryant   M. Gaddis

Prepared by

The Aerophysics Department
Mississippi State University
State College, Mississippi

for

U. S. ARMY AVIATION MATERIEL LABORATORIES
FORT EUSTIS, VIRGINIA

Distribution of this
document is unlimited.

ABSTRACT

The XV-11A is a polyester reinforced fiber glass STOL aircraft
designed and assembled by the Aerophysics Department of Mississippi
State University. This four-place aircraft, powered by a 250-horsepower
T-63 turbine engine, was designed to achieve high-lift coefficients by
means of a variable camber wing with distributed suction boundary layer
control. A shrouded propeller was used for thrust augmentation at low
forward velocities, and beta control on the propeller was successfully
used as a drag increment for glide path control.

To date, the XV-11A aircraft has flown 49 flights with a total
flight time of 35 hours. The majority of the flight time was involved
in aerodynamic research of the shrouded propeller, the distributed suc-
tion boundary layer control system and in an evaluation of the general
handling characteristics of the aircraft. A minimum of performance
data was collected since the primary objective was aerodynamic research.
The fiber glass material has demonstrated the excellent possibilities
of this type of construction when complex, aerodynamically smooth
curvatures are desired.

CONTENTS

ILLUSTRATIONS

SYMBOLS

C_D	drag coefficient - nondimensional
C_L	lift coefficient - nondimensional
C_p	pressure coefficient - nondimensional
d	distance between bifilars - ft.
D	length of bifilar suspension - ft.
db	decibel - nondimensional
dbm	decibel as referred to 1 milliwatt - nondimensional
g	antenna gain - nondimensional
G	acceleration due to gravity - ft./sec.^{2}
Hz	hertz - c.p.s.
MHz	megahertz - 10^6 c.p.s.
GHz	gigahertz - 10^9 c.p.s.
I	moment of inertia - slug-ft.^{2}
I_A	additional moment of inertia about swing axis - slug-ft.^{2}
I_S	moment of inertia of suspension cage about swing axis - slug-ft.^{2}
I_x	mass moment of inertia about the aircraft roll axis - slug-ft.^{2}
I_y	mass moment of inertia about the aircraft pitch axis - slug-ft.^{2}
I_z	mass moment of inertia about the aircraft yaw axis - slug-ft.^{2}
1	distance from swing axis to C.G. of aircraft - ft.
1'	distance from swing axis to C.G. of suspension cage - ft.
L	distance from swing axis to C.G. of pendulum - ft.
L'	length of a standard cylinder for radar reflectivity measurements - meters
$\Delta 1$	distance from bottom axis to middle and top axes - ft.

N_1	engine compressor speed - percent of design speed
N_2	engine turbine speed - percent of design speed
P_r	received power - dbm
P_t	transmitted power - dbm
r	radius - meters
R	distance from the transmitter to the target - meters
T	natural period of pendulum - sec.
$V_0 \rho$	product of aircraft volume and mass density of air - slugs
VTVM	vacuum tube voltmeter
w	aircraft empty weight - lb.
w'	weight of suspension cage - lb.
W	pendulum weight = w + w' - lb.
α	angle of attack - deg.
β	propeller pitch angle - deg.
ζ	damping ratio - nondimensional
λ	wave length - meters
ρ	density - slug/ft.^{3}
σ	radar cross section (RCS)
ω_n	undamped natural frequency - c.p.s.

Subscripts

b	pertaining to bottom axis of rotation
m	pertaining to middle axis of rotation
t	pertaining to top axis of rotation
z	pertaining to vertical (z) axis of rotation

1. INTRODUCTION

For many years aircraft designers have been attempting to decrease the minimum flying speed of fixed-wing aircraft which would enable the aircraft to take off and land in short distances without sustaining a severe drag penalty at high cruise speeds. The attainment of such STOL characteristics is primarily dependent upon increasing the lifting capability of the aircraft wings and increasing the static thrust generated by the propulsion system. Many mechanical devices (such as flaps, slots, and slats) as well as boundary layer control devices (such as blowing and sucking through slots and distributed perforations) have been utilized in an attempt to increase the lift of the wings. Recently, the operation of wings in high dynamic head slipstreams has been successfully used in a number of aircraft. The static thrust of several aircraft has been increased by increasing the propeller size, thereby decreasing the disc loading, as well as by the use of shrouded propellers.

The Aerophysics Department of Mississippi State University has been performing research in high lift and thrust augmentation for a number of years. The Department has designed and assembled a vehicle which uses distributed suction boundary layer control to attain high-lift coefficients and a shrouded propeller to increase the static thrust of a propeller (see Figure 1). The aircraft, designated the XV-11A by the United States Army, was constructed of fiber glass materials to facilitate the construction of the complex shapes required to satisfy the design objectives of the XV-11A. The primary purpose of this aircraft is to investigate the areas of high lift, low drag, and thrust augmentation.

2. HISTORICAL BACKGROUND

In 1958 the Aerophysics Department of Mississippi State University was awarded contracts for aerodynamic research that could be utilized by the armed services towards the development of a relatively high-performance aircraft capable of taking off and landing in small, unprepared fields. A study of the problems involved in the design of such a vehicle indicated the need for major research efforts in three specific areas. These areas of research consisted of increasing the high lift capabilities of the vehicle to allow lower takeoff and landing speeds, augmenting the low speed thrust to provide better acceleration, and reducing the vehicle drag to allow relatively high-speed performance in cruise.

To achieve lift coefficients greater than 3.0 without using slipstream effects, it is necessary to use a boundary layer control system rather than mechanical devices such as flaps or slots. For a boundary layer control system to be effective, it must not only increase the lift of the wings but also utilize sufficiently low horsepower so that a net gain in takeoff performance results when the power for the system is taken from the main power plant. Also, the system must be mechanically simple, light, reliable, and easily maintained. An analytical study (reference 1) showed that the power requirements were minimum for a distributed suction boundary layer control system. Flight experiments performed with TG-3, L-21, and L-19 aircraft demonstrated appreciable increases in maximum lift coefficient; e.g., the L-19 could successfully fly at lift coefficients of 5.7 by means of distributed suction boundary layer control utilizing 12 horsepower from the main engine. The takeoff and landing distances were reduced by 38 and 29 percent, respectively (reference 2). Figure 2 shows the aircraft which were used in the high-lift research.

In order to increase the thrust of the propeller, a shroud was attached. Experiments on an AG-14 showed that the static thrust of a propeller could be increased by as much as 70 percent by means of a shroud (Figure 3). The shroud must be located at the rear of the vehicle for reasons of aircraft stability and pilot visibility. With the shrouded propeller at the back of the vehicle, insertion of the longitudinal and directional controls in the slipstream of the propeller ensures adequate control power at the very low airspeeds necessary for STOL operation.

To ensure a high cruise speed, the drag of the aircraft must be reduced to a minimum by eliminating all external protuberances, by preventing turbulent separation by means of geometric streamlining, and by maintaining laminar flow as long as possible. Geometric boundary layer control was demonstrated on a Navion L-17 and a Beechcraft L-23 by smoothing the wings, using wing-root fillets, making windows flush, sealing undercarriage doors, mounting the radio antenna within fiber

2

glass wing tips, and modifying the cooling systems (Figure 4). A typical result of these modifications on the L-23 was the reduction in horsepower required for level flight from 400 to 310 shaft horsepower at 180 miles per hour.

The results of the research in high lift, thrust augmentation, and low drag were incorporated into a modified AG-14 aircraft which was called the XAZ-1 (Figure 5). This aircraft was not an STOL vehicle because it was underpowered. However, it did demonstrate that a distributed suction, high-lift, variable camber, boundary layer control wing; a shroud for thrust augmentation; and geometric low-drag techniques could be successfully utilized. The results of all the research on the TG-3, the L-21, the L-19, and the XAZ-1 aircraft were directly applied to the design of the XV-11A STOL aircraft.

3. DESCRIPTION OF THE XV-11A AIRCRAFT

The XV-11A aircraft is the result of cumulative research efforts in high-lift boundary layer control, propeller thrust augmentation, and low-drag geometric boundary layer control. With the exception of the landing gear and ducting, the fiber glass components of the vehicle were manufactured by Parsons Corporation and assembled in the Aerophysics Department of Mississippi State University. The first flight was performed on December 1, 1965.

The four-place XV-11A STOL research vehicle is constructed of fiber glass reinforced plastic to achieve a high-rigidity, wave-free structure. This material also allows easy manufacture of complex shapes with a minimum of tooling.

The wing has a camber-changing mechanism which consists of two load-carrying horns in each wing supporting four subspars aft of the main spar. The electrically driven horns rotate through journals in the subspars and the trailing edge of the wing, thereby changing the camber. The subspars are piano-hinged at the top and bottom to facilitate angular movement (Figure 6). The wing leading edge was designed to carry internal fuel tanks, which have a 66-gallon capacity. The wing has a distributed suction boundary layer control system on the upper surface for high lift.

The fuselage is a stiffened shell-type structure with the pilot and passenger compartment glassed-in above seat cushion height. The long side windows are hinged at the top and act as doors. The cockpit contains a gasoline tank with a 30-gallon capacity which is designed to be used as a rear seat support.

The shroud, although similar in external configuration to the XAZ-1 aircraft, does not have the flight controls integrated into the shroud periphery. Cruciform control surfaces operating in the slipstream of the propeller provide adequate control power even at the very low airspeeds encountered with the XV-11A. The controllable pitch propeller has reverse pitch capability and can be used for glide path control.

The propulsion system consists of a T-63 gas turbine engine installed in the fuselage between the wings. The engine shaft rotates at 6000 r.p.m. and drives through a rear-mounted 2.9 to 1 reduction gearbox to the propeller in the shroud. Five bearings support the steel shaft, which is enclosed in a fiber glass housing. The compressor stage of the engine is the suction source for the boundary layer control in the wings. The engine oil and engine compartment cooling is accomplished by an air intake under each wing root. The engine compartment is scavenged by the jet ejector principle, with the turbine exhaust being used as the primary flow.

The pantabase gear was designed for operation from soft, muddy ground where the pantabase would not sink into the mud. The undercarriage was designed for loading conditions equal to eight times the weight of the aircraft.

3.1. ENGINE INSTALLATION

The T-63 engine is mounted in the upper center fuselage just aft of the wing spar carry-through. Rigid sheet and tubular steel mountings support the engine at the sides and top of the accessory drive case. Loads are distributed to a transverse bulkhead and to the upper sides of the engine box. This box is part of a stainless steel enclosure which provides a fire and heat barrier for the rest of the fuselage. Additional barriers are located inside the engine box in order to isolate the hot portions of the engine from the gears and accessories. A ventilating flow of air is branched from the oil cooler inlets under each wing root and is directed to the coolest portion of the engine box. It then flows to progressively hotter sections and is rejoined with the oil cooler flow, where it is exhausted on either side as the secondary flows of the jet pumps formed by the engine exhausts issuing from the trailing edge of the wing fillets (Figure 7). Access to the engine box is by removal of the stainless steel bottom pan of the enclosure. A stressed aluminum hatch is provided in the upper fuselage surface to allow access to the top of the engine.

Power is taken off at the rear power takeoff pad as it is in a helicopter installation. Transmission is via a 1-3/8-inch O.D. tubular steel shaft turning at 6000 r.p.m. to the aft gearbox which supports the propeller and reduces the speed to 2070 r.p.m. The 7-foot-long shaft is supported by a fiber glass housing containing intermediate bearings every 15 inches. A constant-speed universal joint allows the drive to bend through 11 degrees just ahead of the aft gearbox. The shaft, housing, and gearbox are removable from the aft end of the airplane. Photographs of the engine installation and the drive shaft are shown in Figures 8 and 9, respectively.

3.2. BOUNDARY LAYER SUCTION SOURCE SYSTEM

Each wing of the aircraft acts as a single plenum chamber, with the two wings being connected to the suction source by a common duct. The flow from the wing perforations in the upper surface passes through the wing, either back through the spar and inward, or straight inward. It then enters the common duct at the wing root and is guided through a 90-degree turn into the engine compressor. The duct at the compressor inlet has a large-radius bellmouth and a contoured divider at the front center to minimize crossflow. The compressor's inside diameter is 4.50 inches. The duct measures 8 inches by 8 inches at the wing root. At the wing root the duct has a bellmouth averaging .75 inch radius. An

emergency bypass door is provided in the intake air duct to ensure
engine air in the event of stoppage of the wing plenum air due to icing,
etc. The valve is spring-loaded for automatic or manual operation.
Figure 10 gives diagrams of the suction source system.

3.3. OIL SYSTEM

The T-63 engine is lubricated with MIL-7808 synthetic lubricant.
A dry sump system is used with a separate 1-gallon oil tank located
ahead of the engine. A scavenging pump returns the oil from the acces-
sory case to the tank via dual oil coolers which are located beneath
each wing root. The propeller shaft housing incorporates an integral
oil pressure and scavenging system for lubrication of the intermediate
bearings and aft gearbox. Oil under pressure is taken from the engine
to supply the spray nozzles of the shaft and gearbox. Scavenging is
accomplished by an auxiliary scavenging pump which has been added to an
accessory drive pad on the engine.

3.4. FUEL SYSTEM

A simple, single-tank system is used. A flat 39-gallon tank is
located just above the floor in the center fuselage. This is filled
through a recessed cap under a flush cover on the left side of the
fuselage. Fuel is drawn from a drainable tank sump by means of a
submerged electric boost pump. The fuel then goes through a shut-off
valve, filter, and flow meter to the engine. A dual engine-driven fuel
pump, controlled by dual governors, feeds the fuel to the single spray
nozzle in the combustion chamber. The pilot controls the output by
setting the gas producer governor, which also provides overspeed protec-
tion.

3.5. ELECTRICAL SYSTEM

A conventional 28-volt D.C. electrical system is installed in the
aircraft in conjunction with an engine-driven starter-generator. Two
series-connected 12-volt lead-acid storage batteries are located in
the nose of the fuselage for possible in-flight relight. Engine start-
ing is normally assisted by a ground power unit that plugs in at a
flush-covered receptacle located on the right of the fuselage nose.
The electrical load is in the form of motors, such as the starter, camber
change actuator, propeller pitch change, elevator trim tab, and fuel
boost pump. Each circuit is protected by a reclosable breaker, and a
solenoid-operated master switch which opens the entire system.

3.6. CONTROL SYSTEM

Elevators, rudder, and aileron controls are of conventional cable,

push rod, and bell crank construction. A nonfloating trim tab with
manual control was installed in the elevator with a tab position indi-
cator for the pilot; however, this has recently been replaced by an
electrically operated trim tab with the control on the wheel. The ele-
vator is partially counterbalanced.

A dual control column was installed for the elevator and ailerons.
Pendant rudder pedals with toe braking are used. The Mississippi State
University Aerophysics Department designed and installed all controls
in the cabin area, including the front wheel steering attached to the
rudder cables. Cranks, pulleys, and brackets located at the control
surfaces were designed and manufactured by the airframe supplier,
Parsons Corporation.

The camber-changing activator is a single unit mounted in the fuse-
lage between the wings. Both wing camber-changing units are operated
from one electrically driven gearbox with a wing position indicator on
the instrument panel.

An emergency engine intake air bypass door control is provided.

Emergency door hinge releases were installed in both cabin doors
for door jettison.

3.7. PROPELLER

The propeller installed on the XV-11A is the design developed
especially for the T-63. The propeller was obtained from the Air
Force and installed in the shroud after trimming 11 inches off of
each tip (Figure 11).

The propeller, as delivered, utilized a hydraulic pitch control
system which was essentially integral with the T-63 engine. The remote
location of the propeller on the XV-11A did not allow the use of this
control system. An electric pitch change system was designed and
fabricated by the Aerophysics Department. This system uses two electric
motors which are mounted on the propeller hub and drive a screw which
positions the push rod activator of the original propeller control.
Limit switches, brush rings, and a positioning feedback circuit com-
plete the pitch control system. The feedback circuit maintains the
pitch angle selected by the pilot through the position of the propeller
control lever in the cockpit. The pilot may bypass the feedback circuit
by applying electrical power directly to the two electric motors so as
to increase or decrease the blade angle. This alternate method does
not provide an indication of the blade angle to the pilot and is intended
to be used only in an emergency. The circuit diagram for the propeller
pitch change mechanism is shown in Figure 12.

7

3.8. DIMENSIONAL DATA

Dimensions:

Span	26 ft. 2.5 in.
Length	23 ft. 3 in.
Height	8 ft. 6 in.

Weights and Loadings:

Maximum Takeoff Weight	2600 lb.
Maximum Wing Loading	24.5 lb./sq. ft.
Maximum Power Loading	10.4 lb./hp

Wings:

Aspect Ratio	6.5
Chord	4 ft. 10.2 in. on theoretical center line, 3 ft. 2.8 in. at tip
Thickness/Chord Ratio	15 pct.
Dihedral	2 deg.
Incidence	1 deg. at root, -1 deg. at tip
Aileron Area	12.0 sq. ft.
Wing Area (Gross)	106 sq. ft.
M.G.C.	4 ft. 1.5 in.
Taper Ratio	.67
Sweep at 35-Percent Chord	0 deg.
Camber-Changing Span (Including Fuselage)	18 ft.
Aileron Span	3 ft. 6 in.
D Spar at 34.73-Percent Chord	
Wing Airfoil - Modified NACA 63615	

Tail Unit:

Duct	
Inside Diameter	5 ft. 6 in.
Chord	2 ft. 6 in.
Area	15.63 sq. ft.
Horizontal Tail Area	14.4 sq. ft.
Vertical Tail Area	7.3 sq. ft.
Incidence of Tail Unit	1.0 deg. (trailing edge up)

Power Plant:
One 250-horsepower T-63 gas turbine engine driving a two-blade propeller with electrically actuated pitch control by Mississippi State University. Engine is located in mid fuselage and drives the tail-mounted shrouded propeller through a 7-foot shaft and gearbox. Fuel tank, located under the rear seat position, has a 39-gallon capacity. Oil tank capacity is 7 quarts.

Landing Gear:

4-Wheel Pantabase, Steerable

Wheel Track	6 ft. 6 in.
Wheel Base	4 ft.
Wheel Size	5:00 x 5
Brakes, 4-Wheel	Disc

Accommodations:

Four crew members - two abreast seating. Combination doors
and windows on each side of aircraft.

4. AIRCRAFT STRUCTURES

The material used throughout the XV-11A is 9-ounce fiber glass with a general purpose polyester resin. This material provides a strong, lightweight, rigid structure with smooth surfaces and the opportunity to obtain complex curvatures with relatively low-cost tooling. The use of fiber glass is particularly attractive for limited production articles and allows later modifications to be easily made. The chance to experiment with the low radar reflectivity of fiber glass structures is an additional feature offered by this material.

Generally, the structure may be described as a rib or a bulkhead-supported molded skin assembled with an epoxy bond. Views of the aircraft components under construction are shown in Figure 13.

Bonding material used throughout the aircraft was an epoxy, plasticized with 7 percent (by weight) polysulfide. Completed units were post cured after bonding to increase bond strength and decrease the probability of further shrinkage. This post cure was accomplished for most parts where foam sandwich material was used. Polyurethane foam of 4-pound and 6-pound density was used for sandwich material.

High-stress areas in the fuselage skin or bulkhead joints (such as empennage attachment, control brackets, or engine mountings) were reinforced by mechanical fasteners, bolts, or rivets. Generally, bonded joints were lapped or spliced in accordance with current aircraft practice, and efforts were made to obtain sufficiently thick glue lines and filleting of the bonded material at the edges.

In high-temperature areas, such as those around the engine exhaust and the oil coolers, the fiber glass material was laid up with the heat-resistant polyester resin which retains its strength up to a temperature of 350° F. Fuselage structure and skin in the area of the engine compartment were insulated against heat damage by asbestos, fiber glass, and aluminum foil.

Wings, fuselage, and shroud were contoured and smoothed with polyester body putty; the complete airplane was painted with dull-finish white lacquer for heat-reflection purposes and protection of the fiber glass skin.

4.1. LOADS

The XV-11A aircraft was originally designed for limit load factors of +6 and -3 and ultimate load factors of +9 and -4½ based on a 2200-pound aircraft weight. The flight envelope for the 2200-pound case gives a maximum aircraft airspeed of 315 miles per hour. Because of the increases in the weight of the components, the maximum gross weight was

increased to 2600 pounds and the flight envelope was modified as in Figure 14, where the limit load factors are +5.2 and -2.5. This flight envelope has been drawn up according to Federal Aviation Regulations, Part 23. The flight weight is 2400 pounds with pilot only and 2600 pounds with an observer. This flight envelope allows gust criteria of 30 feet per second.

4.2 WING DESIGN

The distributed suction boundary layer control system required that the wing have an even skin thickness on the upper surface and that this surface be smooth and wave-free. Seals were provided at all junctions to prevent air leakage into the wing. The camber-changing mechanism consists of two load-carrying horns in each wing, which support four subspars aft of the main spar. The horns, which take the place of wing ribs throughout the camber-changing area, are of cast magnesium. They rotate through journals consisting of short arc blocks of nylon sliding in a "u" section. These journals are built into the subspars at the proper location to receive the horn (Figure 6).

The single spar wing has a "D" section leading edge with stressed skin construction varying from .050-inch thickness for the top surface to .075 inch at the leading edge and over the main spar. The main spar consists of a "C" section of fiber glass which has varying numbers of layers of stainless steel laminated between layers of cloth in order to form caps at the intersections of the upper and lower skins. Nose ribs and riblets are used to support the leading edge skin. The wing tips outside the aileron are removable and are of the Hoerner-type configuration. The subspars in the camber-changing area join to the skin with piano-type hinges integral with spars and skin. A long pin can be pulled from each hinge point to remove the spars and to expose the horns and mechanism for servicing. Inspection panels are provided forward of the main spar for horn and gearbox inspection.

The machine-drilled suction holes in the fiber glass wing skin have proved to be satisfactory from a structural and maintenance viewpoint. Holes were not drilled in the spar caps, but rib and riblet flanges under the leading edge skin of the wing were drilled when necessary.

The wings are attached to the fuselage by a single wing carry-through spar milled from aluminum and pinned by steel attachment bolts. The carry-through is attached to the fuselage by means of bolts through stainless steel plates laminated into the fuselage bulkhead at the spar location. The wing spar attachment fittings are steel laminations attached to stainless steel and fiber glass build-ups on the main wing spar by means of bolts. Similar fittings on wing and fuselage are provided at the drag fitting location at the wing leading edge. All stainless steel reinforcements in the wing and fuselage were etched and bonded in place with epoxy ("Epon" 901).

11

4.3. WING ASSEMBLY PROOF TESTS

The wing assembly proof tests were performed at Parsons Corporation prior to delivery to Mississippi State University. The wing panel assembly was subjected to static loading of 3508 pounds vertical shear, 900 pounds diag shear, 224,997 inch-pounds vertical bending moment, and 114,300 inch-pounds in-plane bending moment without structural damage.

The aft section of the wing in the camber-changing area and the camber-changing mechanism were power cycled under 50 and 75 percent (528 - 792 pounds distributed) of condition 2 loading,* and proof tested at 100 percent (1057 pounds distributed) for static deflection measurements.

The aileron control connections were checked at 50 percent (314 pounds distribution) of condition 2 aileron loading.

Vertical bending beam stiffness measured agreed with the calculated data to within 6 percent.

The measured torsional stiffness distribution was twice the calculated distribution.

A first-mode natural, fixed-free vertical bending frequency of 8.2 c.p.s. was recorded with the wing assembly mounted in the test fixture.

4.4. FUSELAGE

The fuselage unit was planned as a structure constructed totally of fiber glass. This was accomplished by using a stiffened shell-type structure with bulkheads joined by stringers on the top and bottom and reinforced in the belly by a heavy floor over stringers reaching to the outside skin. A heavy tubular glass skeleton extends from the high wing attachment area to a triangular-shaped ring bulkhead which forms the windshield posts and carries around into the forward end of the built-up floor. The skeleton is the attachment and support for the side and top windows (Figure 13). The complete pilot and passenger compartment was glassed-in above the seat cushion height. The long side windows are hinged at the top and act as doors. The individual glass areas are large and require heavy, mold-contoured, Plexiglas** panels.

---

*Condition 2 loading is defined by the manufacturer, Parsons Aircraft
  Corporation, as a load factor of +3 at 105 miles per hour and a
  weight of 2200 pounds.
**Reg. T. M., Rohn & Haas Company

The heavy bulkheads used to support the wing carry-through attachment are rectangular in cross section and extend around the bottom - fore and aft of the landing gear carry-through. The gear carry-through structure is composed of glass roving compression and tension bars built integrally with floor and bottom skin. The tension bars at the bottom form the hinge points for gear leg attachment.

Floor structure and polyurethane foam sandwich skin, up to the window line, form the main passenger load support. Thrust loads from the aft mounted shroud and propeller are taken through the fuselage skin and stringers at both the top and the bottom. A faired-out lower shroud intersection at the rear forms both aft lower fuselage and the lower one-fourth of the shroud. Shroud attachments consist of reinforced skin with closely spaced anchor nuts for bolting on the remainder of the shroud.

Fuselage skin thickness varies from about .050 inch in the front section to about .030 inch at the rear. Build-up was utilized at points such as landing gear structure, wing carry-through and drag spar fittings, and gearbox mountings. The fuselage skin was laid up in open three-part molds and came together in lapped and bonded joints along the extreme width points on the side and at the top center. Bulkheads were bonded in place, as were stringers and other fuselage structure. Gas tank mounting brackets were bonded and riveted into the floor at locations where side panels bond into the floor. They were positioned fore and aft of the landing gear carry-through.

The gas tank of 39-gallon capacity was constructed of .032 sheet aluminum ribs and wrap. It was bonded and riveted together. Baffles were installed in sufficient number so that the tank would be rigid enough for a rear seat support.

4.5. SHROUD AND EMPENNAGE

The Aerophysics Department of Mississippi State University paid close attention to the design of the shroud and tail surfaces of the XV-11A, since problems had arisen pertaining to excessive weight of these components on the XAZ-1 aircraft. Construction is of a single spar and closely spaced ribs covered by skin .030 inch thick on the inner surface and .020 inch thick on the outer one. Skins are bonded to spar and ribs. The trailing edge is a glass-covered foam wedge bonded inside the skins.

The stabilizer and fin form a cross in the shroud behind the propeller and effect a part of the shroud stiffening. They are of a heavier build-up, about .050-inch-thick skins. The skin of the rudder and elevator are .020 inch thick, and the ribs are reinforced by steel tubing at hinge points. Rib spacing is 6 inches in the rudder and elevator as compared to 3 inches on the shroud.

13

The weight of the complete shroud and control surfaces, minus the two bracing struts, was 68 pounds. Some trouble was encountered in obtaining a close tolerance on the propeller tip clearance due to slight warpage during the post curing of the shroud; however, this was overcome by cutting and reapplying a small area of glass. The Department found that this light structure was sensitive to warpage inherent in polyester in lay-ups.

The shroud-to-fuselage struts consist of two fiber glass roving spars and stressed skin with a polyurethane foam core.

4.6. LANDING GEAR

The landing gear used on the XV-11A is a compromise between a pantabase operation and test flying from hard-surface runways. The result is a four-wheel gear with wheels mounted in skids or elongated pants and sprung to the fuselage by laminated fiber glass leg members. These leg members were built into a faired torque box which absorbed landing loads.

The leg members (6 per side) are composed of glass roving caps laminated into, and bonded to, side webs. The leg section is fastened into the two-wheel pant, wrapped with fiber glass cloth, and then covered with an airfoil-shaped fairing (Figure 15).

Pants are constructed of aircraft birch plywood laminated with fiber glass cloth. Wheel axle loads are properly distributed with bolted-on flanges. Front wheels are steerable by connection to the rudder cables. The rear wheels are fixed. Brakes operate on all four wheels.

Initial shock loads are absorbed by a rubber pad fitted between the compression side of the gear and fuselage carry-through. As this hardens under load, the fiber glass landing gear legs and the fuselage carry-through members flex with the loading.

A tail skid constructed of fiber glass roving is positioned under the shroud.

Individual landing gear leg components were static tested in a mocked-up mounting to simulate pant and fuselage attachment. The tests were carried out in a 200,000-pound testing machine. After some bonding surfaces were enlarged, the leg was static tested to $7\frac{1}{2}$ G's, the ultimate load. At this point the roving parted at the hinge line, thus assuring the maximum strength attainment of the structure. Previously, a fiber glass landing gear strut of a lighter build-up than the XV-11A's had been torque tested to better than 6 G loading. Thus, it was felt that sufficient preliminary test work had been done to assure a reasonable margin of safety on the landing gear.

Nevertheless, after 24 landings, it was apparent that considerable delamination was occurring on the fiber glass webs. The undercarriage was removed, inspected, and repaired. It was found that instead of the load being carried equally by the six struts on each side, it was being carried by both the rear legs due to torsional loading of the relatively stiff gear. This apparently caused successive delamination. However, there was little danger of the undercarriage's collapsing because the load was simply shifted to the next strut as the web in the rear leg delaminated and separated. In the reassembly of the undercarriage, care was taken to insure that the load was more equally distributed among all six struts on each side.

15

5. CONSTRUCTION TECHNIQUES USED IN FABRICATING
THE FIBER GLASS COMPONENTS

All fiber glass bulkheads, ribs, and skins of the XV 11A were constructed either at Parsons Corporation or Mississippi State University's Aerophysics Department. Matched molds were used for structural parts, yielding pieces with approximately 60-percent glass content. These pieces were oven cured to facilitate assembly without warpage. Open lay-up of glass laminate, used for large skin areas, resulted in glass content of approximately 53 percent and room temperature cure.

5.1. WING

Wing skins were laid up in large wooden molds with matching plaster male molds clamped in place with three bolts passing through inspection panel openings. Stainless steel spar caps were laminated in place with successive overlays of cloth. All spars, ribs, and camber-changing mechanism supports were bonded into the top skin as it lay inverted in the mold (see Figure 13). The camber-changing horns and drive mechanism were added at this time. Subspars were fitted into their piano-hinge counterparts which were built into the wing skins. Wings were completed by bonding on bottom skins which contained the inspection panels for the camber-changing mechanism.

5.2. FUSELAGE

The fuselage skin was laid up on an open female mold of fiber glass, reinforced with steel tubing. This mold was constructed over a fiber glass and plywood mock-up furnished by the Mississippi State University Aerophysics Department. The three-part mold consisted of a lower section to the maximum width of the fuselage, and a pair of sides parting at top center. A lap for bonding was provided for at each joint. The build-up of additional layers of glass at the nose, belly, wing locations, and landing gear locations was made on the original mold. The lower mold was used as a jig for the bonding-in of bulkheads and stringers before addition of side skins. Sliced polyurethane foam was bonded to the sides and floor of the cabin area and covered with fiber glass laminate. The floor was 1/8-inch-thick laminate laid up separately, then bonded in place.

5.3. EMPENNAGE

Cylindrical, wooden molds were used for open lay-up of the shroud skins. Inner and outer surfaces were molded, then bonded at leading and trailing edges. Contour accuracy was critical for the inner surface

16

of the shroud. Elevator and rudder "D" sections and skins were open
lay-ups in wooden molds, and the ribs were match-molded.

5.4. LANDING GEAR

Landing gear leg sections were laid up in metal molds constructed
to facilitate the winding of wet glass roving through the tension and
compression sides of the strut and over an aluminum bushing at the hinge
point. Light tension was maintained on the roving wrap. Sections were
joined to the fuselage through a piano-type hinge and fitted into the
wheel pant ahead of the rear wheel. Spaces were then filled with poly-
urethane foam. Biased cloth lay-up of .072-inch thickness was bonded
to the top and bottom of the leg in order to complete the torque box.
The fiber glass pad which transferred compression loads to the fuselage
was match-molded and bonded to the leg assembly before attachment to the
pant. Pant attachment was a combination of bolted flanges, bonding, and
reinforcing fiber glass cloth wrap (Figure 15).

5.5. SHAFT HOUSING AND DUCTING

The fiber glass drive shaft housing, gearbox front housing, and
attachments were open lay-up of heat-resistant resin and glass cloth
over male molds turned from hardwood. Alignment of shaft and bearings
was achieved in the housing by seating bearings in glass and resin and
by using the actual metal shaft for alignment purposes. Oil lines and
the oil scavenging chamber were bonded to the housing. Coned housing
attachment flanges were fitted to the housing at bulkhead intervals.
They were stepped in diameter to allow removal to the rear as the pro-
peller and gearbox were removed. The shaft housing is shown in Figure 9.

The ducting from the wings to the engine compressor was constructed
over a male mold mock-up and was fitted with bellmouth fairings at the
wing root inlets and at the compressor outlet. Oil and engine cooling
ducts were laid up over wooden molds and were bonded into the fuselage
duct at the lower front sides of the wing roots. Intake, oil, and engine
cooling ducts are shown in Figure 7.

17

6. WEIGHT AND BALANCE

All components of the XV-11A that arrived from Parsons Corporation were weighed prior to assembly. Similarly, all parts that were designed and manufactured in the Aerophysics Department were also weighed and their distance from the aircraft datum measured. Those items which could not be weighed were estimated by using the best available data from the handbooks. The weight of the polyester putty filling that went into the wings, fuselage, and shroud is only a rough estimate at best; however, the error involved should be small in comparison to the total weight of the vehicle.

The following paragraphs give a weight and balance breakdown of the aircraft as well as the moments of inertia about all three axes which were determined experimentally.

6.1. WEIGHT BREAKDOWN OF XV-11A AIRCRAFT

The weight and center-of-gravity location of the various components of the XV-11A are given in Table I.

TABLE I
WEIGHT BREAKDOWN OF XV-11A

Component	Weight (lb.)	Longitudinal Moment Arm (in.)	Vertical Moment Arm (in.)
WINGS (201 Pounds Each)	402.0	115.6	+22.75
Tubing (In R.H. Wing)	20.0*	-	-
Wing Fairings	7.0*	-	-
Wing Spar Carry-Through	20.0	-	-
Wing Flap End Plates	3.0*	-	-
FUSELAGE (Bare Shell As Purchased)	382.0	113.6*	+0.4
Plexiglas	58.0*	60	+15.00
Door Latch Installations	10.0*	65	-2.00
Instrument Panel, Cowl, and Battery Box	27.0*	20	-2.00
Pilot's Control	20.0*	28	0
Additions to Fuselage, Structure, etc.	25.0*	142	0
Cables and Control Linkages	20.0*	122	-1.00
Seating (2 With Belts and Shoulder Harness)	40.0	66	-6.00
Instruments (Flight and Permanent Control Readout, Radio, Wiring, Ignition)	60.0*	32	+4.00
Fire Extinguisher	7.5	70	-13.00

18

TABLE I - contd.			
Component	Weight (lb.)	Longitudinal Moment Arm (in.)	Vertical Moment Arm (in.)
ENGINE INSTALLATION, COMPLETE WITH MOUNTING, DUCTING, INSULATION, COVERS, OIL TANK, AND ACCESSORIES (Dry Engine Wt. 140 lb.)	260.0	135	+16.50
GAS TANK EMPTY INSTALLATION	25.0	106	-10.50
SHROUD	41.0	246	+38.00
Controls Surfaces	43.0*	263	+30.90
Fittings	3.0*	-	-
Tab Installation	3.0*	-	-
Struts	7.5*	236	+41.50
Tail Skid	4.5	248	-8.50
PROPELLER AND PITCH CHANGE MECHANISM	69.0*	248	+30.90
DRIVE SHAFT AND HOUSING	29.5	188	+22.50
PROPELLER DRIVE GEARBOX	20.0	238	+30.90
CAMBER CHANGE GEARBOX (Electrically Driven)	10.0*	122	+23.50
BATTERIES (2 - 12 Volt)	54.0	12	-5.00
LANDING GEAR (Including Fairings and Rubber Pads)	220.0	100	-27.90
TOTAL	1891.0		

*Estimated values required because the particular value was not obtained prior to assembly of aircraft.

The longitudinal moment arm is measured from the zero fuselage station, positive aft. The vertical moment arm is measured from the fuselage reference line, positive up. The location of most of these components is illustrated in Figure 16.

At the time the XV-11A design was finalized, the available information on the use of fiber glass for load-carrying structures was limited. For this reason, conventional metal aircraft techniques were used in the design and fabrication of the XV-11A structure. Considerable weight savings could be realized with an optimized fiber glass structure using current state-of-the-art knowledge in fiber glass construction.

19

6.2. MOMENT OF INERTIA DETERMINATION

The mass moment of inertia of a compound pendulum about its swing axis, neglecting the effects of the surrounding air and considering small oscillations, is given by the equation

$$I = \frac{WLT^2}{4\pi^2}. \tag{1}$$

Since the pendulum in this analysis was the XV-11A aircraft plus the suspension cage, this equation was altered as described in Reference 4 to define the aircraft's moment of inertia about its body axes through the center of gravity. It is necessary to subtract the contribution of the inertia of the suspension cage which was attached to the fuselage. Another term accounts for the air mass inside the aircraft, and a final term estimates the so-called "additional mass" contribution resulting from the inertia of the surrounding air which is disturbed by the swing. The centroids of both of these air masses are assumed to coincide to the first approximation with the aircraft center of gravity. The additional mass factor I_A is estimated from consideration of the projected areas of aircraft surfaces which are oriented normal to the swinging motion of the pendulum. The procedure and empirical coefficients employed for this purpose are described in reference 5.

The resulting equation for the mass moment of inertia of the aircraft about its C.G. is

$$I = \frac{WLT^2}{4\pi^2} - (\frac{w}{g} + V_0\rho)1^2 - I_A - I_S. \tag{2}$$

This includes both the inertia of the aircraft structure and the enclosed air. The mass of enclosed air is considered as part of the aircraft mass, being about 1 percent of the total.

6.2.1. Instrumentation for Moments of Inertia Measurements

The principal instrumentation components are a light source, a light detector, a shutter attached to an extremity of the XV-11A, a second shutter to permit light passage only when desired, and an electronic counter for measuring the time lapse between the momentary passages of light from source to detector. The amplitude and the decay of the oscillations were determined by the maximum position of the beam of light on the large shutter attached to the XV-11A.

6.2.2. Moments of Inertia

For determining the moments of inertia of the XV-11A, the following procedure was followed:

The suspension cage was arranged symmetrically on the aircraft so that swings could be made about three axes parallel to the X body axis of the airplane with all three swing axes lying in the plane of symmetry. The data from two of these swings provided a means for determining the Z coordinate of the aircraft C.G.

The mass moment of inertia of the aircraft about the roll axis was finally determined as

$$I_X = 905 \pm 11 \text{ slug-ft}^2.$$

The possible error values are discussed later.

A slightly different technique was employed for the pitch mode swing since the location of the C.G. of the suspension cage made it impossible to maintain the centers of gravity of the cage and the aircraft in a plane with the suspension axes. For this reason, the two swings performed in this mode were not used to provide another estimate of l_b, but rather were used only to determine the vertical position of the C.G. of the pendulum; i.e., the whole suspended mass, aircraft plus cage. The fore and aft location of the pendulum C.G. was found by dropping a vertical from the swing axis. With the pendulum C.G. thus established and the C.G. of the suspension cage known, the principle of moments provides the means of finding the position of the aircraft C.G.

The mass moment of inertia of the aircraft in pitch was found to be

$$I_y = 1768 \pm 12 \text{ slug-ft}^2.$$

The moment of inertia about the yaw axis was determined by suspending the airplane as a bifilar pendulum by means of two lengths of 3/16-inch aircraft cable, as illustrated in Figure 17. The C.G. of the suspension cage and the aircraft fell out of the plane of the bifilars which resulted in the following equation for the moment of inertia of the aircraft in yaw.

$$I_z = \frac{Wd^2 T^2}{16\pi^2 D} - (\frac{w}{g} + V_o \rho)l^2 - I_A - I_S.$$

From this,

$$I_z = 2370 \pm 15 \text{ slug-ft}^2.$$

6.2.3. Error Estimate

The possible error in determination of the moment of inertia depends upon the precision attained in each of the following procedures:

(a) Weighing
(b) Timing
(c) Scaling lengths
(d) Estimating additional mass contribution and aircraft volume.

Of these, the first and last predominate. The highest order of
precision was obtained in the electronic system for measuring the period
of pendulum oscillations. Millisecond accuracy was achieved in measuring
the damped periods T_d which were then corrected to determine the natural
periods T_n retained to the same accuracy.

The four scales used for weighing were checked against each other
and found to vary about 5 pounds in a thousand from their common mean.
To accommodate this fact and to allow for human inaccuracies in weigh-
ing, the corrected weight values were assumed to be in doubt $\pm\frac{1}{2}$ percent.
Each term of an equation which involves weight then has an error contri-
bution of $\pm\frac{1}{2}$ percent irrespective of the algebraic sign of the term.

Because of the approximate empirical procedure involved in esti-
mating the additional mass factors (reference 5), the possible error in
this term was assumed to be 10 percent, which is probably conservative
according to reference 4. The air mass enclosed inside the airplane is
so small that error in its calculation is insignificant.

Figure 18 shows the general layout of the XV-11A aircraft in the
suspension frame, and Table II summarizes the results of the moments of
inertia tests.

22

TABLE II

RESULTS OF THE MOMENTS OF INERTIA TESTS

Axis of Rotation	Roll			Pitch		Yaw
	X_b	X_m	X_t	Y_b	Y_t	Z
Axis Position	bottom	middle	top	bottom	top	
Symbol						
w	1890	-	-	-	-	-
w'	214	-	-	-	-	246
W	2104	-	-	-	-	2136
Δl	0	1.0833	2.1666	1.0833	2.1666	-
l	2.2566	3.3399	4.4232	2.2634	4.4267	0.125
l'	-0.815	+0.268	+1.353	-	-	1.194
L	-	-	-	1.9377	4.1043	-
T	3.5756	3.2318	3.1690	4.5332	3.6960	11.702
$V_o\rho$	0.559	-	-	-	-	-
I_A	39.5	43.3	48.3	24.3	24.3	24.3
I_s	24.1	20.2	32.1	38.1	45.8	26.2
d	-	-	-	-	-	4.305
D	-	-	-	-	-	14.06

23

7. INSTRUMENTATION

7.1. NORMAL AIRCRAFT INSTRUMENTATION

The instrument panel of the XV-11A aircraft is shown in Figure 19. In addition to the usual flight instruments, engine instruments, and radio, a number of control deflection indicators and a wing internal pressure gauge are located on the right side of the panel.

7.2. FLIGHT TEST INSTRUMENTATION

In order to fully monitor the flight tests of the XV-11A aircraft and to determine its flight characteristics, several additional instruments were required.

The instrument panel data were recorded by a 16-mm camera, taking one frame per second during the first flights. The camera served the primary purpose of a crash recorder. The instruments used in addition to normal flight instruments are shown in Table III.

TABLE III **PANEL MOUNTED FLIGHT TEST INSTRUMENTATION**		
Instrument	Range	Type of Sensor
Aileron Position	±10 deg.	Potentiometer - ½ of resistance bridge operating from Zener diode regulates supply
Rudder Position	±20 deg.	"
Elevator Position	±30 deg.	"
Elevator Trim Position	±20 deg.	"
Camber Angle	0-29 deg.	"
Yaw Angle	±15 deg.	"
Angle of Attack	0-35 deg.	"
G-Meter (Vertical)	±12G, -4G	Spring-mass, dial indicator

In addition to photographic recording, a CEC Type 5-144 P3 oscillograph recorder was used to record continuous flight data. The recording paper speed was 0.6 inch/second, limiting the frequency response to a maximum of approximately 10 hertz. The maximum recording time per cartridge of photographic paper was 30 minutes.

The data channels recorded are shown in Table IV.

TABLE IV		
OSCILLOGRAPH RECORDED FLIGHT TEST INSTRUMENTATION		
Information Recorded	Range	Type of Sensor
Control Stick Force	±30 lb.	Strain-gauge bridge - Zener diode regulated supply
Normal Acceleration	±2G	Strain-gauge bridge - Zener diode regulated supply
Horizontal Acceleration	±1.5G	"
Rate of Roll	±18 deg./sec.	Potentiometer - ½ bridge, Zener diode supply
Rate of Pitch	±18 deg./sec.	"
Rate of Yaw	±6 deg./sec.	"
Aileron Position	±10 deg.	"
Rudder Position	±20 deg.	"
Elevator Position	±30 deg.	"
Airspeed	0-150 m.p.h.	"
Altitude	0-10,000 ft.	"

   A multitube water manometer was installed in the aircraft to record wing pressure distributions, boundary layer measurements, rake surveys, and quantity flow measurements. To use this manometer, it was necessary for the flight observer to face the rear of the aircraft.

8. PERFORMANCE

The preliminary phase of the XV-11A flight test program consisted of 49 flights with a total flight time of 35 hours. The majority of this flight time was devoted to aerodynamic research of the shrouded propeller, the distributed suction boundary layer control system, and an evaluation of the general handling characteristics. A minimun of performance data was collected since the primary objective was aerodynamic research. No takeoff and landing performance measurements were recorded, because the existing suction source system was unable to provide full boundary layer control during landing.

8.1. STATIC THRUST

The variation of static thrust as a function of engine shaft horsepower is shown in Figure 20. The broken line on this figure represents the ideal thrust as given by the momentum theory. The theoretical values assume that 90 percent of the engine power output is effectively transmitted to the slipstream by the propeller. The difference between the actual and ideal thrust curves indicates the improvement that may be realized through changes in propeller configuration.

Further testing will be conducted to evaluate the capabilities of the present propeller and to define the needed changes in the propeller configuration.

8.2. LEVEL FLIGHT

The power required for level flight as a function of equivalent airspeed was obtained from flight test data shown in Figure 21. The data points shown in this figure were obtained at various times during the flight test program and do not represent a systematic attempt to determine the engine and propeller settings for minimum power at a given airspeed. A systematic investigation was not performed because of the known inadequacies of the present propeller. Although the various values of power required, obtained at a given airspeed, reflect to some extent the normal scatter in flight test data, it is felt that the different engine and propeller settings used for the individual test points are the major cause of the scatter. For this reason, the faired curve shown on this figure is considered to be representative of the minimum power required for level flight with the present propeller. There is every reason to believe that an improvement in this curve will result from the anticipated increase in efficiency of the new propeller.

On two flights, at altitudes of 5000 and 15,000 feet, fuel flow data were taken; the results are plotted in Figure 22.

9. STABILITY AND CONTROL CHARACTERISTICS

At this time, only limited test data pertaining to the stability and control characteristics of the XV-11A have been obtained. Most of this information is in the form of a qualitative evaluation of the aircraft, with emphasis being placed on safety of flight; however, some quantitative data were recorded in connection with other phases of the flight test program.

9.1. STATIC CONTROL CHARACTERISTICS

The variation in static longitudinal, lateral, and directional control forces as a function of surface deflections is shown in Figure 23. A comparison of the maximum allowable breakout forces considered to be acceptable according to MIL-F-8785 (ASG) and the average static breakout forces obtained from Figure 23 is shown in Table V.

TABLE V BREAKOUT FORCES		
	MIL-F-8785 (1b.)	XV-11A (1b.)
Elevator	4	11.0
Aileron	3	3.5
Rudder	7	30.0

The military specification values are for observation-type aircraft. The XV-11A values are considered to be excessive, but they have not proven to be a noticeable problem to the pilot. It may be noted that the large elevator breakout force does not show up in the variation of wheel force to trim given in Figure 24. This difference between static and flight characteristics may be due to the level of vibration in flight, particularly with the control surface located immediately behind the propeller. The high breakout force in the directional control system is in part due to the unusual landing gear, with front-wheel steering, resulting from the pantabase concept. It is interesting to note that these measured breakout forces are in the same order of magnitude as those measured on some current general aviation aircraft (reference 6).

9.2. LONGITUDINAL TRIM CHARACTERISTICS

Figure 25 shows the elevator angle required to trim for three wing camber settings as a function of indicated airspeed. Elevator angle data were available for this one flight only. Thus, an evaluation

27

of the stick-fixed neutral point is not feasible. However, it is quite apparent that an acceptable level of static longitudinal stability is available with the C.G. located at 36.6 percent of the wing mean geometric chord. This is the most aft C.G. position tested. A significant increase in apparent static stability may be noted with the 10- and 30-degree camber settings. This is probably a result of the progressive wing separation that occurs with the present boundary layer control system. Anticipated improvements in the boundary layer control system should reduce this effect.

The variation of wheel force required to trim as a function of indicated airspeed is found in Figure 24. These data do not lend themselves to determining a control-free neutral point because of a somewhat erratic variation in slope with the C.G. position. These data do illustrate satisfactory levels of control-free static stability for the range of velocities and C.G. positions tested. The curves for 10 and 30 degrees f wing camber reflect the apparent increase in control-fixed stability discussed in the preceding paragraph.

The change in elevator deflection and wheel force required to trim at a constant flight velocity due to changes in wing camber setting is shown in Figure 26. These changes are typical of the current, high-wing general-aviation aircraft. These forces are higher than desirable, but they are considered to be acceptable because of the rather low rate of change of wing camber and the improved electric trim system now installed in the aircraft.

9.3. LONGITUDINAL DYNAMIC STABILITY

Although there are no quantitative flight test data pertaining to the dynamic stability of the XV-11A, some analytic work has been accomplished on the longitudinal dynamic characteristics. Figures 27 and 28 show the predicted short period and phugoid frequency and damping characteristics for two C.G. positions. The moment of inertia used in these calculations is slightly larger than the subsequently measured value of 1760 slug-ft^2 discussed in section 6.2. MIL-F-8785 (ASG) specifies that the short-period longitudinal oscillations should "damp to one-tenth amplitude in one cycle" and that the phugoid oscillations "shall be at least neutrally stable" if the period "is less than 15 seconds". A short-period damping ratio in excess of 0.345 is required for the oscillations to damp to one-tenth amplitude in 1 cycle. A phugoid period of greater than 15 seconds requires a frequency of less than 0.066 cycle per second. The predicted short-period and phugoid characteristics satisfy both of these requirements.

Since the aerodynamic characteristics used in this analysis were obtained without benefit of wind-tunnel test data, these predicted results can be considered as only rough approximations. Also, the requirements of MIL-F-8785 (ASG) do not ensure that satisfactory flying

28

qualities will be provided. The results of this analysis do seem to verify the pilot observations that the longitudinal characteristics are at least acceptable within the present operational flight envelope.

9.4. HANDLING QUALITIES

The qualitative evaluation of the handling qualities of the XV-11A can be summarized as follows:

1. The aircraft has adequate control for the presently authorized flight envelope.

2. The control forces are somewhat high with rather large static breakout forces in the longitudinal and directional control systems; however, the large breakout forces were not apparent in flight.

3. The aircraft is stable for the range of aircraft weights and C.G. positions that can presently be developed. Low-speed flight at low power settings and wing camber settings of 10 degrees or greater produces undesirable lateral/directional oscillations in moderately turbulent air. These oscillations are damped and are in part attributable to the present inadequacies of the boundary layer control system. The stabilizing effect of the propeller when operating in reverse pitch is quite noticeable on the oscillations.

4. The use of reverse propeller thrust was successful for glide path control and for increasing the rates of sink of the aircraft. The longitudinal and directional control power was decreased when this technique was used; however, the control power was still considered to be acceptable.

5. An apparent decrease in lateral control power was found at low velocities and low power settings. This relative ineffectiveness was partially due to the present ineffectiveness of the boundary layer control system; however, other contributing factors are considerable. Aileron float, as observed in flight, and the velocity ratio of pilot control movement to aileron movement seemed to be excessive.

6. The stalling maneuvers investigated in the flight test program have demonstrated a mild stall with no excessive wing dropping and recovery within 100 feet when normal recovery techniques are used. Stall warning is less than desirable.

7. Visibility from the cockpit is excellent in all directions except directly aft; however, because of the large window area, the temperature inside the cabin becomes excessive in hot weather.

29

8. Ground handling was acceptable with a turning radius of 21 feet with steering alone and 13 feet with differential braking. In rough ground the aircraft had a tendency to porpoise because of the short coupled landing gear.

10. AERODYNAMIC MEASUREMENTS

A large portion of the preliminary flight test program was devoted to aerodynamic measurements associated with the high-lift suction boundary layer control system. An effort was made to optimize the suction velocity distributions so that the aircraft would have acceptable handling qualities both in the takeoff and the landing phases of the operation. Tuft pictures, pressure distribution and boundary layer measurements were taken at various flight velocities. Aerodynamic measurements were also taken of the shroud inflow and outflow as well as boundary layer measurements on top of the fuselage.

10.1. WING PRESSURE DISTRIBUTIONS

Typical measured wing pressure distributions on the XV-11A wing in flight are shown in Figure 29. The pressure taps were located on the starboard wing midway out on the cambered portion of the wing. The data are shown for 75 miles per hour indicated airspeed with wing camber settings of 0, 10, 20, and 30 degrees. Suction was being applied when these data were obtained, but it was not of sufficient quantity to maintain attached flow on the high camber configurations. The internal wing pressure, as well as the chordwise position of the first row of open suction holes, is shown on each plot. The first seven rows of available suction holes were sealed to prevent any outflow due to the local external wing static pressures that were more negative than the internal wing pressures. The pressure distribution for the zero-degree camber setting shows that there was still a small amount of outflow in the neighborhood of 0.1 X/C; however, the flow was attached. The approximate chordwise position at the start of separation, as shown by the tuft pictures, is also noted on each plot. The local (section) lift coefficients obtained by integrating these pressure distributions are noted on each plot. Although the total aircraft lift coefficient is the same for each camber setting, the changes in span loading and tail load required to trim result in different values of local lift coefficient.

10.2. FLOW VISUALIZATION

One advantage of fiber glass construction, especially for limited production or a one-of-a-kind vehicle, is the relative ease of fabricating complicated, compound curvatures free of any joints or other protuberances. The XV-11A is an excellent example of the possibilities of this type of construction, and the photographs in Figure 30 show the resulting disturbance free flow. The tuft pictures of the cruise configuration for a range of flight velocities are presented in Figure 31. The numbers displayed in the aircraft window represent the indicated airspeed in miles per hour. The airspeeds of 120 and 130 are represented by 20 and 30 in the photographs. There is no detectable area

31

of flow separation for the cruise configuration. Figure 30 presents
the tuft photographs for the 30-degree camber configuration. Except
for the separated flow on the wing, which is discussed in the following
paragraph, there is no area of separation apparent with this config-
uration.

Figures 32 through 35 show wing tuft photographs obtained at wing
camber settings of zero, 10, 20, and 30 degrees, respectively. Tuft
pictures were not obtained while the XV-11A was in stalled flight
because of the minimum separation between the chase aircraft and the
test aircraft required to produce quality tuft photographs. Stalled
flight in this discussion is considered to be that condition in which
either the developed lift is less than the aircraft weight or the motions
of the aircraft are not completely under the control of the pilot. The
minimum speed for the tuft photographs was within 1 or 2 miles per hour
of the stalled flight condition.

Figure 32 (zero camber) and, to some extent, Figure 33 (10-degree
camber) illustrate that the flow is essentially attached to the wing
for flight speeds within 2 miles per hour of stall. The loss of lift
is quite abrupt with little warning. Recovery from the stall is normal.
Figures 34 and 35 show the more progressive development of flow separa-
tion with the 20- and 30-degree camber configurations. Lift is still
being maintained at the minimum speeds shown with 20- and 30-degree
camber; a pronounced lateral/directional oscillation develops at speeds
below those shown in these figures. The oscillations are of sufficient
magnitude to make further increases in angle of attack unfeasible.
These oscillations are apparently a result of unsymmetric, unsteady flow
separation on the wings. In spite of the progressive flow separation
with the 20- and 30-degree camber configurations, there is no pronounced
warning of the approaching stall.

The relatively high minimum flying speeds indicated by these pic-
tures are of course the result of the present inadequacies of the
boundary layer control system.

10.3. SHROUD INFLOW MEASUREMENTS

For the static thrust condition, the variation of inflow velocity
across the shroud for a number of engine power settings is shown in
Figure 36. It is apparent that a decrease in blade loading is taking
place near the shroud for the higher power settings. Further investi-
gation is necessary to provide a better understanding of this shrouded
propeller installation.

Figure 37 presents the measured shroud inflow profile at a number
of flight velocities. The propeller thrust was the thrust required for
level flight. Although the significance of the change in inflow velocity
with flight velocity is masked by the as yet unknown variation of thrust

required with flight velocity, the consistent change in inflow velocity is quite pronounced. Essentially, the change in inflow velocity is equal to the change in flight velocity.

The variation in the shroud inflow velocity due to changing wing camber position at a constant 80 miles per hour indicated airspeed is illustrated in Figure 38. The mechanism of this small, but measurable, change in the velocity profile is not known at this time.

All of the inflow measurements depicted in this section were obtained on a shroud radial which makes an angle of 45 degrees with the aircraft plane of symmetry in the lower, starboard quadrant of the shroud. The rake was mounted $7\frac{1}{2}$ inches forward of the propeller plane.

10.4. BOUNDARY LAYER CONTROL SYSTEM

The present boundary layer control system does not produce sufficient suction velocities through the surface of the wing to prevent flow separation, especially at wing camber settings above 10 degrees. Lift coefficients of the order of 2.5 have been achieved with the uncambered wing; however, this falls far short of the lift coefficients of 5.0 which were anticipated with the cambered wing. The suction source for the present boundary layer control system is the compressor of the T-63 main propulsion engine. Unfortunately, flight testing has shown that the airflow characteristics of the engine compressor and the boundary layer control system are not compatible. Figure 39 presents the range of suction pressures; i.e., the pressure differential across the skin that can be developed with the present system assuming that the compressor is working at 90 percent N_1. The original porosity distribution was that calculated with the existing boundary layer theories with transpiration, under the assumption of an evenly distributed porosity distribution. Since the suction holes were drilled prior to flight testing, sealing rows of existing suction holes was the only way that increased suction pressure could be developed. Figure 39 shows that a suction pressure of only 2.6 inches of water could be developed with the original hole distribution at 90 percent N_1. It also shows that about half of this pressure was obtained at the flight idling compressor speed which is the landing condition. The design suction pressure was 9.0 inches of water, which could be achieved only after 49.5 percent of the suction holes were sealed. A higher percentage must be used if the flight idle condition is to be satisfied. This situation is obviously unfeasible, since the use of suction for boundary layer control involves the assumption of distributed porosity. The need for high-lift coefficients in landing also precludes the use of the present system at the low power setting, although a waste gate or bypass system which could partly solve the landing problem has been designed for the T-63. The only feasible solution to the mismatch problem is the use of an auxiliary blower to provide the necessary suction velocities for both the takeoff and landing conditions irrespective of the power output

33

of the main engine. Also, possible modifications to the wing and the porosity distribution may be necessary to obtain satisfactory suction velocity distributions and still maintain a close approximation of an evenly porous wing surface.

10.5. FUSELAGE BOUNDARY LAYER MEASUREMENTS

The intended use of an auxiliary blower for providing the necessary boundary layer control system suction has brought about the need for a suitable inlet for the T-63 intake airflow. One of the most promising locations for this inlet is on top of the fuselage at the aft end of the large upper window. A Keil tube was mounted at this location to provide a measure of the local boundary layer. The variation of the measured velocities, in terms of the velocity ratio, as a function of the distance from the fuselage surface is shown in Figure 40. These data are for 70 miles per hour and zero-degree wing camber. This configuration and speed yield about 22 degrees angle of attack. Identical results were obtained at low angles of attack. The attached and relatively thin boundary layer shows that this is probably a satisfactory location for the proposed intake.

34

11. RADAR REFLECTIVITY EVALUATION

Since the XV-11A is constructed of fiber glass, there was a possibility that the aircraft would be a poor radar target.

To determine the radar cross section (RCS) of the XV-11A, tests were performed to measure the microwave power reflected from the XV-11A and to compare this to the microwave power reflected from a standard reflector. Comparisons were also made of the reflected power of the XV-11A and two all-metal aircraft, i.e., a Cessna 319 and an Anderson-Greenwood 14.

11.1. EQUIPMENT

A block diagram of the equipment used in these tests is shown in Figure 41. The receiver section of the equipment consists of a horn antenna, a precision attenuator, a heterodyne receiver having a 30 MHz intermediate frequency, a circuit for suppressing the D.C. output voltage of the receiver when no input signal is present, and a D.C. vacuum tube voltmeter (VTVM).

The transmitter section consists of a sweep oscillator capable of covering the X-band, a traveling wave tube amplifier with a gain of 30 db and an output power of one watt, a power meter, and a horn antenna.

The receiving and transmitting antennas were identical horn antennas with a beamwidth of 20 degrees and a gain of 19 db.

11.2. RECEIVER CALIBRATION

The receiver was designed with a peak holding, automatic gain control circuit. The long time constant of this circuit allowed voltage readings, which were a function of received power, to be made with a high input impedance D.C. VTVM.

Using the setup shown in Figure 41, the local oscillator of the receiver was set to 8.62 GHz and with no output from the transmitter; the D.C. output voltage was suppressed to read zero on the VTVM. With the sweep oscillator set to sweep from 8.6 GHz to 8.7 GHz at a sweep frequency of approximately 100 H , the receiver was calibrated in 1 db increments from -100 dbm to -40 dbm.

11.3. RANGE CALIBRATION AND MEASUREMENT METHOD

The reflectivity measurements were made on an abandoned section of asphalt runway on the Starkville Airport. A distance of 50 meters

was chosen to give a maximum returned signal while assuring that the entire target remained within the 3 db (beamwidth) of the antennas.

As a check on the overall accuracy of the range, an aluminum cylinder with a radius of .073 meter and a length of 1.23 meters was used as a standard reflector.

The RCS of a cylinder is given by the expression

$$\sigma = \frac{2\pi L'^2 r}{\lambda}$$

where $\pi = 3.1416$, L' is the length, r is the radius, λ is the wave length, and σ is the radar cross section. In this case, the RCS is 20 square meters or 13 db greater than 1 square meter.

The ratio of the reflected power to the transmitted power is given by

$$\frac{P_r}{P_t} = \frac{g^2 \lambda^2 \sigma}{(4\pi)^3 R^4}$$

where P_r is reflected power, P_t is transmitted power, g is the gain of the antenna, and R is the distance from the transmitter to the target.

With a range of 50 meters, a RCS of 20 square meters, a frequency of 8.65 GHz, and a transmitted power of 1 watt (30 dbm), the above expression gives

$$P_r = 1.24 \times 10^{-5} \text{ milliwatts or } -49.1 \text{ dbm.}$$

The return from the standard cylinder was found to be -52.5 dbm, which indicates an error of 3.4 db. Part of this error was probably due to difficulty in reading voltage with sufficient accuracy in this volt-meter range. This problem was overcome by using additional zero sup-pression, which allowed the VTVM to be switched to a lower range. A precision attenuator was added to the input circuit of the receiver to allow the voltmeter to be returned to the same reading for each data point. Using this method, the difference in power reflected from the aircraft and the standard reflector could be read directly from the attenuator.

11.4. RESULTS

The results of the static RCS measurements made on the three air-craft are best shown in Figure 42. In this figure, the RCS is plotted in db greater than 1 square meter for every 7.5 degrees around the aircraft. It can be seen from the figure that all three aircraft have large reflections from the sides. On the two metal aircraft, this was probably due to large, flat surfaces along the sides of the aircraft

and the vertical control surfaces. On the XV-11A, this side peak was probably due to metal in the engine compartment and the exhaust ducts. There is also a considerable amount of metal throughout the cabin; also, the fuel tank, propeller, and numerous control cables are of metal. All of these metal objects form small "scattering centers" which contribute to the overall reflected power. It should be noted that although the maximum reflections from the XV-11A are equal to the maximum reflection from the AG-14, which is all metal, the AG-14 is a much smaller aircraft. When the XV-11A is compared to the Cessna 319, which is about the same physical size, the XV-11A peak reflections were 6 db less than those from the 319.

The fact that the XV-11A is a good radar target is also evidenced by observations made with search and approach control radar equipment. With these tests, the "blip" from the XV-11A was about the same as that of the Cessna 319 at a range of 10 miles. Since the weather was very poor on the day that these tests were made, it was not possible to determine which plane would lose radar contact first when flying away from the radar equipment.

11.5. CONCLUSION

Although the XV-11A is a good radar target in its present state, it is not inconceivable that its RCS could be reduced considerably. Most of the aircraft's "scattering centers" are so located that micro-wave absorbing material could be used to "hide" them with no major changes in the aircraft structure. The one major exception is the pro-peller. This might require a considerable effort - possibly going to a wooden or fiber glass propeller to reduce its RCS. Although these efforts would probably not make the XV-11A completely invisible to radar, there is a chance that the maximum radar detection range of the aircraft could be greatly reduced.

12. STRUCTURAL FATIGUE TESTS

At the start of the XV-11A flight research program, it was deemed wise to conduct fatigue tests on the fiber glass structural components of the aircraft. Of primary importance were the glass lay-up, as utilized in construction, landing gear buildup, rudder and elevator panels, and the wing structure through the variable camber section.

12.1. FIBER GLASS COUPONS

Fiber glass lay-up of 181 Volan 'A' fabric and a general purpose polyester resin were laminated in an approximation of the density used throughout the aircraft. Flexural fatigue tests were conducted on plain coupons and on coupons drilled to match the wing suction hole pattern. The resin-rich (glass content 53.2 percent) coupons were statically tested to an average of 35,600 p.s.i. However, the fatigue strength, tested at zero mean stress and 10×10^6 cycles, was found to be 11,500 p.s.i., which is 32 percent of static tensile strength. The complete S-N curves for the coupons with and without holes are shown in Figure 43. Drilled coupons with 0.020-inch-diameter holes tested to 25,000 p.s.i. tensile strength, 70 percent of the undrilled static tensile strength. Fatigue-wise, the drilled laminate demonstrated 90 percent of the strength of the undrilled laminate at 10×10^6 cycles.

Computations for tensile and fatigue strength disregard the loss in cross-sectional area from hole drilling. The S-N curves obtained, while tending to flatten as cycling reached the 50,000,000 point, still did not show indications of reaching an endurance limit. Fatigue strength of coupons was markedly lower when cycling was performed without forced air cooling.

12.2. LANDING GEAR STRUT

Static testing was performed on a pair of undercarriage legs in a compression testing machine, and it was found that failure occurred at an equivalent load of $7\frac{1}{2}$ times the weight of the aircraft. A fatigue test was designed which would load the leg in a manner similar to the actual installation. This test had a repeated flexing action which covered the load range from 1 G to failure. Strain gauges were attached to the leg at various points to determine the elongation under the progressive loading to reveal possible bond failure at the web-cap junction. A sketch of the fatigue testing arrangement is shown in Figure 44. Ten thousand cycles of flex were used for each loading, and the loading was increased in $\frac{1}{2}$ G increments. Table VI summarizes the progressive flexural loading of the undercarriage legs.

38

		TABLE VI	
	FATIGUE TEST RESULTS FOR LANDING GEAR STRUT		
Load (lb.)	Equivalent Stress in G's	Number of Cycles	Remarks
200	1 G	12,286	-
250	-	11,129	-
300	1.5 G	11,125	-
350	-	10,012	-
400	2 G	12,287	No visible changes in gear leg, first rubber pad worn out.
500	2.5 G	11,126	-
600	3 G	10,123	Bond failure at root of tension member, second rubber pad worn out.
700	3.5 G	10,239	Shear failure beginning at pad to compression member.
800	4 G	10,020	Separation of pad to web cloth wrap, third rubber pad worn out.
900	4.5 G	5,000	Whole pad worked loose from web and caps. Aluminum hinge on frame split.
1000	5 G	5,000	Rubber pad replaced with laminated metal and rubber pad.
1100	5.5 G	2,748	Compression member sheared away portion of pad. No damage visible in gear leg other than bonding at the hinge point. No further flexing is possible at this point due to worn-out pad.
	TOTAL	111,095	

The strut was cycled 80,000 times through a 3 G equivalent loading before any failure began to appear. At this point the cloth wrap over the joint at the pad began to split. This indicated that the web bonding to the tension cap was creeping or had separated at the hinge area. This separation continued until at 5.5 G loading the pad failed under compression at 110,000 cycles.

12.3. RUDDER PANEL

The longitudinal and directional control surfaces operating in the slipstream of the propeller would appear to be the most critical areas on the XV-11A with regard to fatigue. A copy of the rudder panel was loaded in torque to match the aircraft cruise condition, and it was subjected to intermittent loading to match propeller induced air loads. The induced air loads were determined from a wake survey of the propeller in the static condition.

To date, the test panel has been vibrated a total of 212 hours and no failure of the material or the bonding has occurred. However, it must be noted that the rudder panel has been lightly loaded and that the vibration amplitude is small, i.e., 0.063 inch, giving a 74.9-pound centrifugal force. The fiber glass seems to do an excellent job of damping the imposed vibrating loads. Careful inspection of the hinges and hinge pins on the aircraft rudder after 35 hours of flight shows no wear. If the number of blades in the propeller is changed or the propeller speed is increased, then possible vibrational and fatigue problems could arise.

12.4. VARIABLE CAMBER WING

The variable camber wing of the XV-11A presented an unusual fatigue problem, since several kinds of loading were involved and no prolonged testing of the mechanism had been previously performed. A full-scale section of the variable camber wing was constructed, and the wing was loaded to simulate the loading condition at 80 miles per hour (Figure 45).

To date the variable camber wing panel has been cycled 30,000 times with no indications of fatigue in wing skins, horn, or spars. This is equivalent to approximately 15,000 flights.

13. FEASIBILITY STUDY OF RETRACTABLE UNDERCARRIAGE

A study was made of existing retractable landing gear configurations which might be compatible with the design and STOL mission of the XV-11A aircraft. Consideration was given to weight, ruggedness, and applicability. Possible designs were examined from the retractable skid type to the more simplified three-wheel retractable system. Of particular interest was the retractable skid as used on the prototype model of the AH-1G. This design was examined with the idea of determining the practicality of a retractable skid installation on the XV-11A.

A detailed examination of the space available for retracting nose and main landing gear was made on a fuselage mock-up of the aircraft. Possible C.G. changes were examined along with changes necessary to existing structure for gear mounting. Wheel size, braking, and steering requirements were examined.

A three-wheel retracting gear was determined to be the most practical system. Space available in the fuselage would be sufficient with the possible exception of a bulge in the instrument panel cowling in the nose to allow clearance for the retracted nose wheel.

A rearward and upward retracting pair of main gears would be most practical with a maximum tire diameter of 20 inches. A modification of, or a design similar to, the Cessna "210" retractable gear would be the simplest installation (Figure 46). This is a spring steel leg which was mounted with a pivot at the base, so that retraction to the rear and upward of the complete leg was possible. Leg and wheel would lie completely retracted under the engine compartment. A new bulkhead with fore and aft bracing would be required for mounting. In addition, the existing landing gear carry-through structure should be removed to save weight.

A nose gear design of the "knee" type, where the wheel deflects to the rear and upward, was deemed most desirable for its rough field capability. This should be steerable and should retract forward to suit space and C.G. requirements. A wheel diameter of about 14 inches is maximum without fuselage bulges at the lower nose of the fuselage. The beefing up of one or more bulkheads and the addition of fore and aft load bracing members would be required for installation. The battery box and some equipment would have to be relocated, and steering controls would have to be added to the rudder controls system.

Results of the installation described above would be:

1. A net weight of approximately the same as the existing panta-base gear (220 lb.).

2. A probable retracted gear C.G. location rearward of the present location.

3. Lower rough field capability than with present gear; though, by using maximum size wheels on the rear gear, a considerable degree of this capability would be retained.

4. Lower drag gained by complete retraction of landing gear.

An alternative extension of the rough field capability of the above installation would be the use of a beefed-up fuselage bottom with small skid plates for "wheels-up" landing on extremely rough fields or plowed ground, etc.

14. CONCLUDING REMARKS

The XV-11A aircraft has flown a total of 49 flights with no serious problems due to structure, power, or control systems.

The relative ease of fabricating complicated compound curvatures free of any joints or protuberances by the use of fiber glass has been successfully demonstrated in the XV-11A aircraft. An illustration of the success in contouring and smoothness is seen by the minimum shaft horsepower required to fly at 80 miles per hour. This was found to be 30.1 horsepower, notwithstanding the large fixed undercarriage on the aircraft.

The structure of the XV-11A was designed around the use of polyester fiber glass reinforced resin. These techniques were not well known a number of years ago, and the result of this has been that the structural weight of the vehicle is heavy in comparison to an equivalent metal aircraft. However, with the techniques of today, when the components would be optimized for epoxy fiber glass construction, considerable weight savings would be obtained.

The static thrust of the shrouded propeller was lower than anticipated because of the inability of the existing propeller to use the existing horsepower efficiently. A new propeller configuration shall be designed when further shrouded propeller flow measurements have been made.

The stability and control characteristics of the XV-11A are acceptable except in the STOL landing mode with camber when undesirable lateral/directional oscillations occur in turbulent air. These oscillations are due to the inability of the boundary layer control system to suppress separation at high camber settings.

The handling qualities of the XV-11A are adequate for the mission of the vehicle; however, stall warning is less than adequate even though the stalls are mild with no wing dropping.

The use of reverse propeller thrust for glide path control and to increase the rates of sink of the XV-11A was successfully demonstrated on all 49 flights. The longitudinal and directional control power was decreased by using this technique; however, the drag increment of the propeller at the rear of the vehicle was stabilizing and the control power was still considered to be acceptable.

Aerodynamic measurements of the wing internal pressures, inflow velocity distributions, wing porosity characteristics, and engine compressor characteristics show a mismatch of the boundary layer control requirements and the engine airflow requirements. This condition dictates the use of an auxiliary blower to provide boundary layer control

suction power both for takeoff and landing irrespective of the power output of the main engine. Such a blower could easily be driven from the normal aircraft power takeoff pad on the T-63 engine and could be operated at high settings both at takeoff and landing. Modifications to the wing may be necessary to satisfy suction velocity criteria and the assumption of an evenly porous wing surface.

Boundary layer measurements on top of the fuselage indicated that this would be an acceptable position for a flush-mounted air intake for the T-63 if an auxiliary blower for the boundary layer control is used.

No separation flow was found on the XV-11A in the cruise or in the high-lift condition except on the wings prior to stall.

Radar reflectivity measurements on the XV-11A show that although the radar cross section is less than that of a metal aircraft of equivalent size, it is still a good radar target because of the propeller and the engine. It is felt that this radar cross section could be considerably reduced by a fiber glass propeller and by radar absorbing devices around the engine.

The fatigue strength of the fiber glass components of the XV-11A aircraft has been found to be high, with the undercarriage being capable of taking 110,000 landings at 5.5 G loading before failure.

It is felt that a retractable undercarriage could be designed for the XV-11A, with the use of a conventional tricycle gear, with no increase in aircraft empty weight; however, there would be a reduction in rough field capability.

Figure 1. XV-11A Research Aircraft.

45
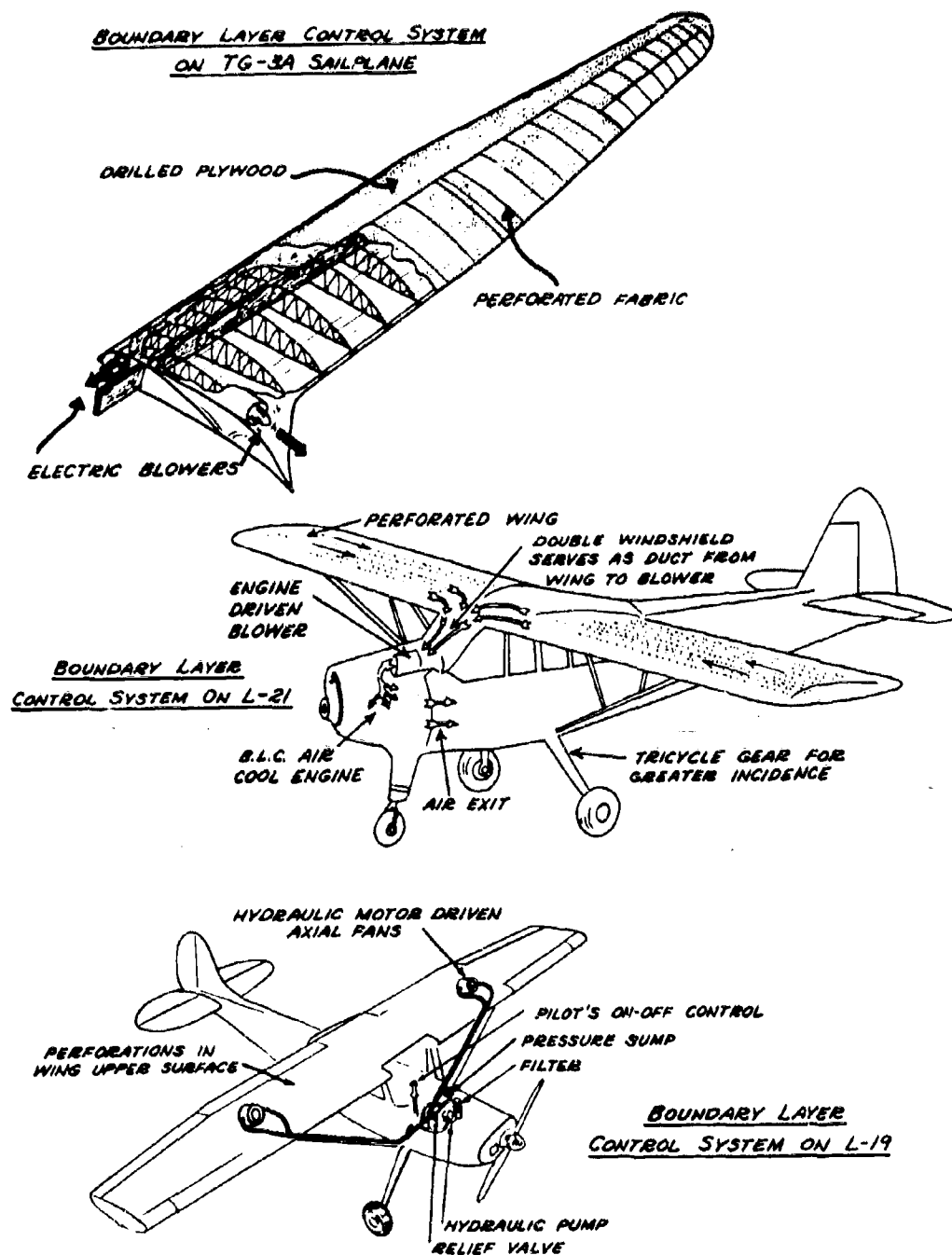
Figure 2. Schematics of Aircraft Used in the High-Lift Research Program.
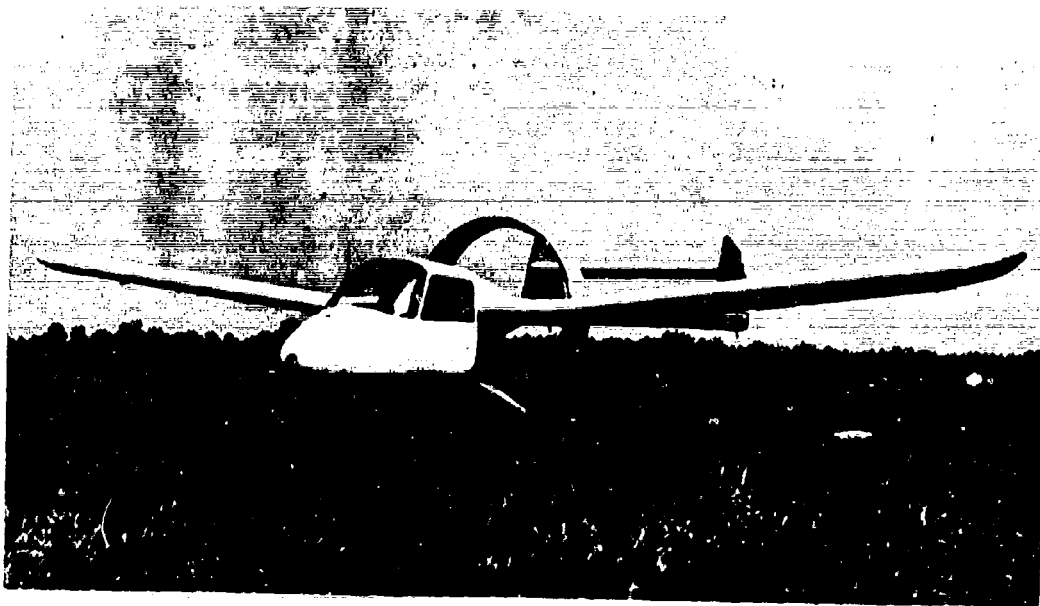
AG-14 Aircraft With Shrouded Propeller.
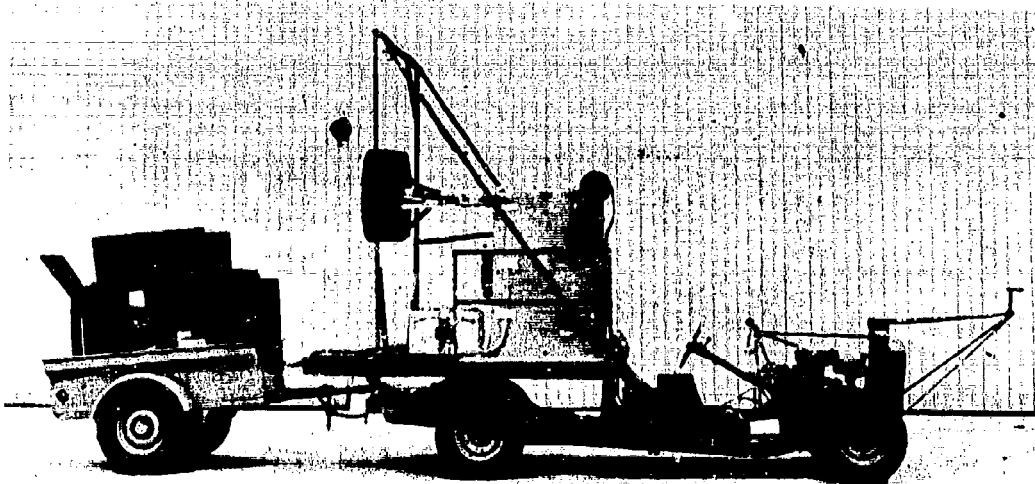
Shrouded Propeller Test Stand.

Figure 3. Shrouded Propeller Research.

47
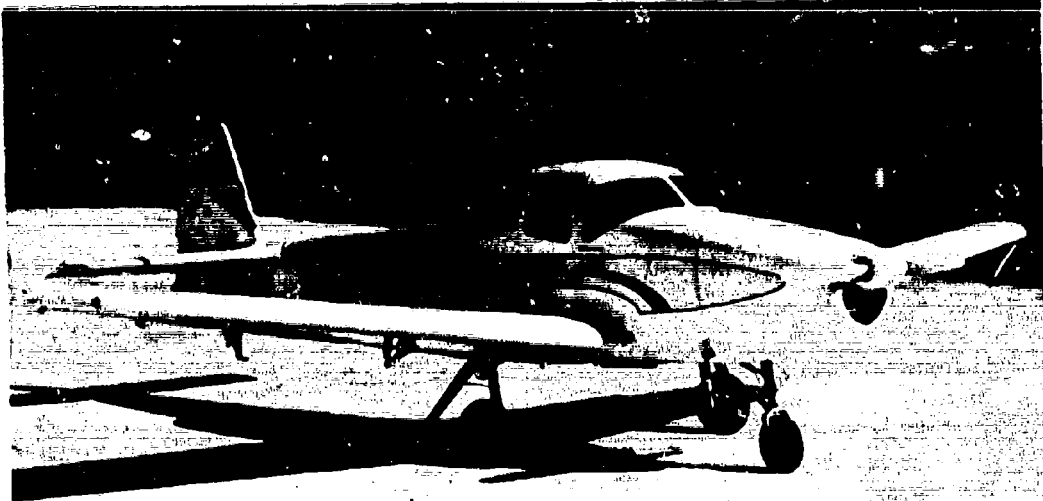
Navion L-17.
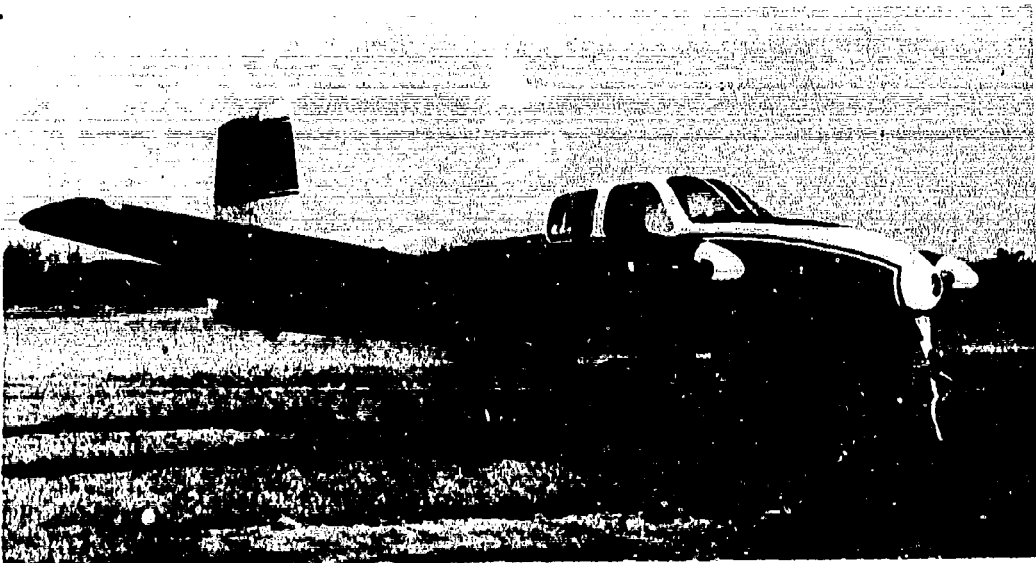
Beechcraft L-23.

Figure 4. Aircraft Used in Geometric Boundary Layer
Control Studies for Low Drag.
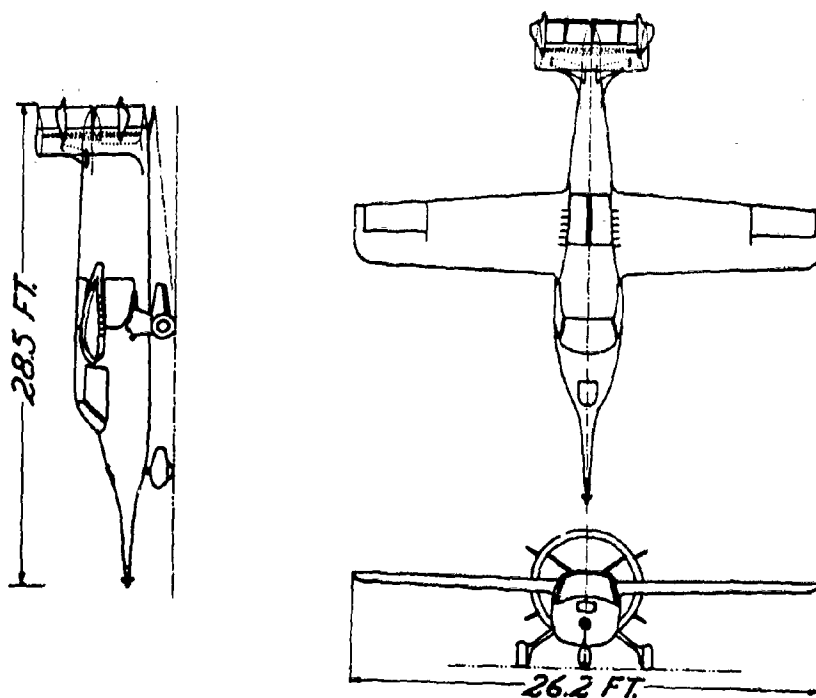
Figure 5. XAZ-1 Research Aircraft.
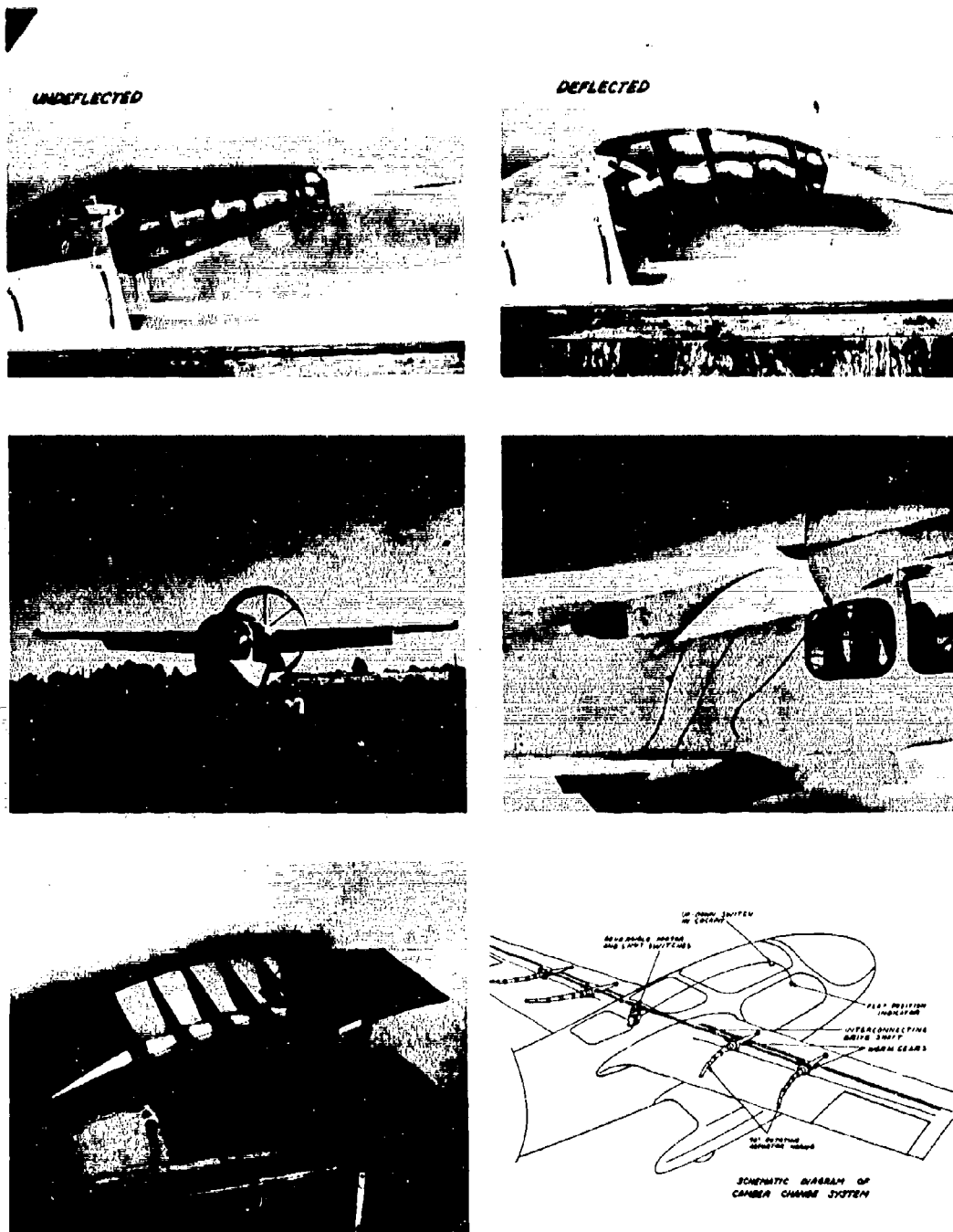
Figure 6. Variable Camber Wing on XV-11A.

ENGINE COMP'T.

MIXED EXHAUST

OIL COOLER

RAM AIR

COOLING AIR

ENGINE EXHAUST

ENGINE COMP'T.
HOT AIR EXHAUST
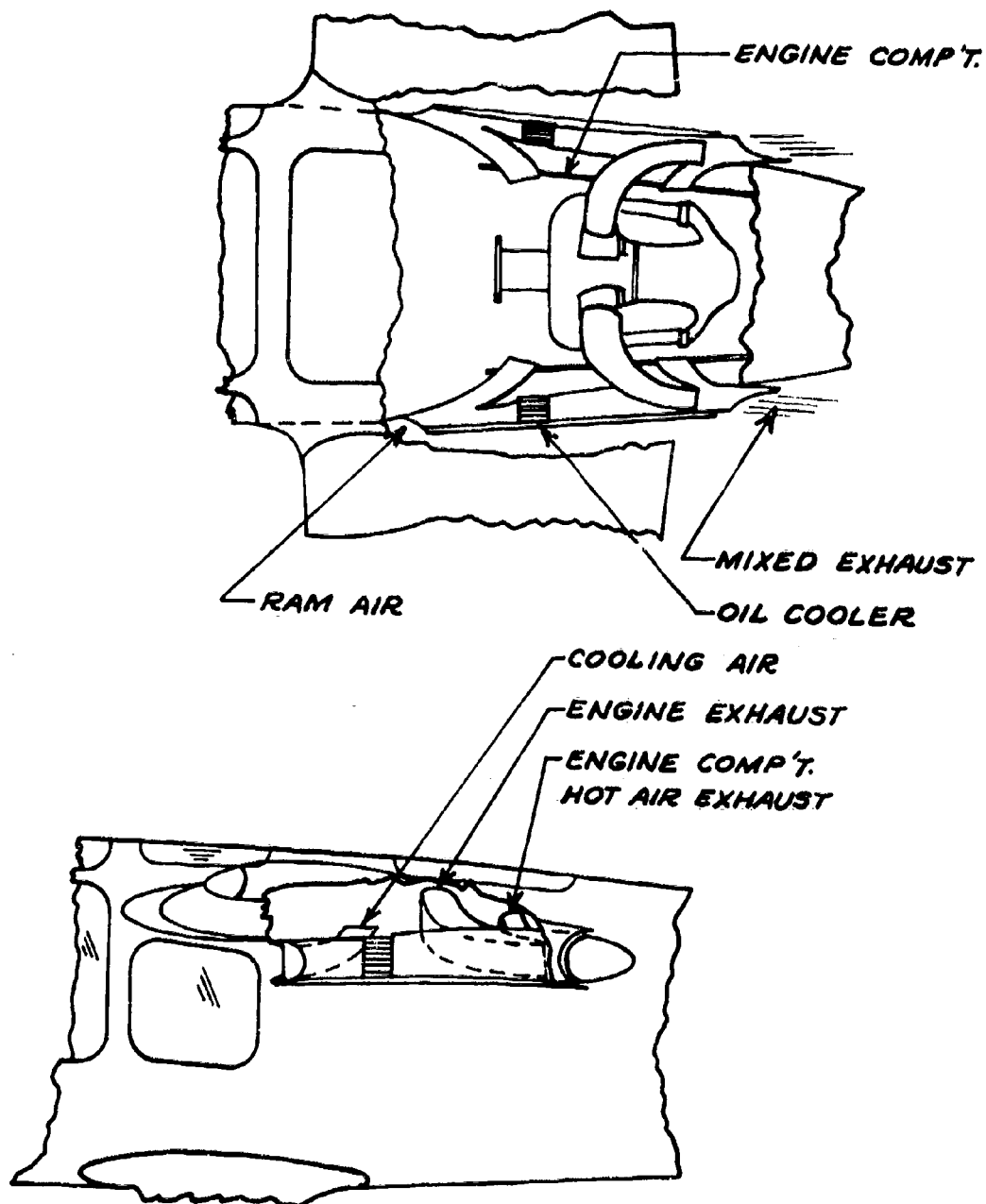
Figure 7. Oil and Engine Cooling System.
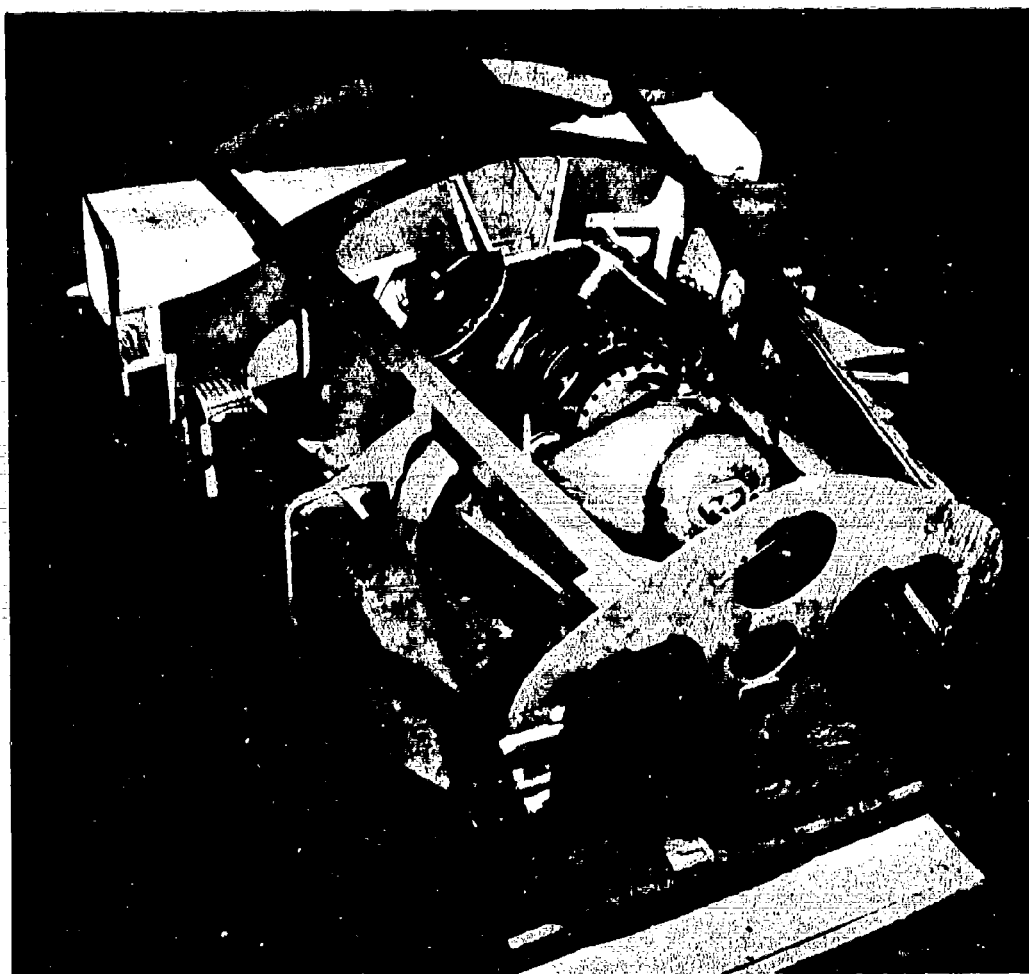
Figure 8. Engine Installation in Fuselage Mock-Up.

a. Propeller Shaft and Fiber Glass Housing.
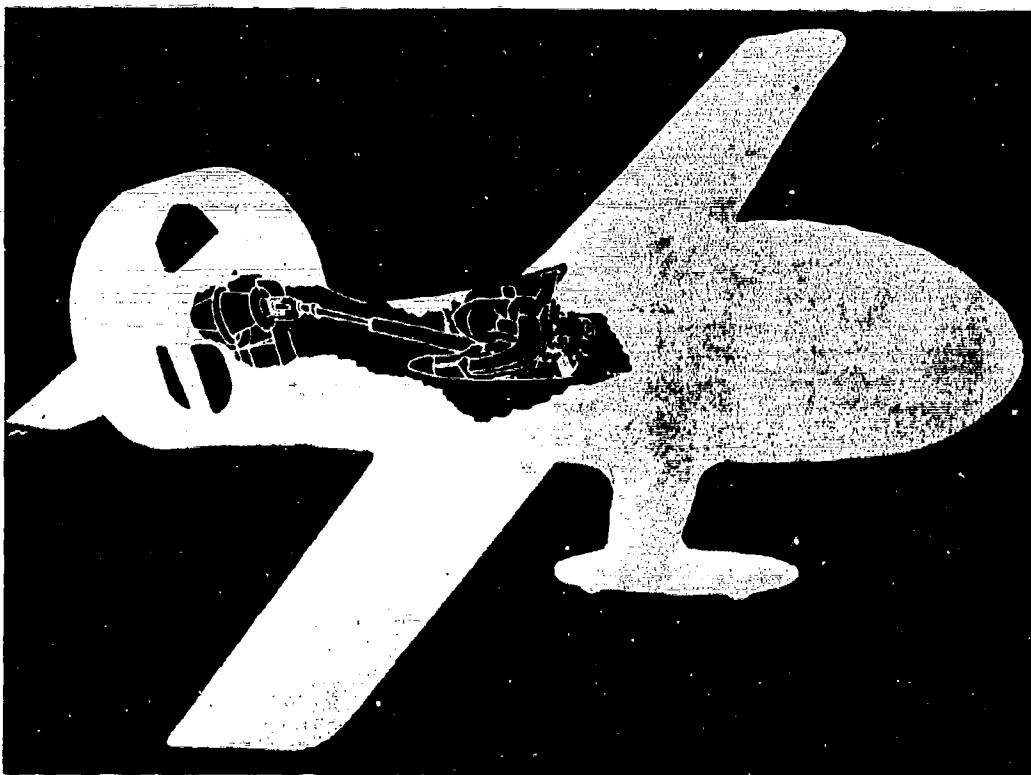
b. Shaft Installation in Aircraft.

Figure 9. Propeller Drive Shaft.

EMERGENCY VALVE

ENGINE
EXHAUST

COMPRESSOR
AIR DIVIDER
WING CARRY-THRU
SPAR
WING AIRFLOW

INTAKE DUCT   TURBINE ENGINE

INTAKE DUCT
AT COMPRESSOR
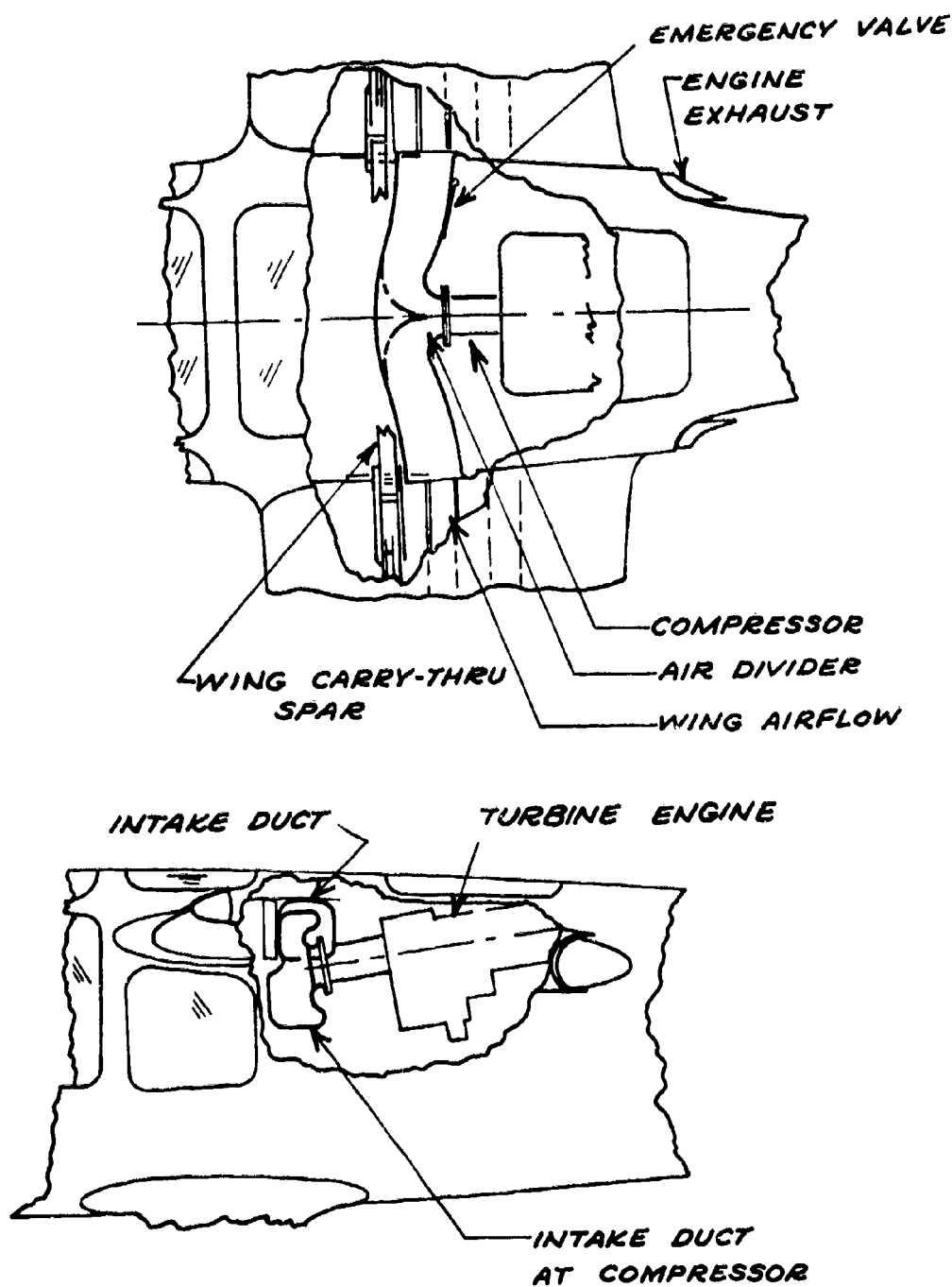
Figure 10. Diagram of the Boundary Layer Suction Source System.

54
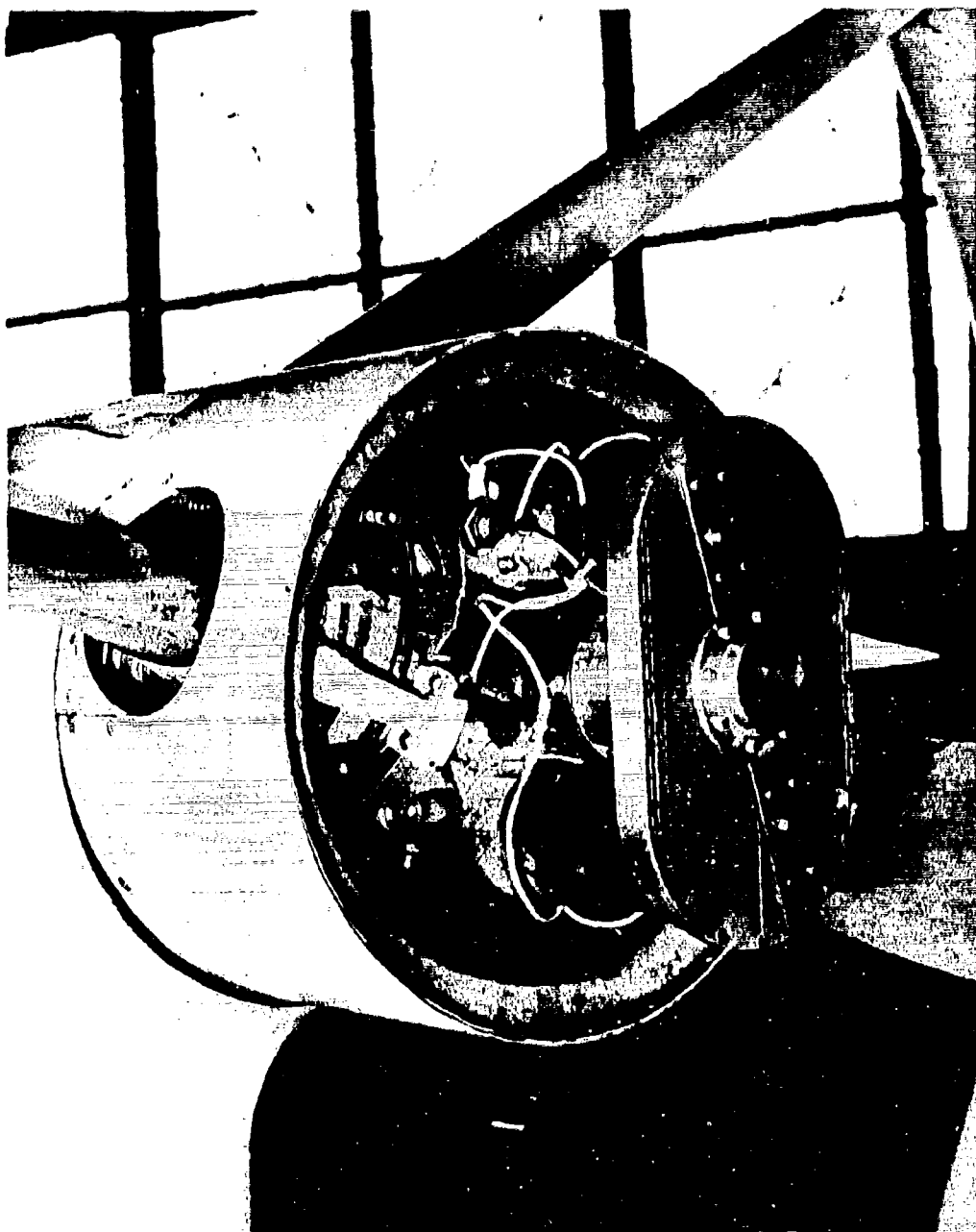
Figure 11. Propeller With Aerophysics' Electrical Pitch
Change Mechanism.
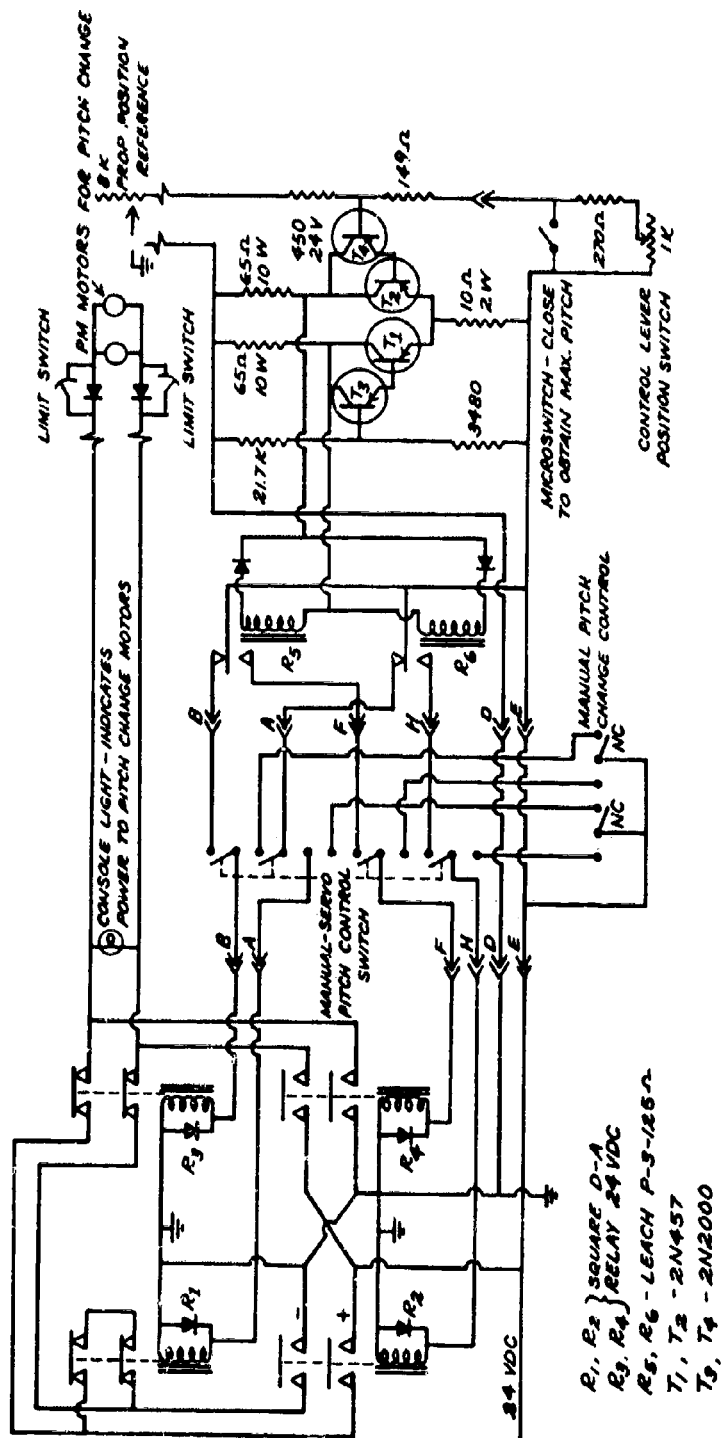
Figure 12. Circuit Diagram for the Propeller Pitch Change Mechanism.
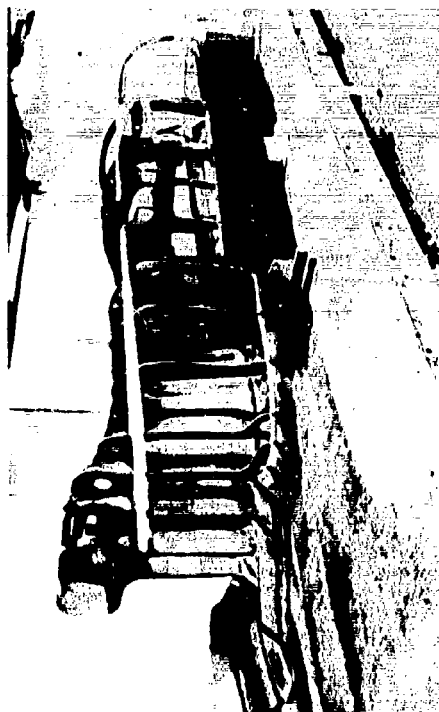
Figure 13. Views of the Aircraft Under Construction.
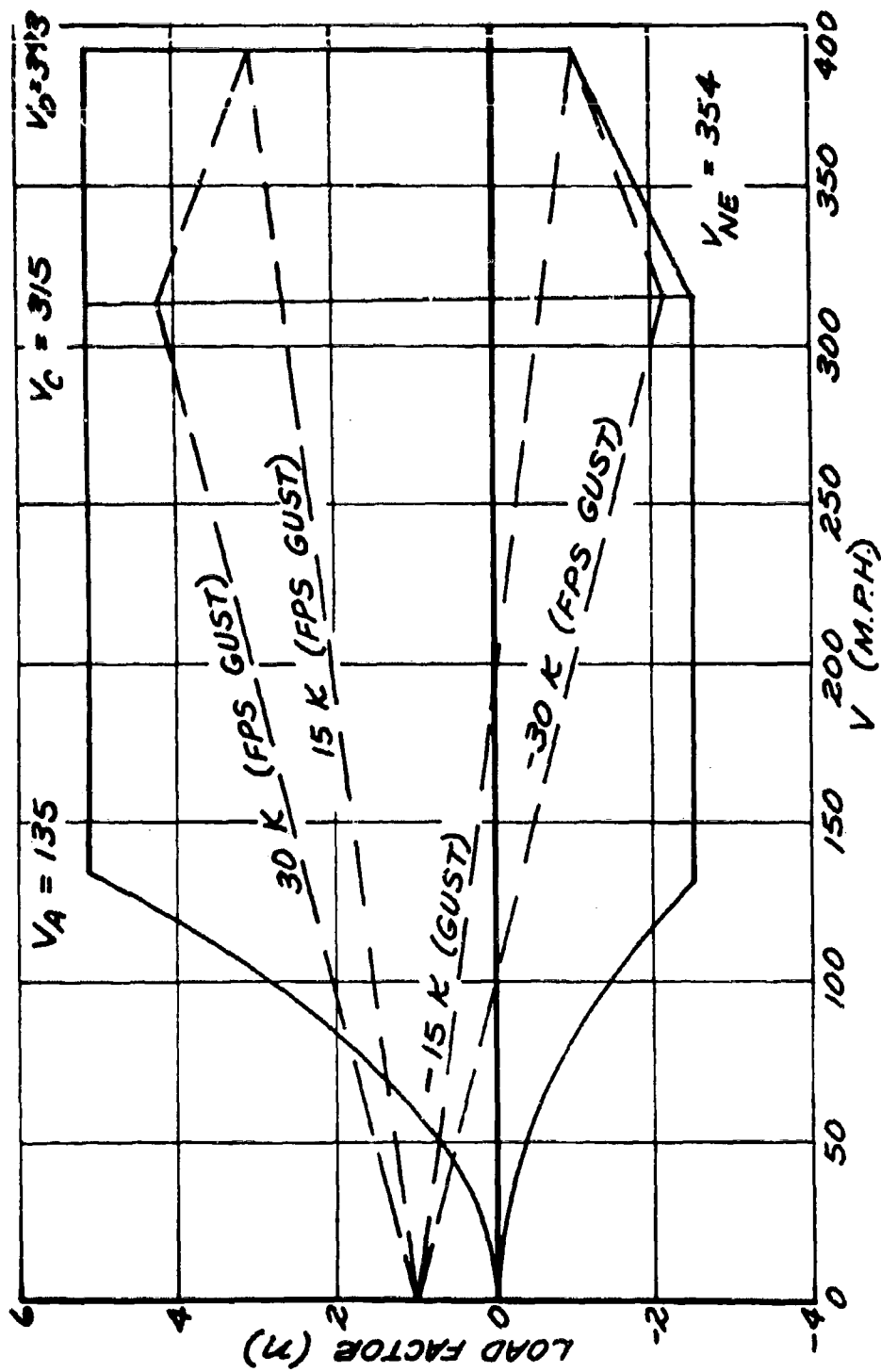
Figure 14. Flight Envelope of XV-11A Modified for a Weight of 2600 Pounds.
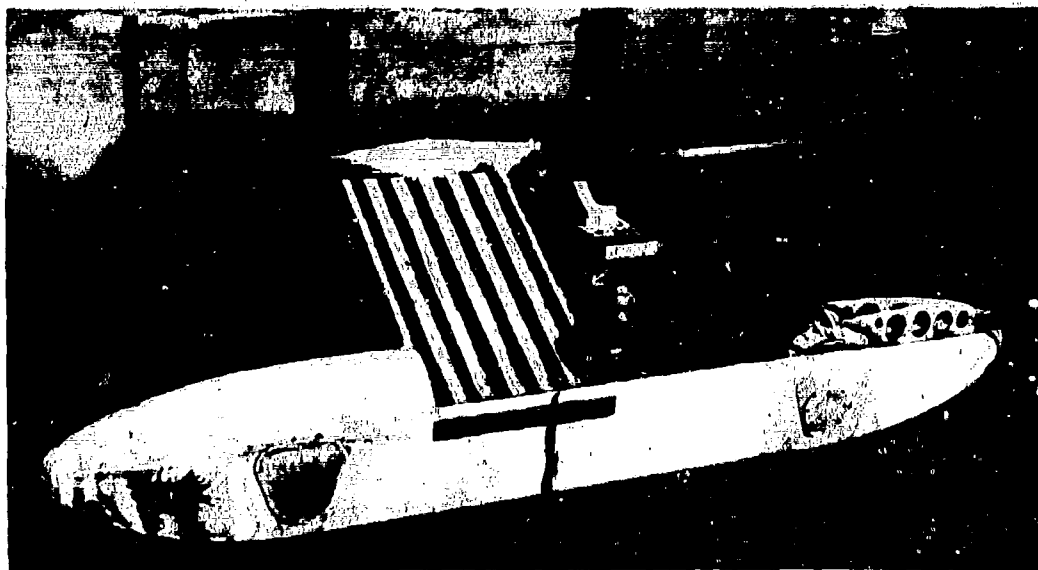
Figure 15.   Landing Gear Assembly.

59
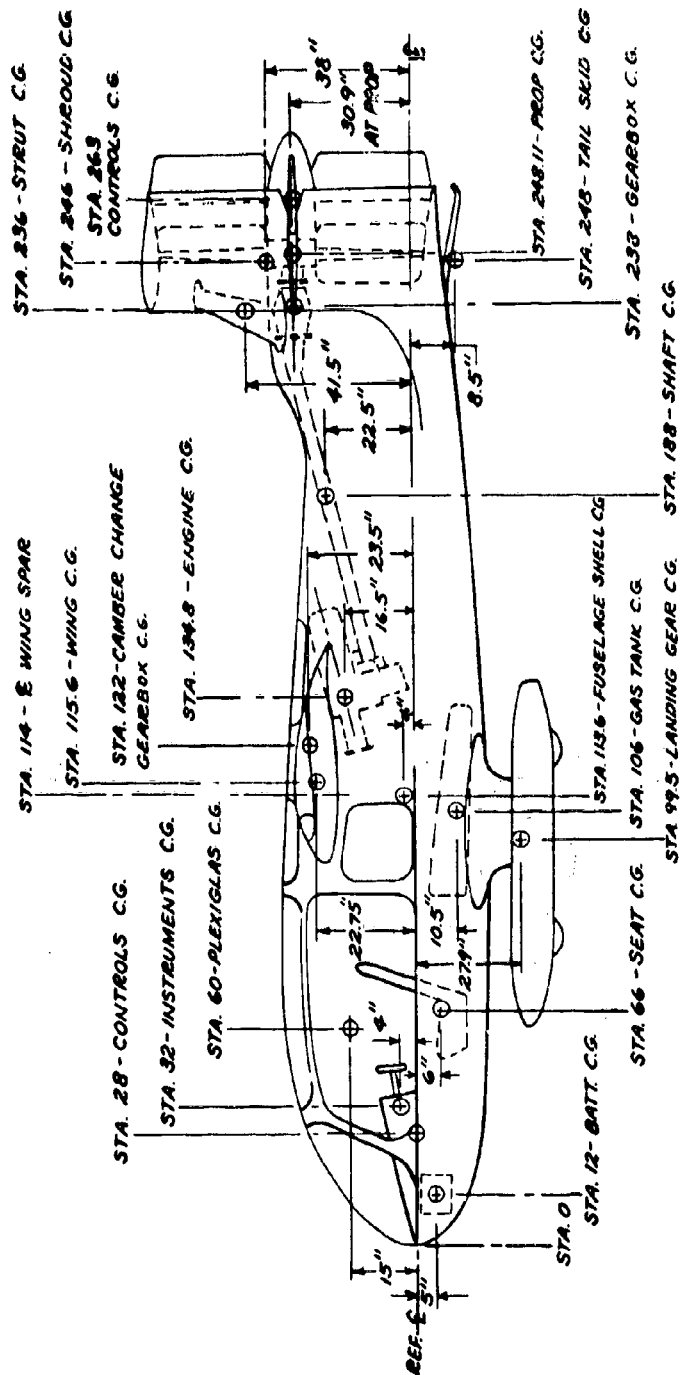
Figure 16. XV-11A Component C.G. Locations.

60

Figure 17. Bifilar Suspension for Determination of
the Moment of Inertia in Yaw.

Figure 18. Suspension Frame for Pitch and Roll
Moment of Inertia Measurements.

61
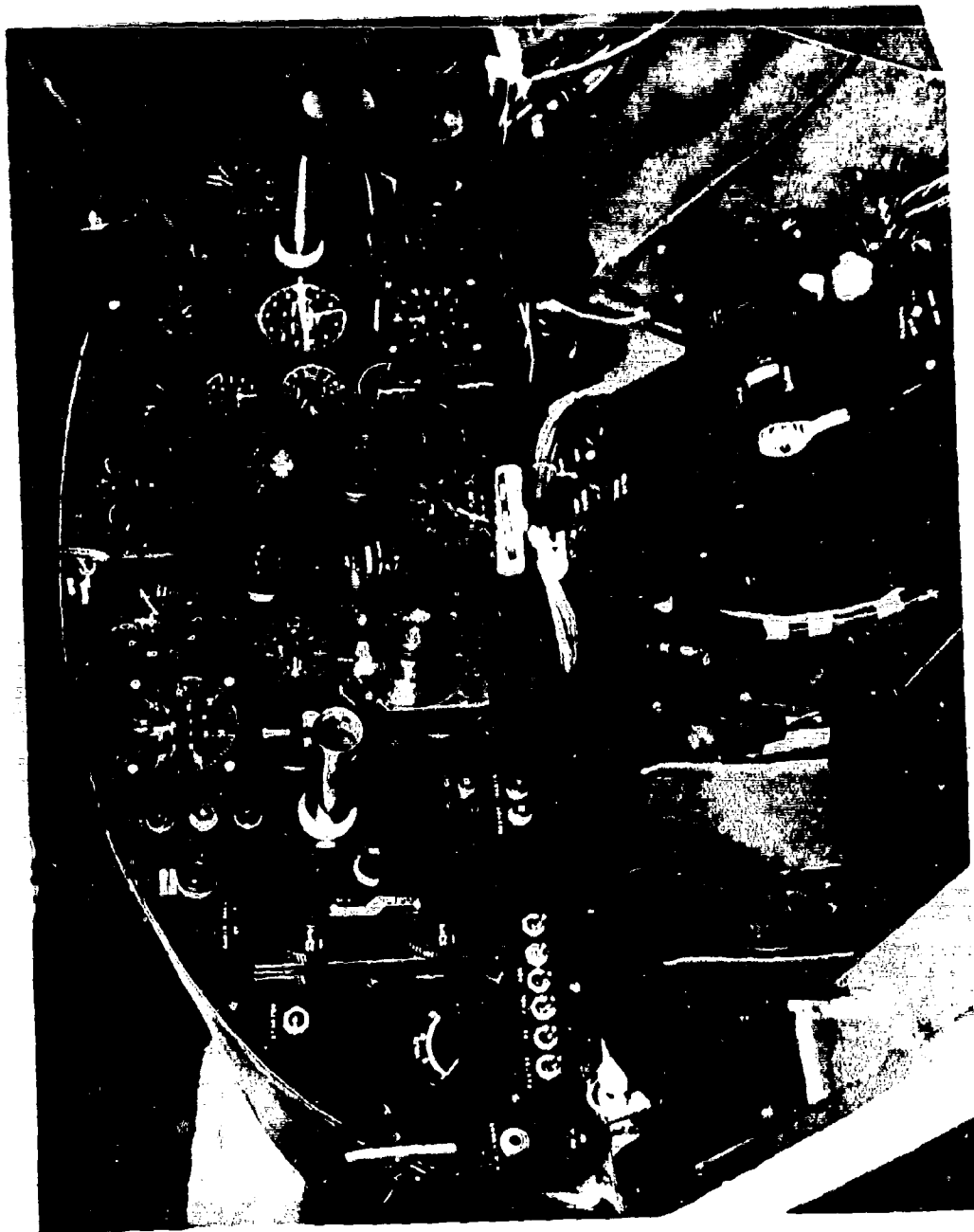
Figure 19. Panel of the XV-11A Aircraft.
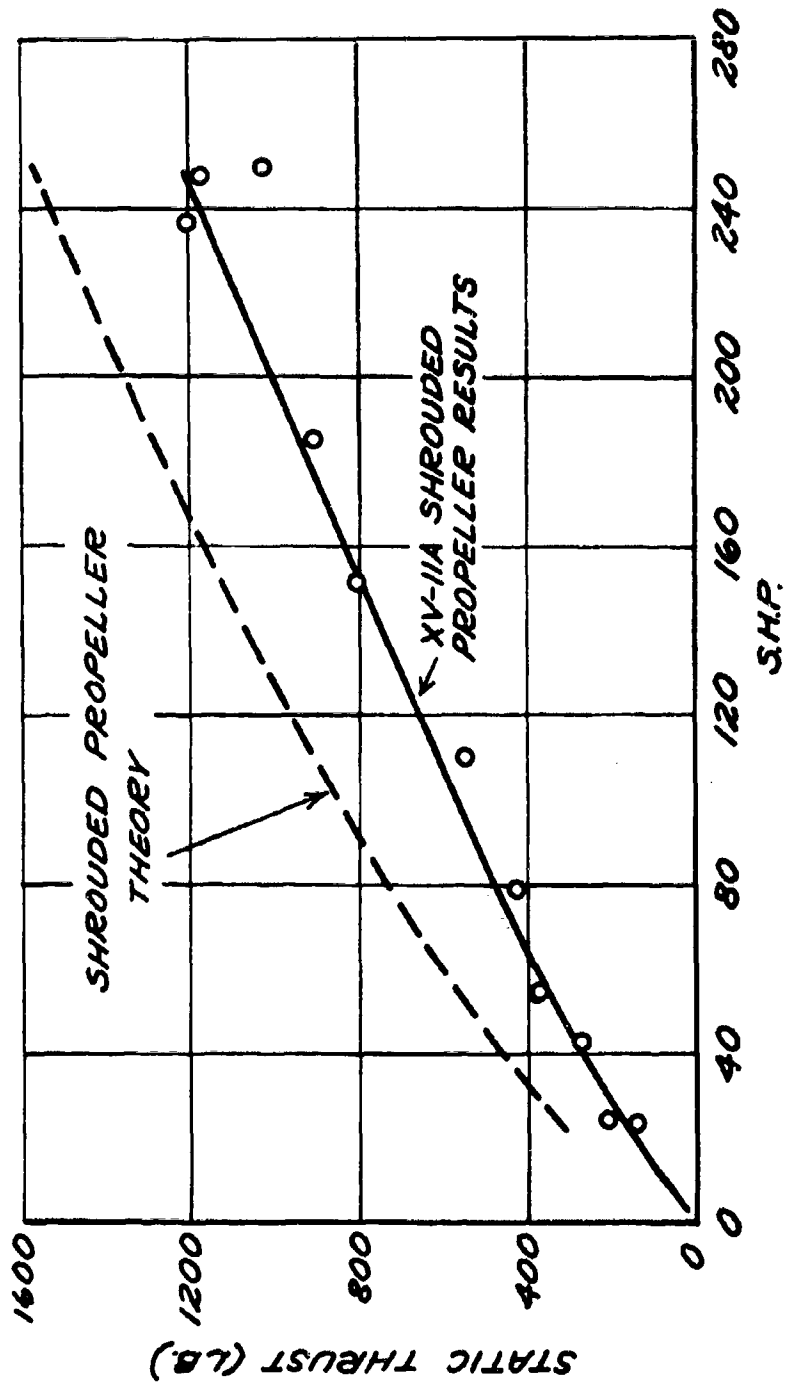
Figure 20. Static Thrust Results.
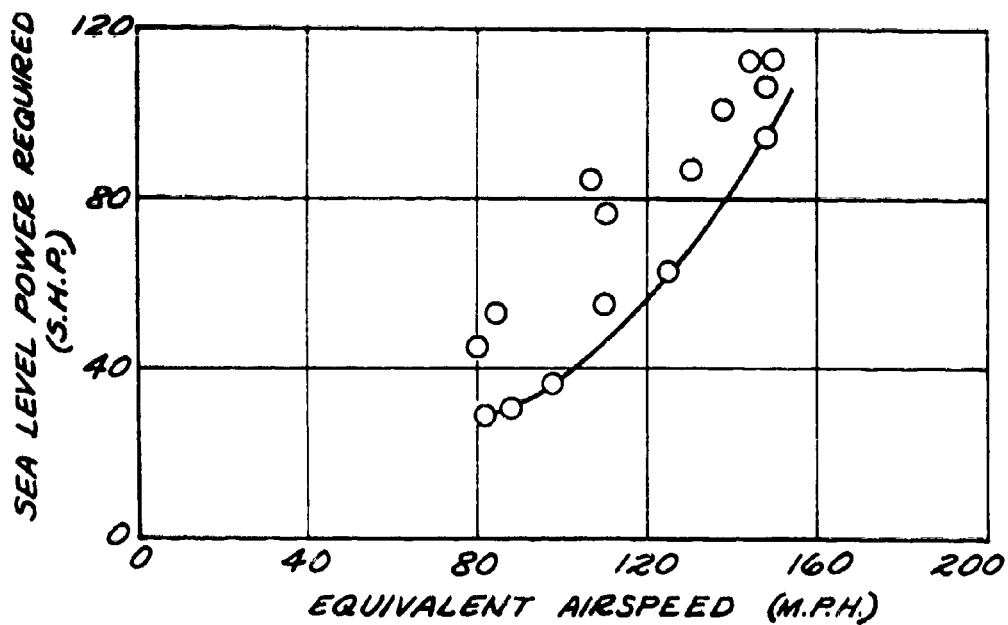
Figure 21. Power Required for Level Flight.
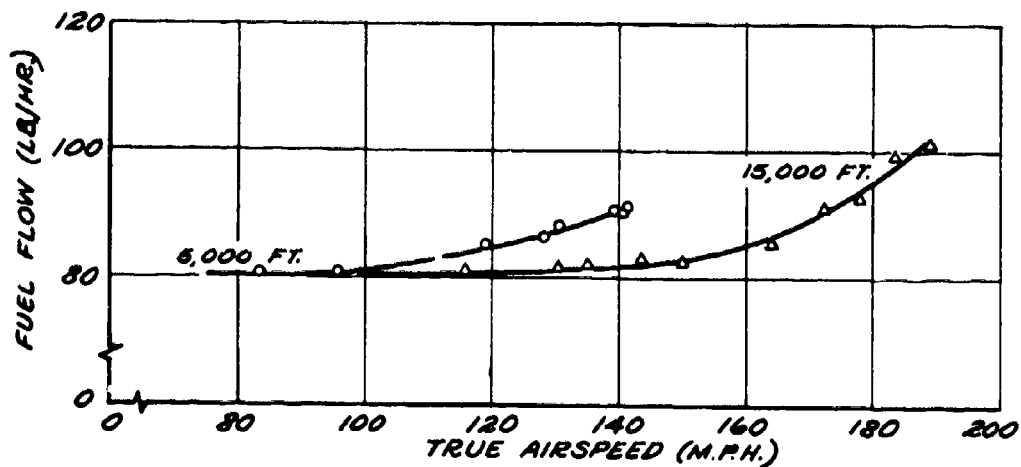
Figure 22. Level Flight Fuel Curves.

64
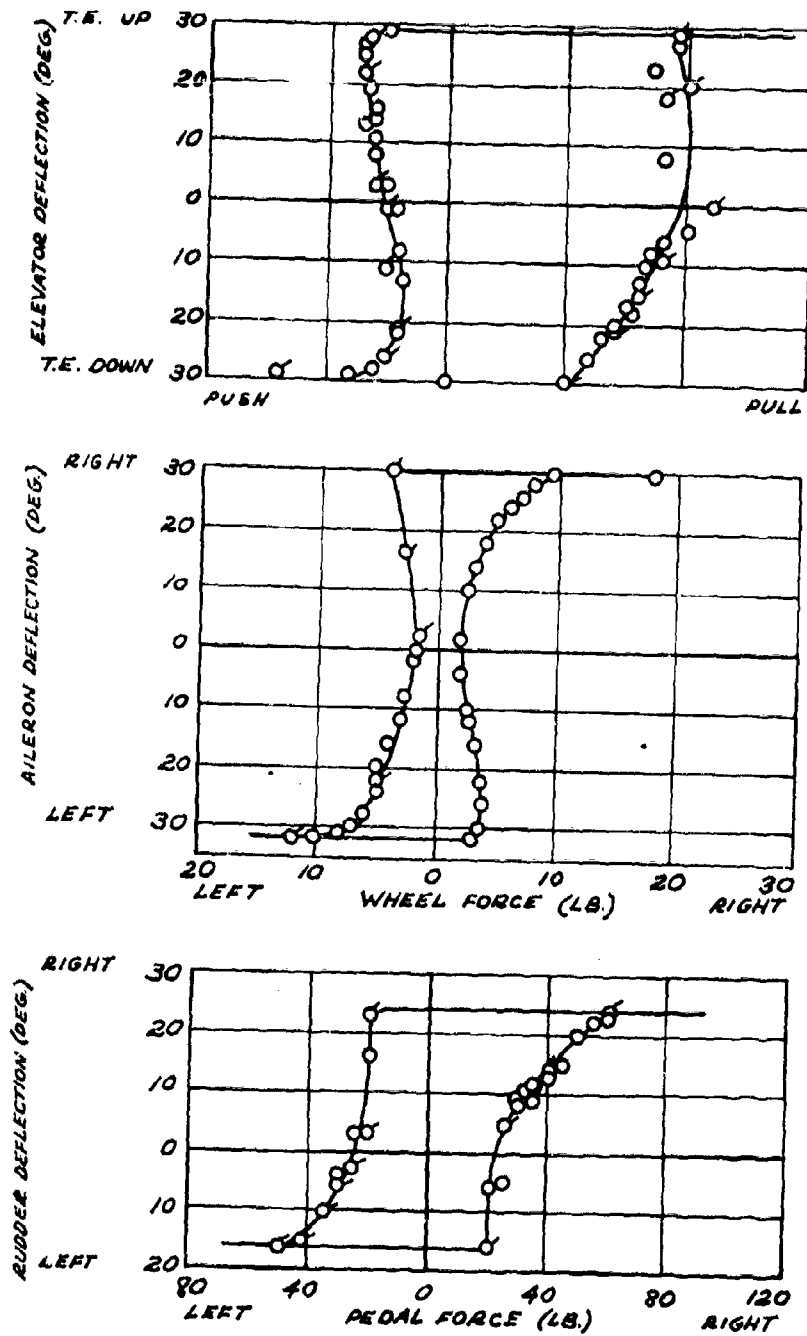
Figure 23.   Static Control System Characteristics.
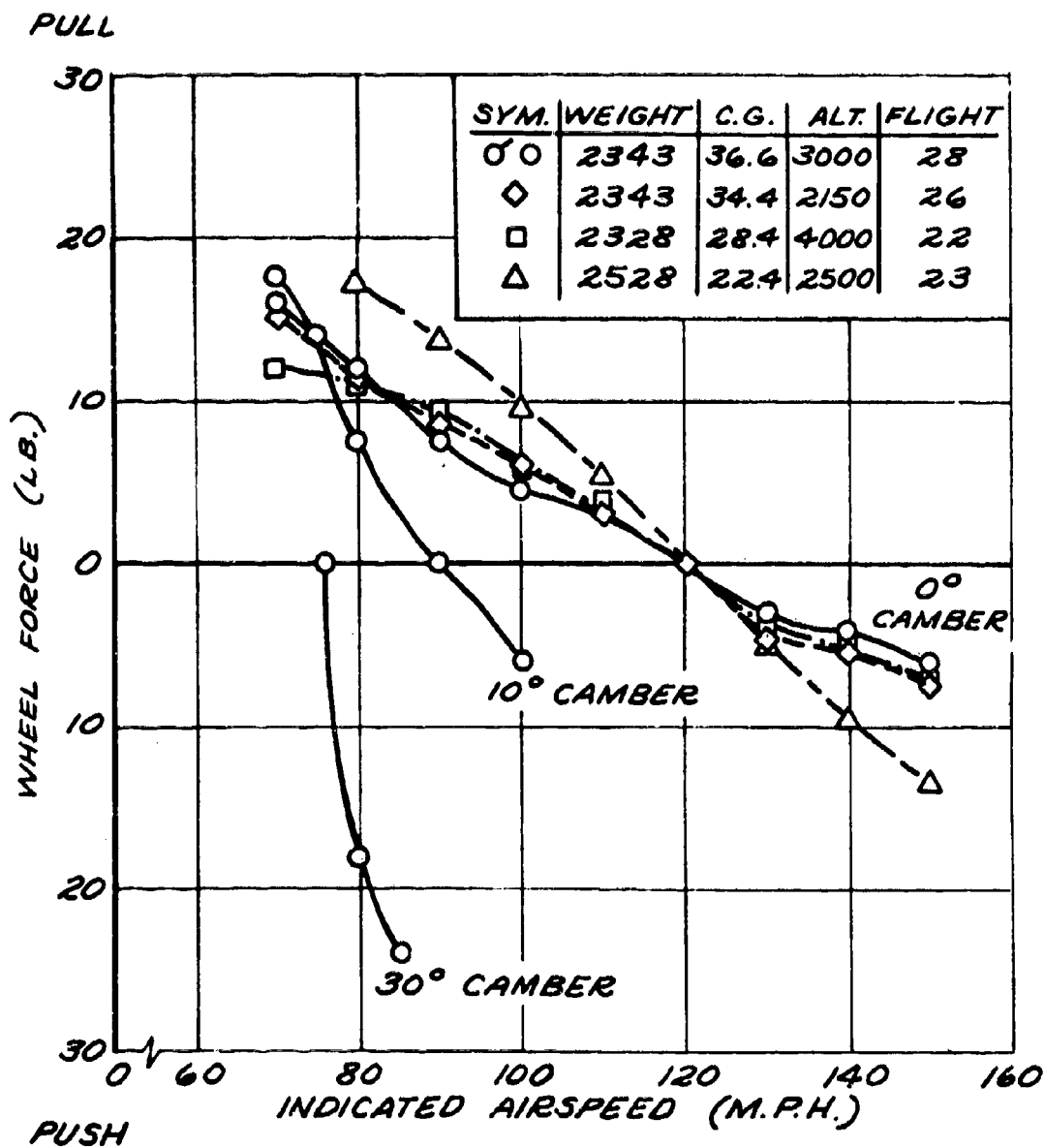
Figure 24. Wheel Force Required to Trim.
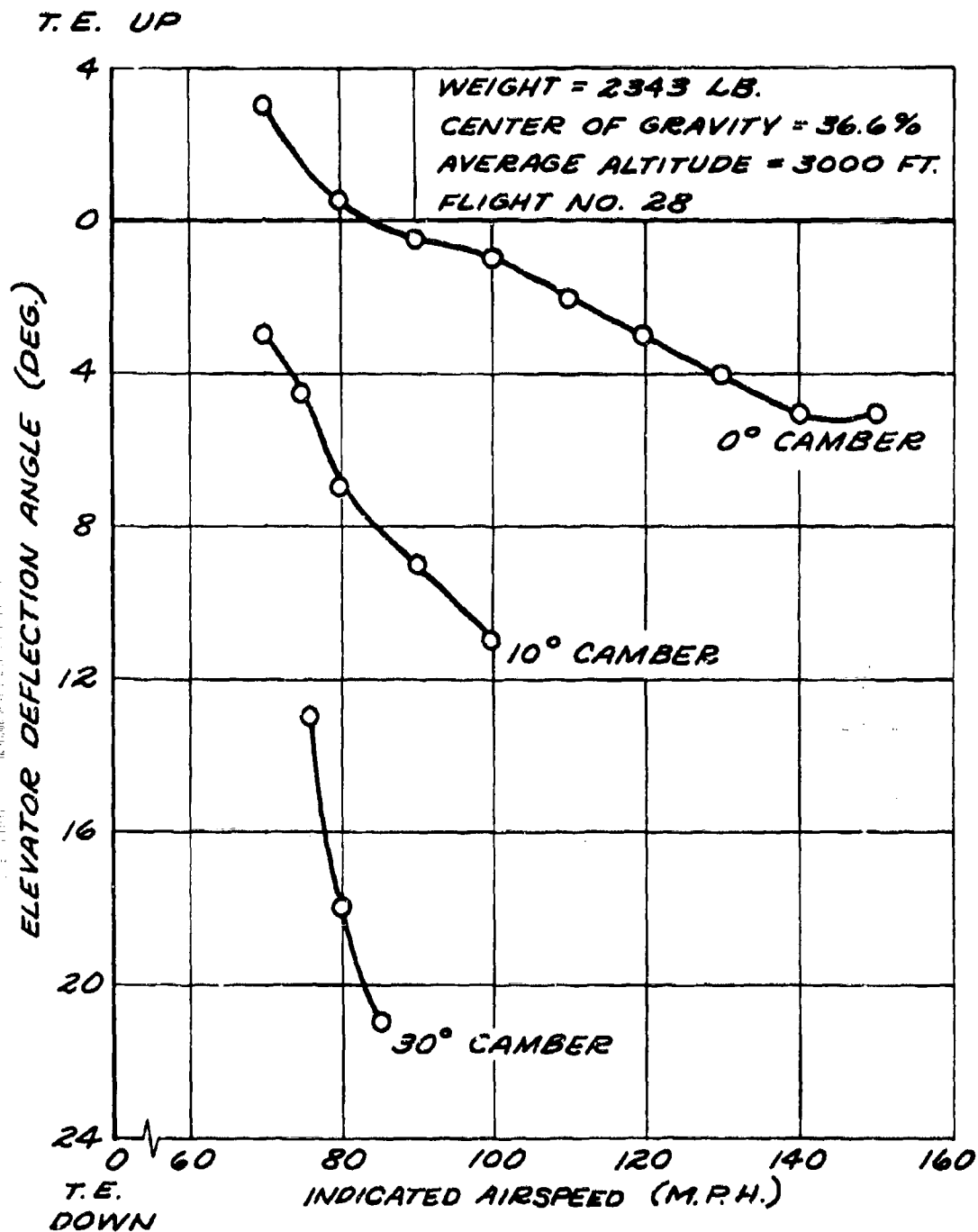
Figure 25. Elevator Required to Trim.
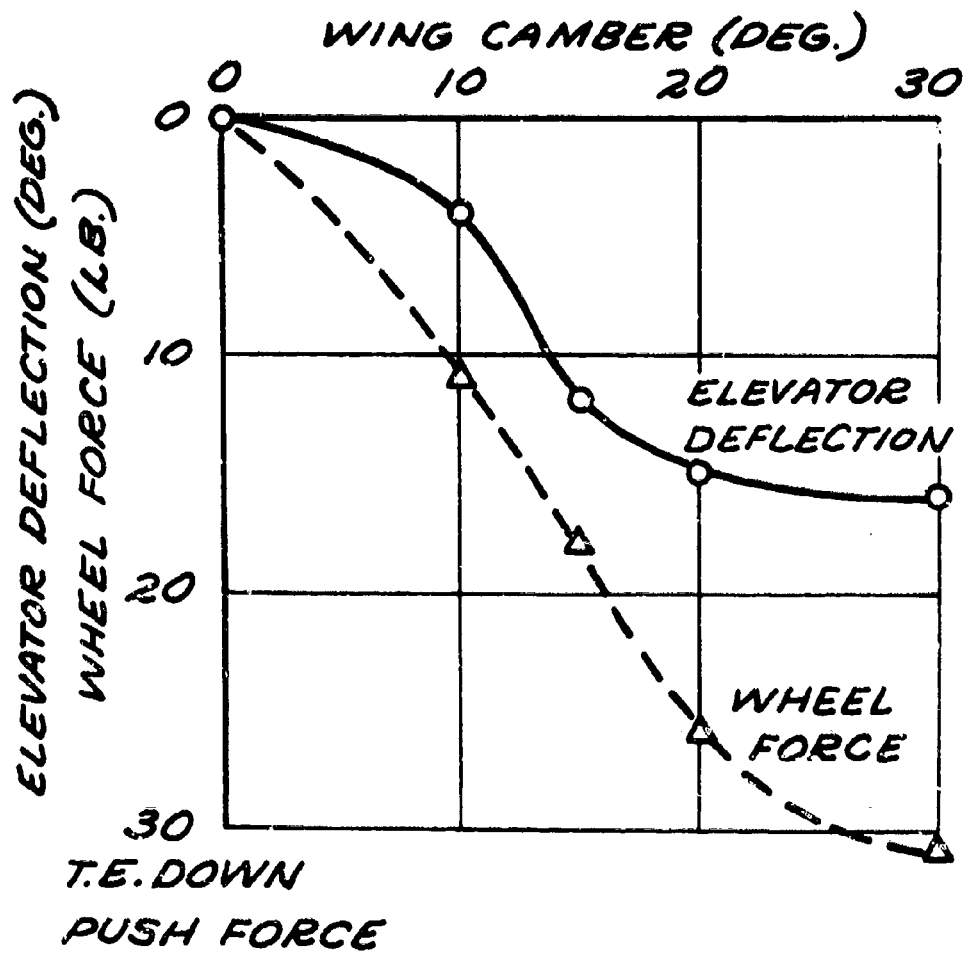
Figure 26. Trim Change Due to Wing Camber Change.
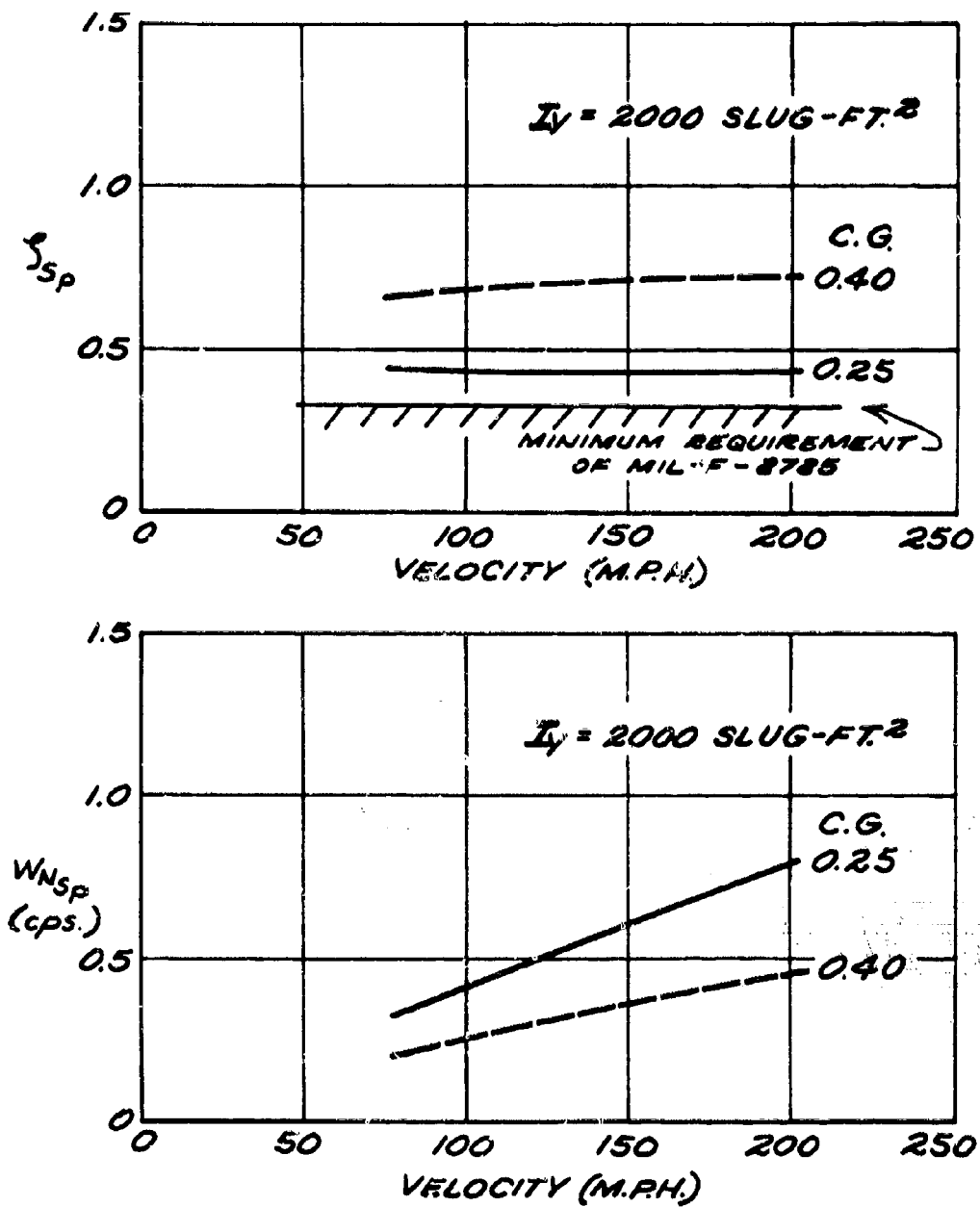
Figure 27. Short Period Frequency and Damping Characteristics.
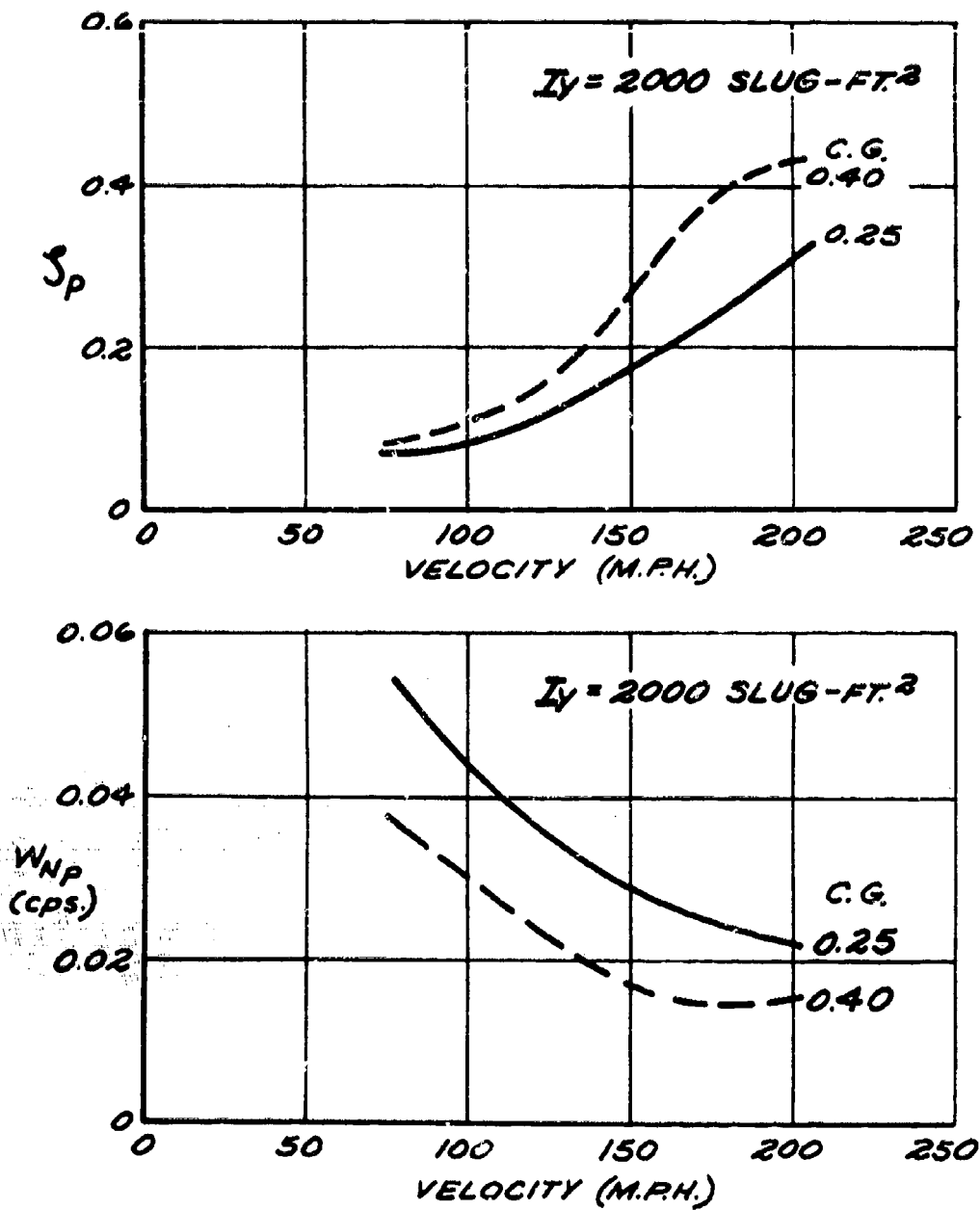
Figure 28. Phugoid Frequency and Damping Characteristics.
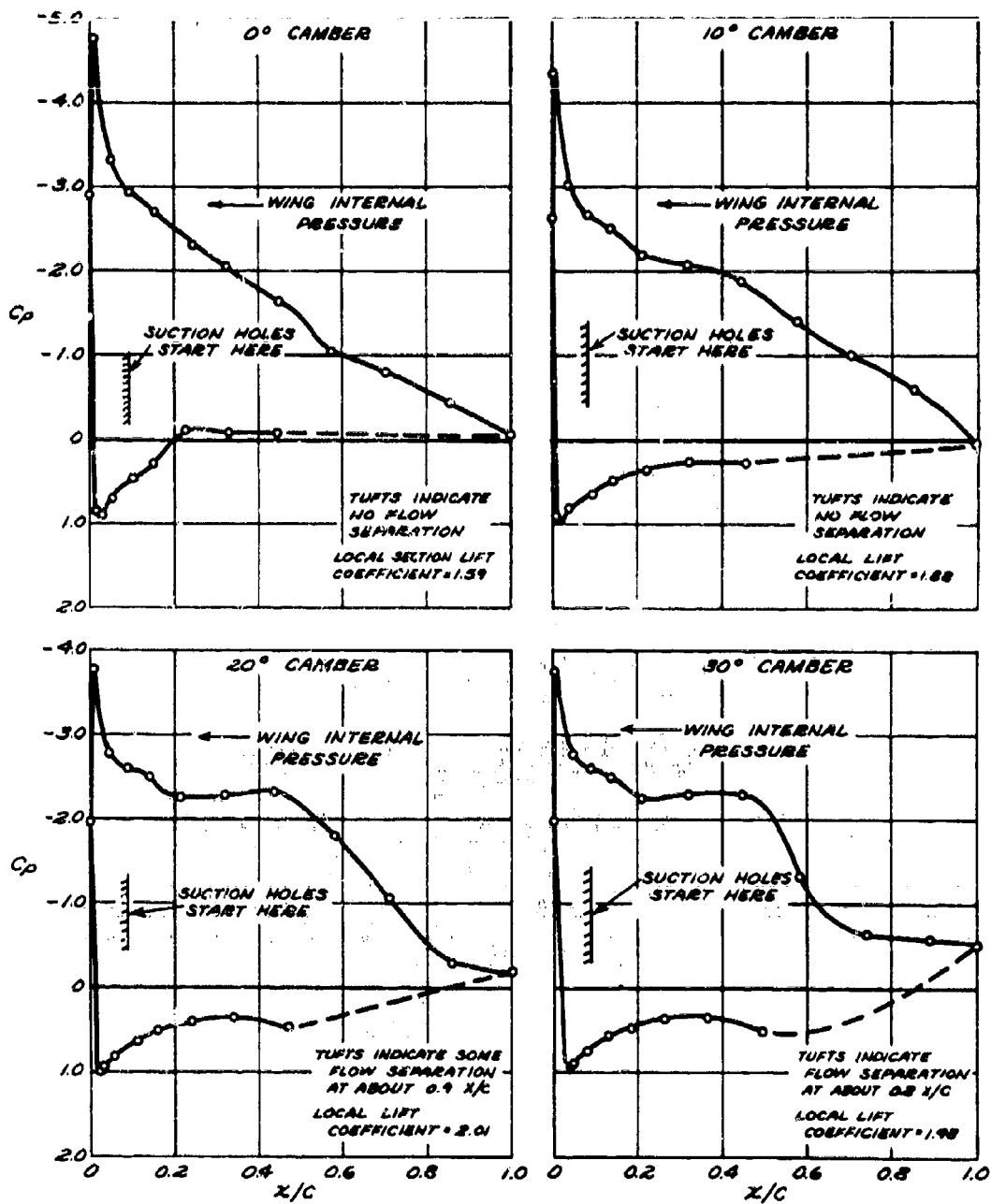
Figure 29. Wing Pressure Distributions Measured on XV-11A.

71
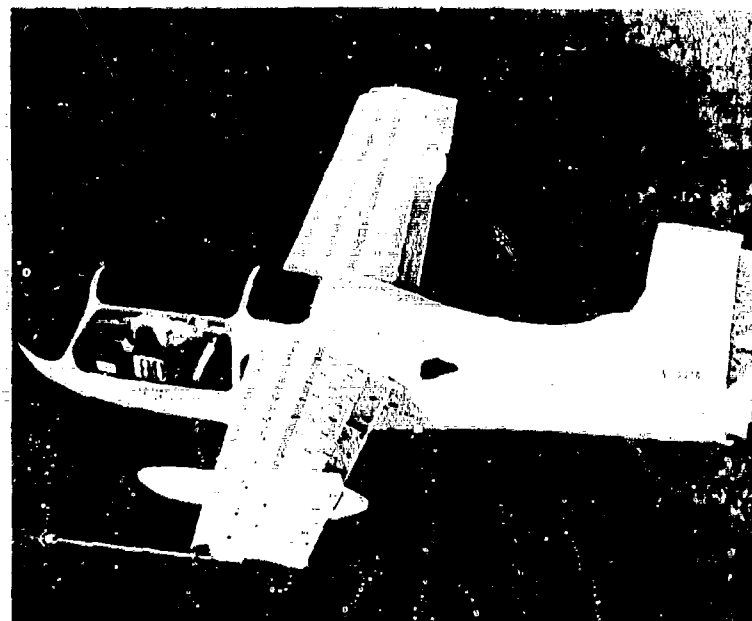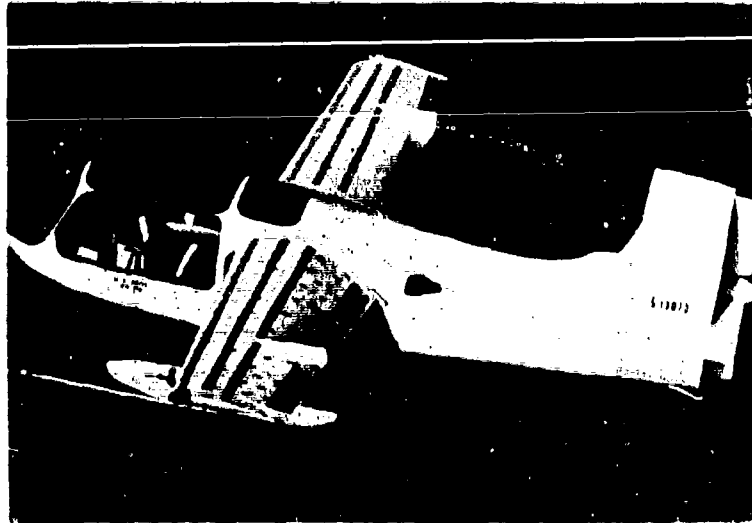
Figure 30. Aircraft Tuft Pictures, 30-Degree Camber.
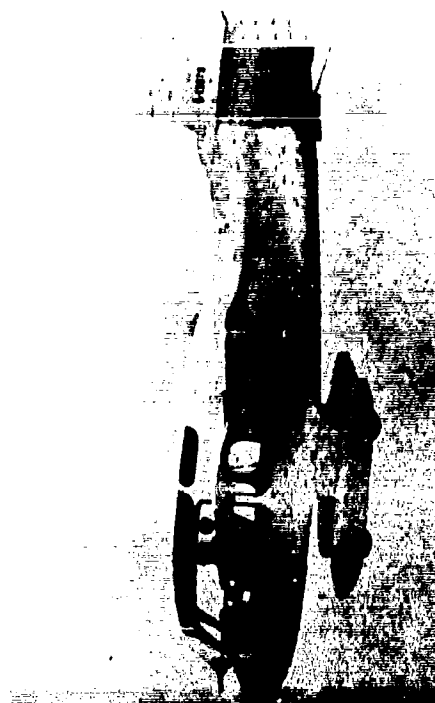
Figure 31. Aircraft Tuft Pictures, Cruise Configuration.

73
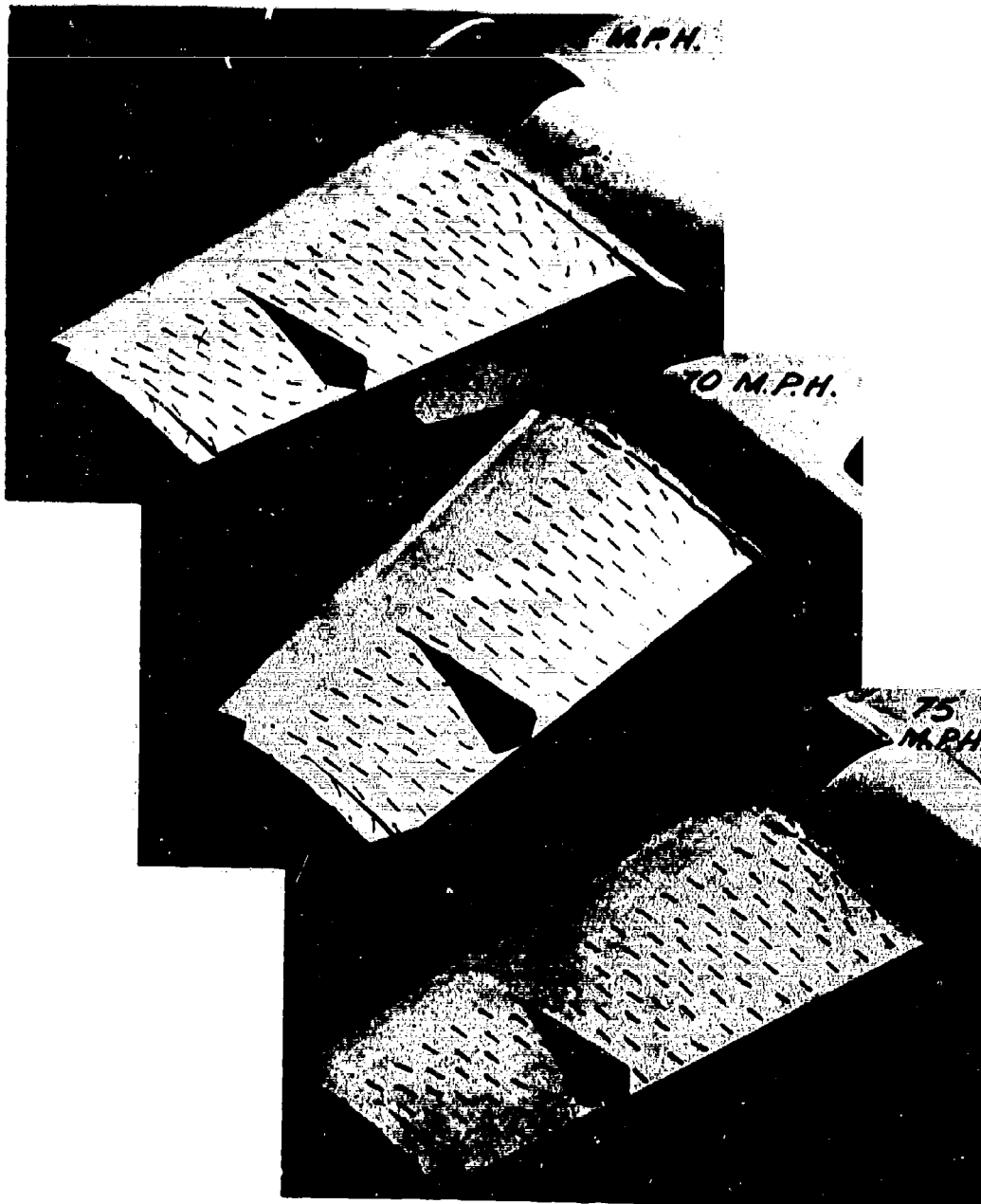
Figure 32. Wing Tuft Pictures, 0-Degree Camber.
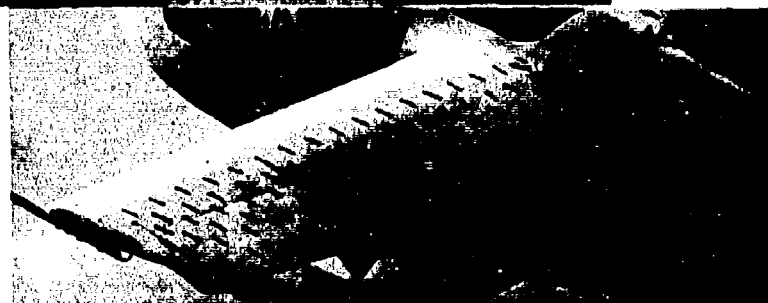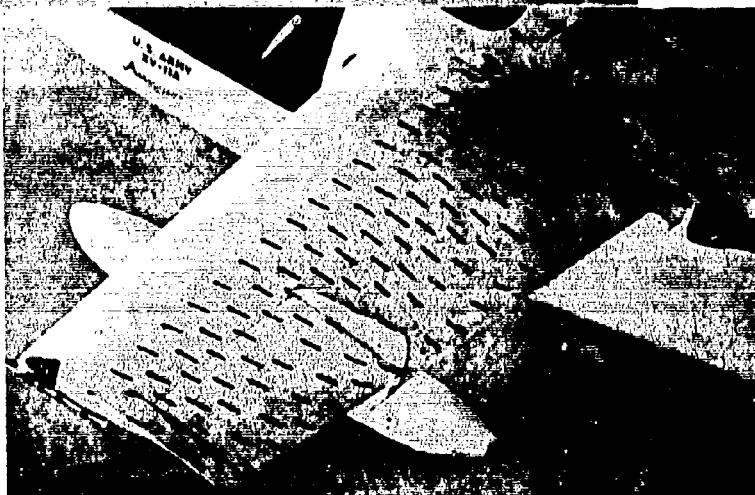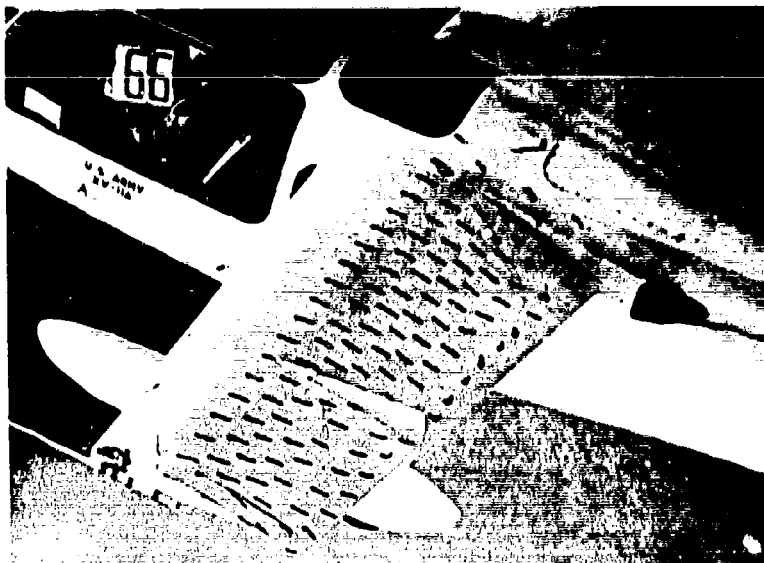
Figure 33. Wing Tuft Pictures, 10-Degree Camber.
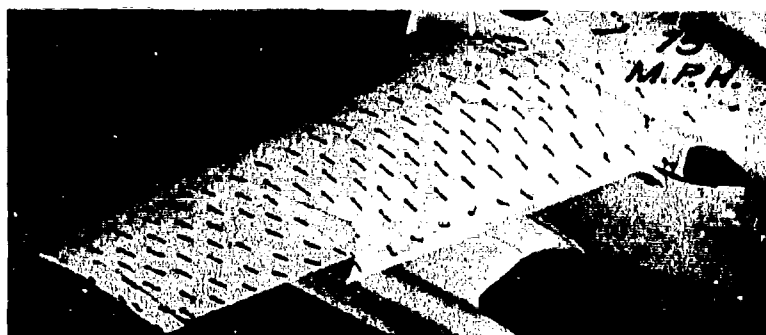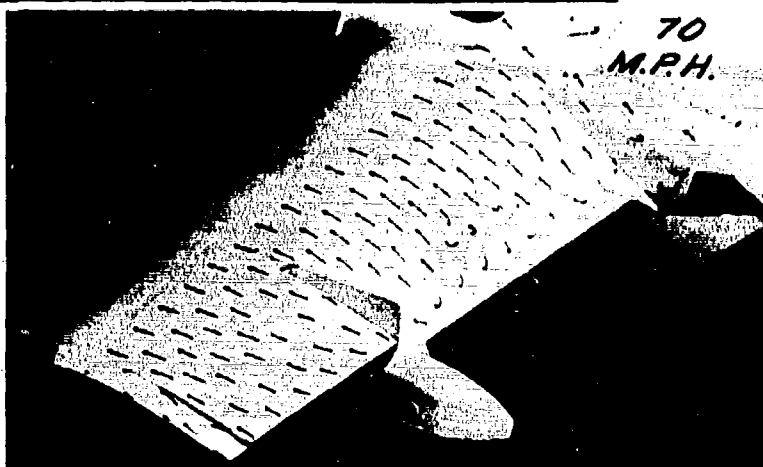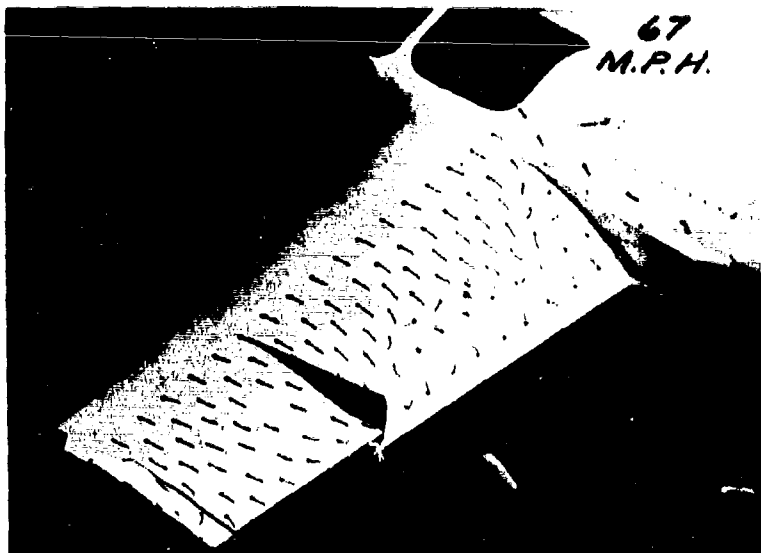
Figure 34.   Wing Tuft Pictures, 20-Degree Camber.
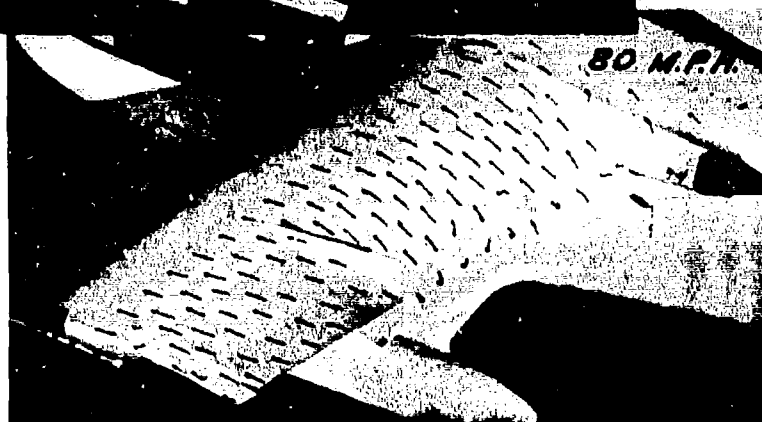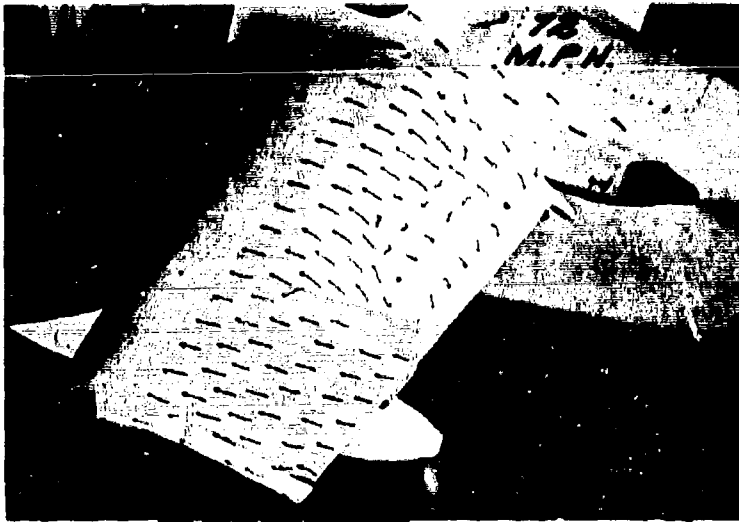
Figure 35.   Wing Tuft Pictures, 30-Degree Camber.
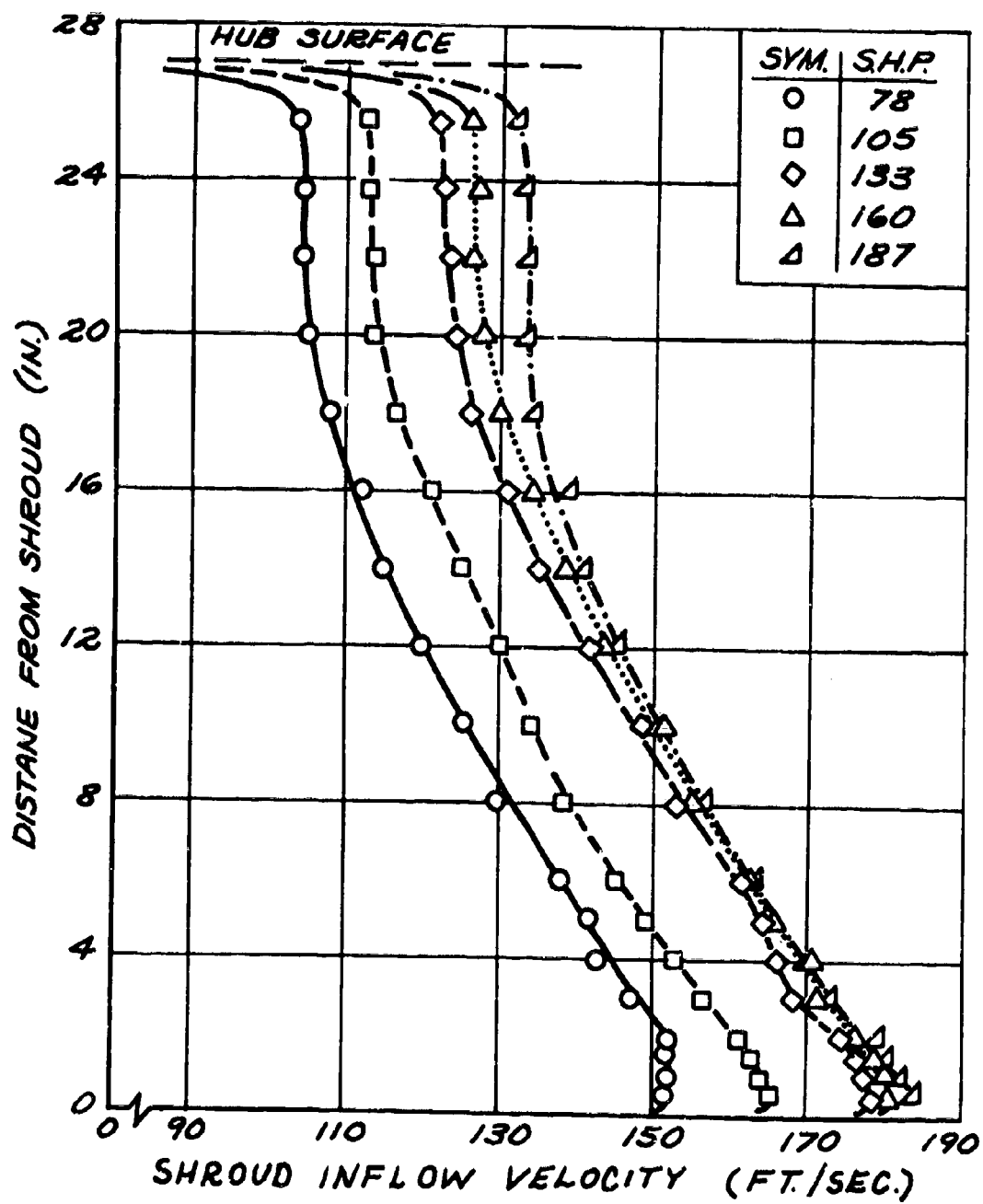
Figure 36. Shroud Inflow Measurements for the Static Condition.
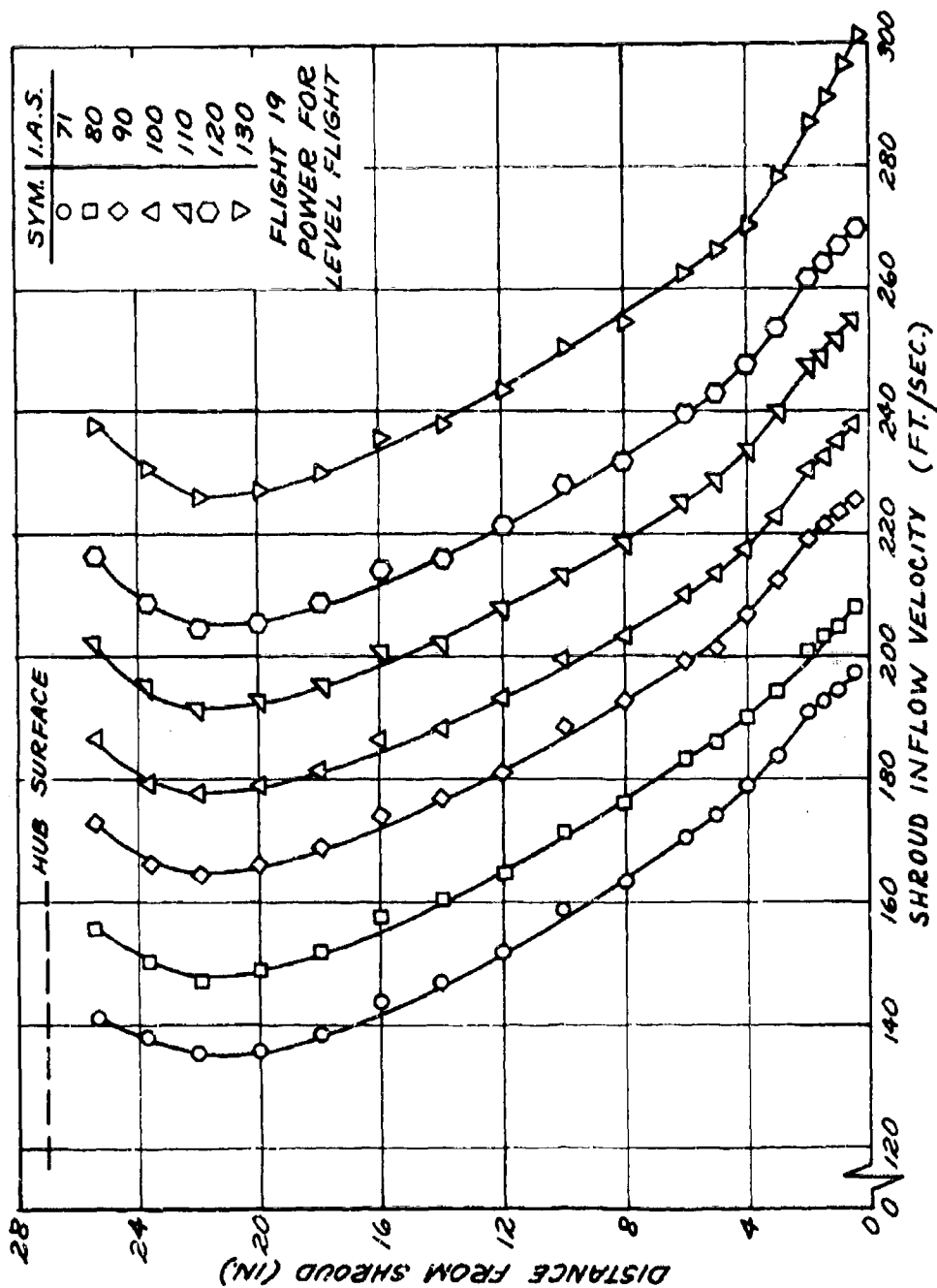
Figure 37. Level Flight Shroud Inflow Measurements.

79
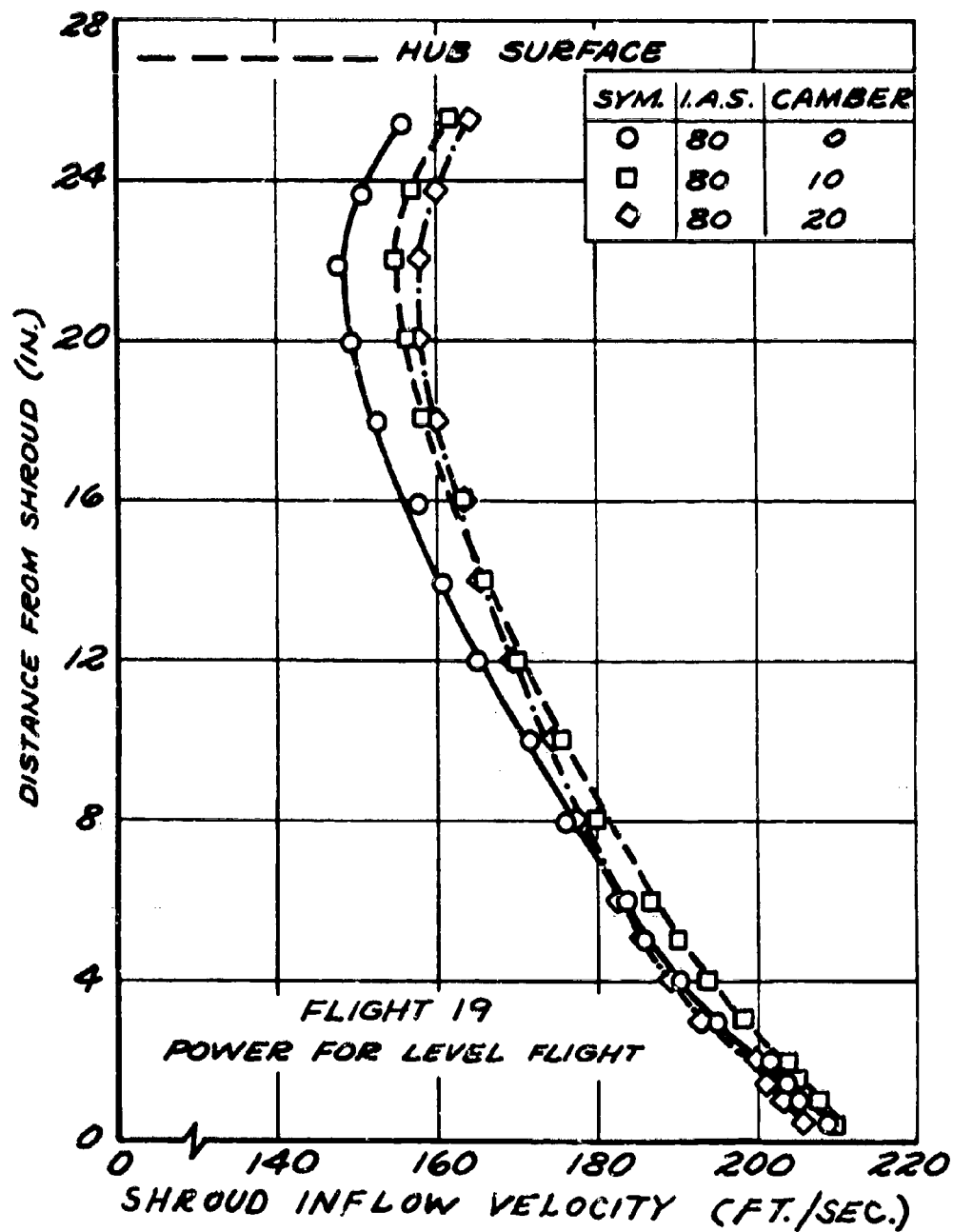
Figure 38. Variation in Shroud Inflow Velocity
Due to Changing Wing Camber.
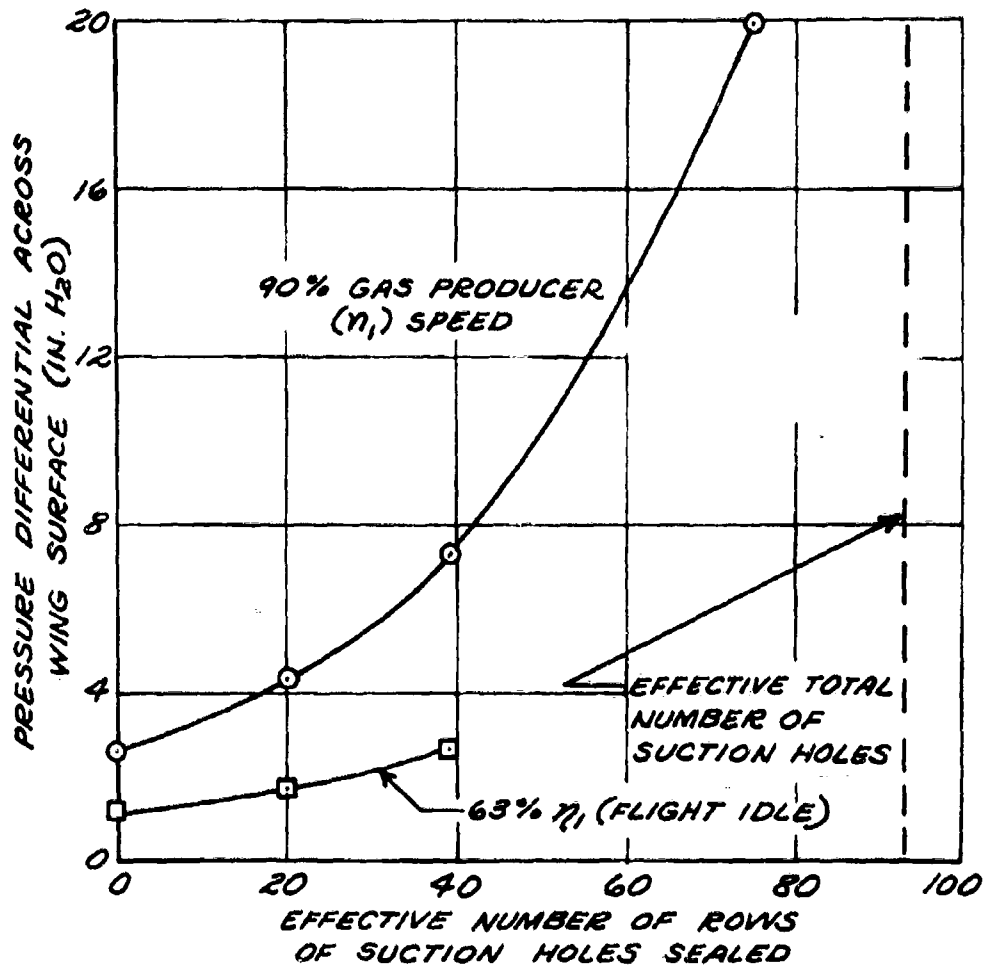
Figure 39. Variation of Pressure Differential Across the Skin as a Function of the Number of Suction Holes Sealed.
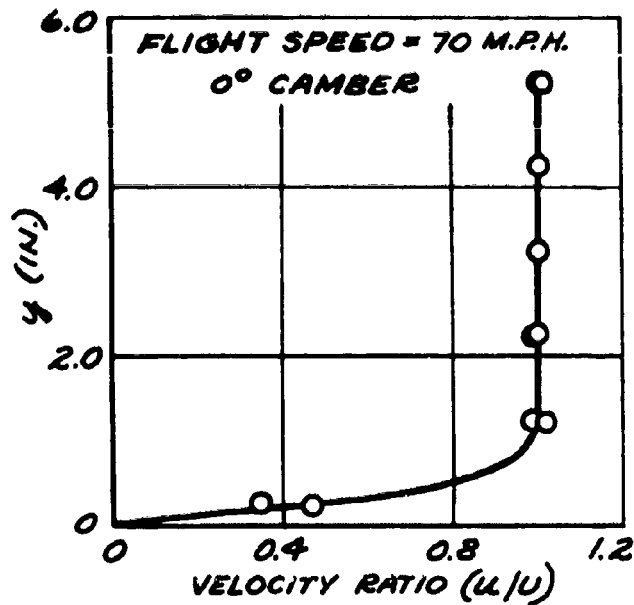
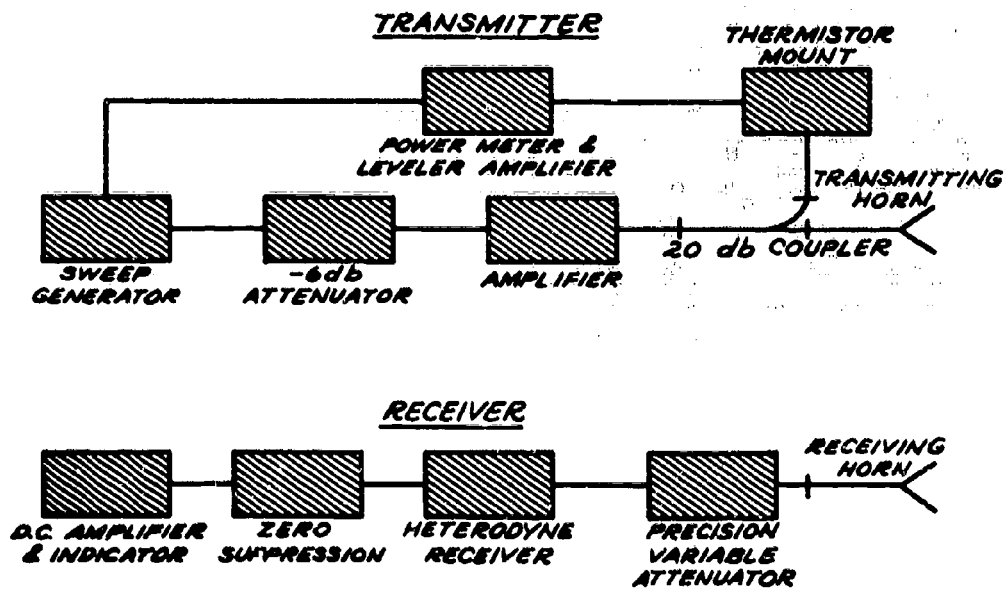Figure 40. Boundary Layer Measurements on Top of Fuselage, $\alpha = 22^\circ$.

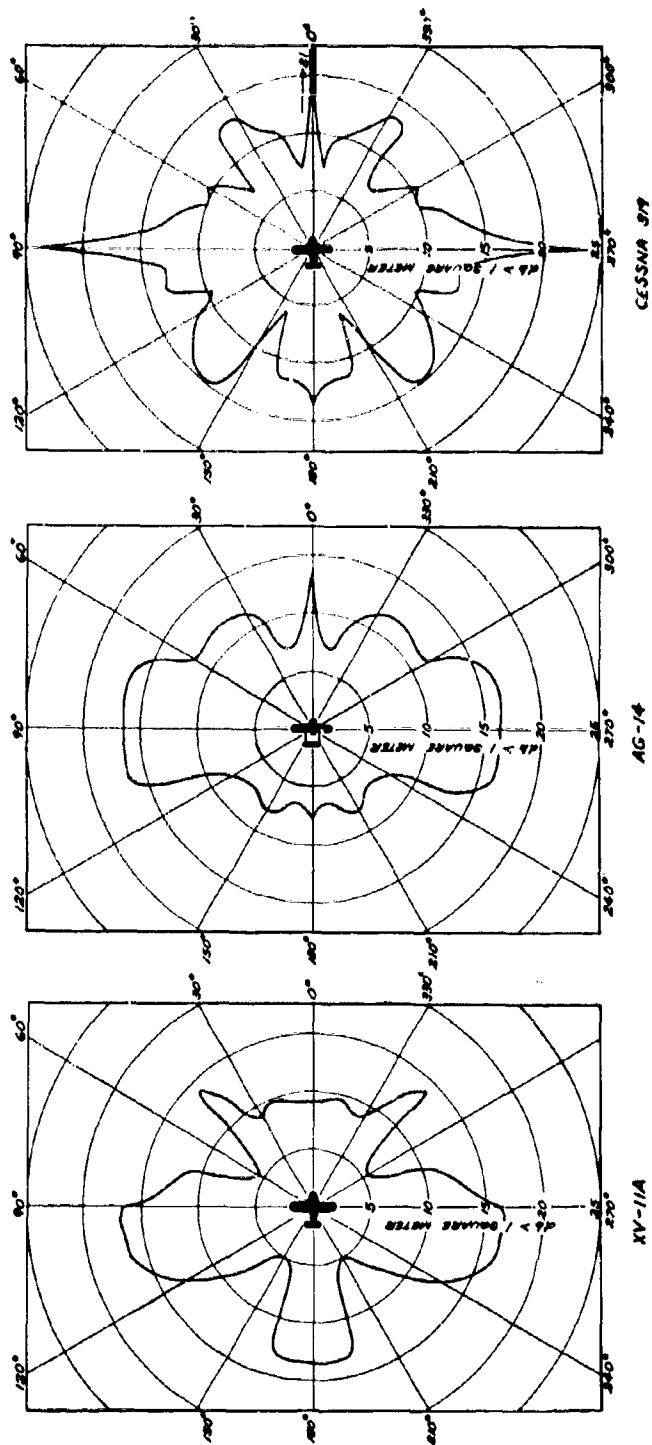Figure 41. Block Diagram of Equipment Used in Radar Reflectivity Tests.

Figure 42. Radar Cross Sections of the XV-11A, the AG-14, and the Cessna 319.
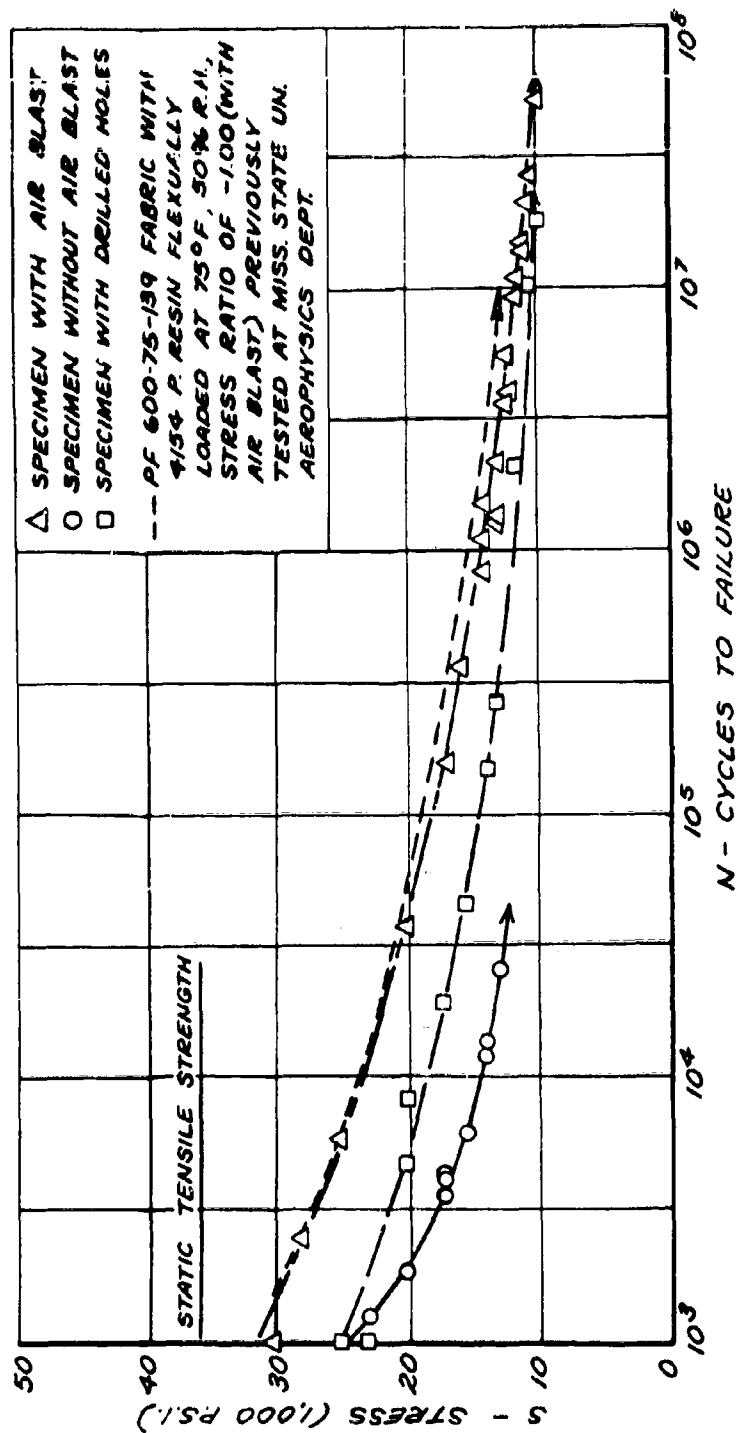
Figure 43. Fatigue Results of Fiber Glass Coupons.

CROSS SECTION

1.25"

0.26"
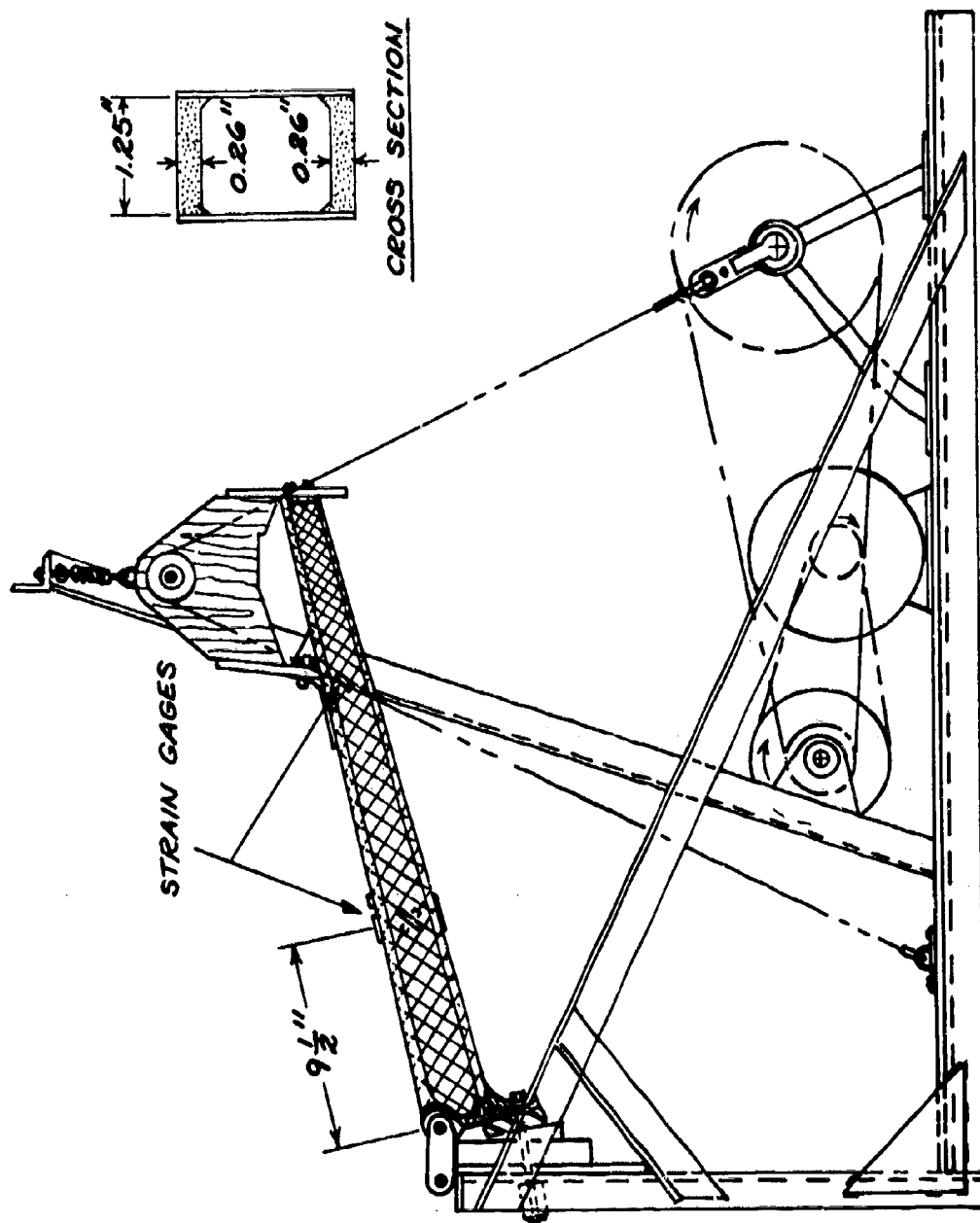
0.86"

STRAIN GAGES

9½"

Figure 44. Sketch of the Landing Gear Strut Fatigue Testing Machine.
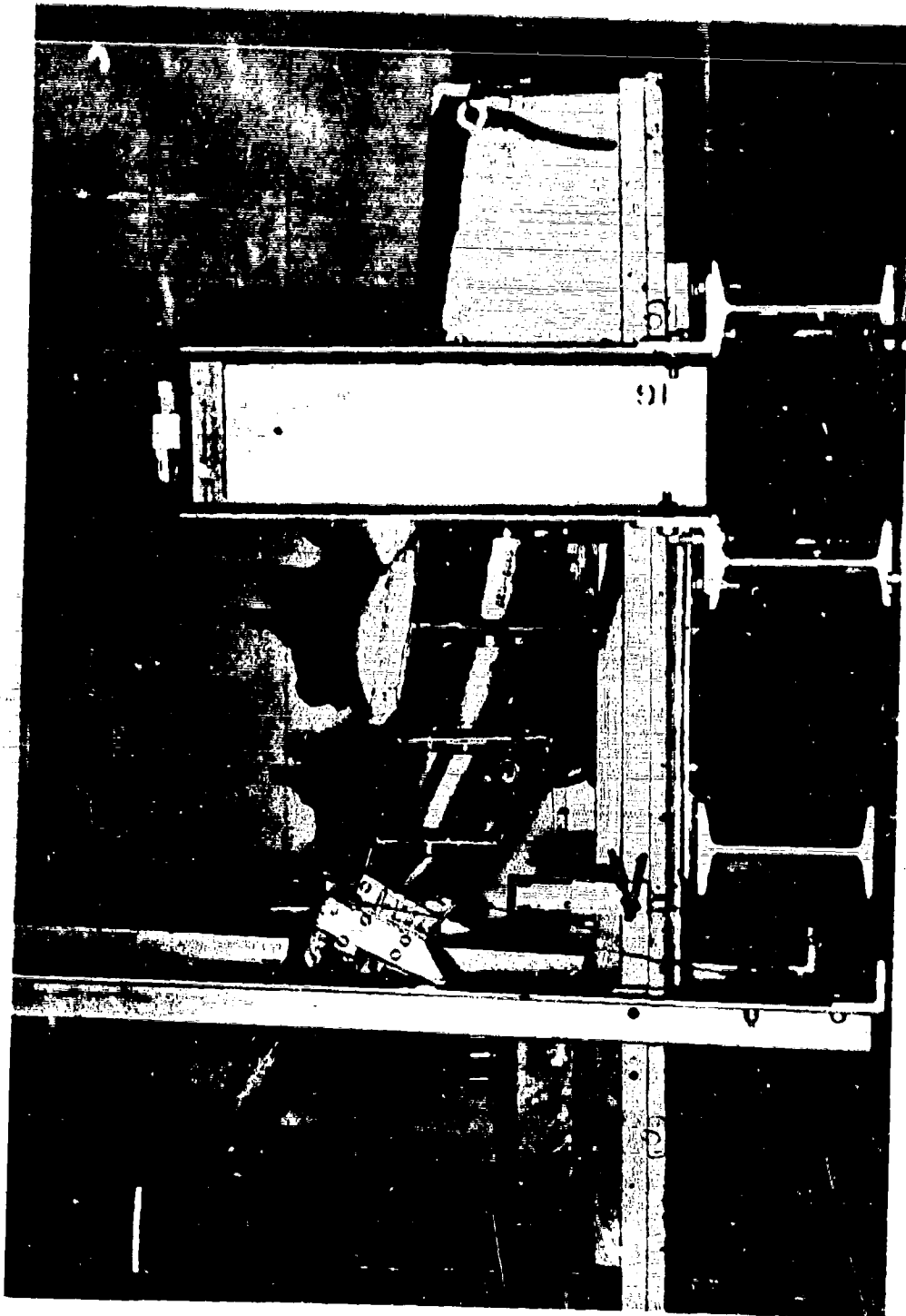
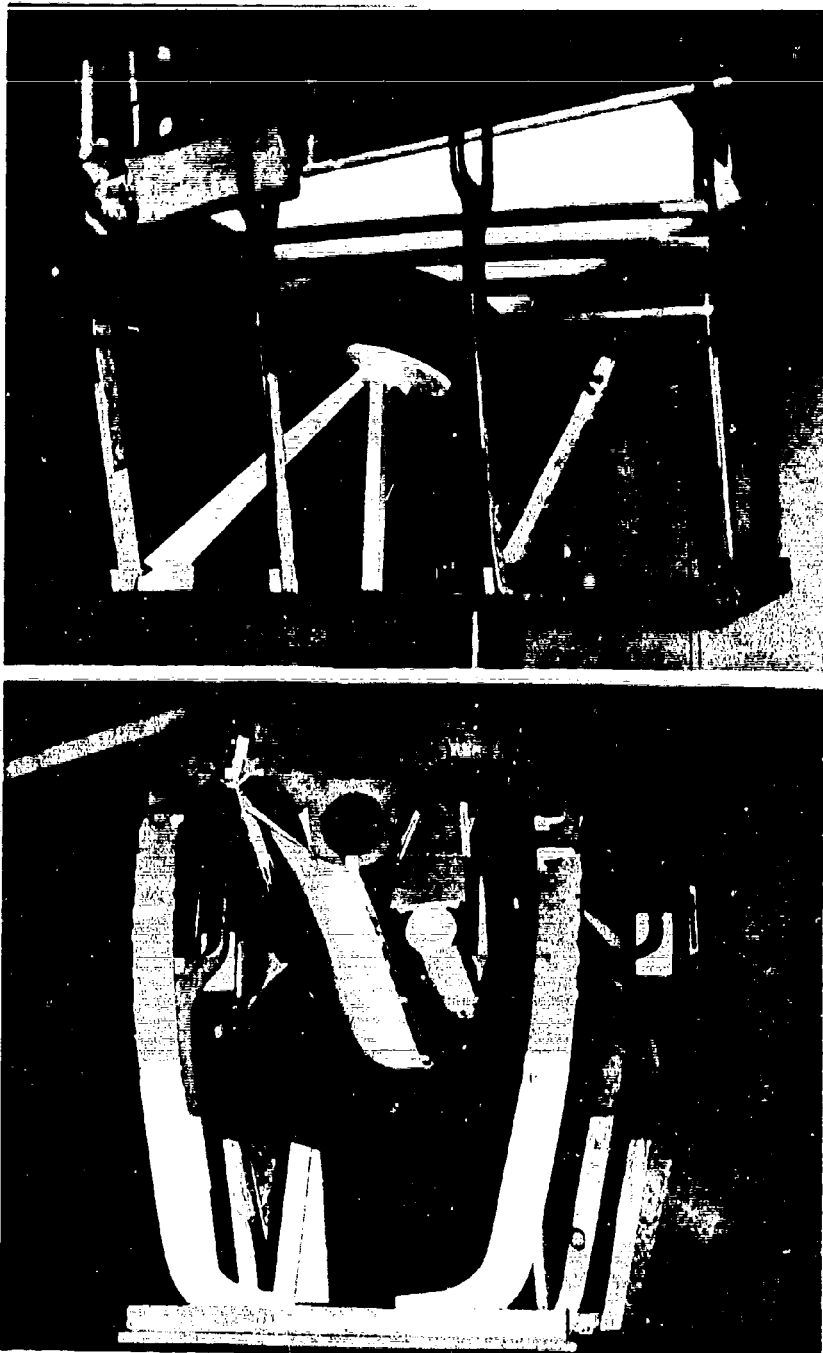Figure 45. Fatigue Test of Variable Camber Wing Section.

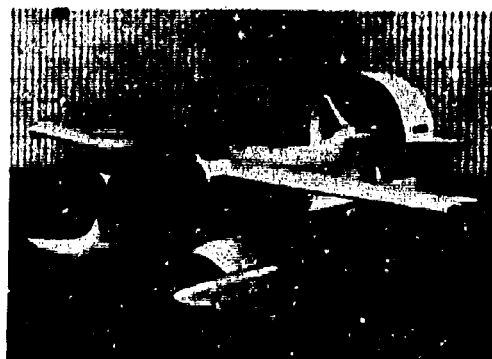Figure 46.   Mock-Up of Retractable Undercarriage in XV-11A Fuselage Mock-Up.

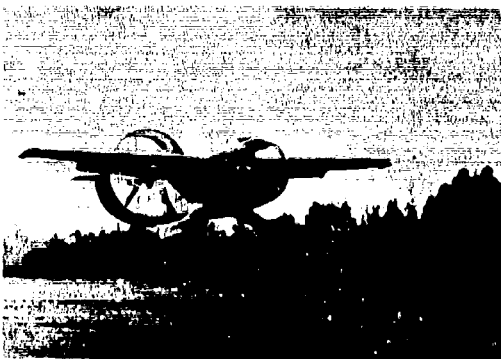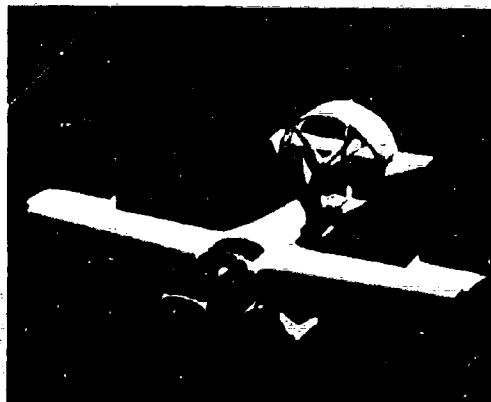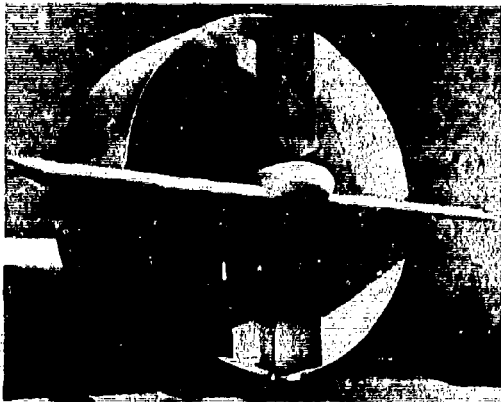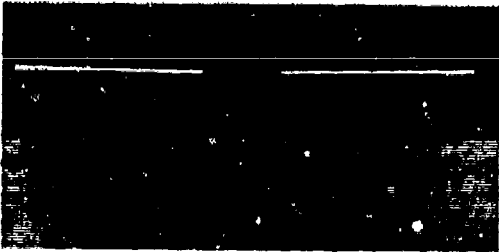Figure 47. Three-View Drawing of XV-11A.

Figure 48.   Various Views of the XV-11A.

REFERENCES

1. Cornish, J. J., III, A Comparison of the Power Requirements of
   Distributed Suction and Jet Blowing to Increase Lift,
   Aerophysics Department, Mississippi State University, State
   College, Mississippi, May 1959.

2. Roberts, S. C., Smith, M. R., and Clark, D. G., Flight Test Eval-
   uation of a Distributed Suction High-Lift Boundary Layer Control
   System on a Modified L-19 Liaison Aircraft, Research Report
   No. 66, Aerophysics Department, Mississippi State University,
   State College, Mississippi, and USAAVLABS Technical Report 66-
   36, United States Army Aviation Materiel Laboratories, Fort
   Eustis, Virginia, June 1966.

3. Roberts, S. C., An Investigation of the Shrouded Propeller Propul-
   sive System in the Marvelette Aircraft, Research Report No. 48,
   Aerophysics Department, Mississippi State University, State
   College, Mississippi, and USAAVLABS Technical Report 64-41,
   United States Army Aviation Materiel Laboratories, Fort Eustis,
   Virginia, August 1964.

4. Gracey, W., The Experimental Determination of the Moments of Inertia
   of Airplanes by a Simplified Compound-Pendulum Method, NACA
   TN No. 1629, Langley Memorial Aeronautical Laboratory, Langley,
   Virginia, 1948.

5. Malvestato, F. S., Jr., and Gale, L. J., Formulas for Additional
   Mass Corrections to the Moments of Inertia of Airplanes, NACA
   TN No. 1187, Langley Memorial Aeronautical Laboratory, Langley,
   Virginia, 1947.

6. Barber, M. R., Jones, C. K., Sisk, T. R., and Haise, F. W., An
   Evaluation of the Handling Qualities of Seven General-Aviation
   Aircraft, NASA TN D-3726, Flight Research Center, Edwards,
   California, November 1966.

7. Bandari, D. R., Fatigue Tests of Glass-Fabric Base Laminates Sub-
   jected to Flexural Loading, Aerophysics Department, Mississippi
   State University, State College, Mississippi, August 1965.

8. Boller, K. H., Resume of Fatigue Characteristics of Reinforced
   Plastic Laminates Subjected to Axial Loading, T.R. No. ASD-TDR-
   63-768, AFCS, Wright-Patterson Air Force Base, Dayton, Ohio,
   1963.

9. Nordby, G. M., The Effect of Resin Content and Voids on the Strength
   of Fiberglass-Reinforced Plastics for Airframe Use, USAAVLABS
   Technical Report 65-66, United States Army Aviation Materiel
   Laboratories, Fort Eustis, Virginia, November 1965.

10. Hoehne, V. D., _A Method of Design of Shrouded Propellers_, Engineering Report No. 213-8, University of Wichita, Wichita, Kansas, October 1959.

11. Kuchmann, D., and Weber, J., _Aerodynamics of Propulsion_, McGraw-Hill Book Company, New York, 1953.

12. Lippisch, A. M., _Some Basic Deviations About the Action of a Ducted Propeller_, Collins Aero-Research Laboratory, 1956.

13. Theodorsen, T., _Ducted Propeller Aerodynamics_, Republic Aviation Corporation, New York, 1960.

14. Cornish, J. J., III, "Some Aerodynamic and Operational Problems of STOL Aircraft With Boundary Layer Control", _Journal of Aircraft_, March 1965.

15. Raspet, A., Cornish, J. J., III, and Bryant, G. D., _Delay of the Stall by Suction Through Distributed Perforations_, IAS Preprint 56-587, January 1958.

16. Clark, D. G., _Flight Development of a High-Lift Research Aircraft Using Distributed Suction_, Presented at AGARD Flight Mechanics Panel, Paris, 1965.

DOCUMENT CONTROL DATA - R&D

(Security classification of title, body of abstract and indexing annotation must be entered when the overall report is classified)

1. ORIGINATING ACTIVITY (Corporate author)	2a. REPORT SECURITY CLASSIFICATION
Mississippi State University Aerophysics Department State College, Mississippi 39762	Unclassified
	2b. GROUP

3. REPORT TITLE

XV-11A Description and Preliminary Flight Test

4. DESCRIPTIVE NOTES (Type of report and inclusive dates)

5. AUTHOR(S) (Last name, first name, initial)

Roberts, Sean C., Stewart, Aberdeen W., Boaz, Virgil L., Bryant, Glenn D., Mertaugh, Lawrence J., Jr., Wells, William G., Gaddis, Edwin M.

6. REPORT DATE	7a. TOTAL NO. OF PAGES	7b. NO. OF REFS
May 1967	103	16

8a. CONTRACT OR GRANT NO.	9a. ORIGINATOR'S REPORT NUMBER(S)
DA 44-177-AMC-266(T)	USAAVLABS Technical Report 67-21
b. PROJECT NO. TASK 1F125901A14203	
c.	9b. OTHER REPORT NO(S) (Any other numbers that may be assigned this report)
d.	Aerophysics Research Report No. 75

10. AVAILABILITY/LIMITATION NOTICES

Distribution of this document is unlimited.

11. SUPPLEMENTARY NOTES	12. SPONSORING MILITARY ACTIVITY
	U. S. Army Aviation Materiel Laboratories Fort Eustis, Virginia 23604

13. ABSTRACT

The XV-11A is a polyester reinforced fiber glass STOL aircraft designed and assembled by the Aerophysics Department of Mississippi State University. This four-place aircraft, powered by a 250-horsepower T-63 turbine engine, was designed to achieve high-lift coefficients by means of a variable camber wing with distributed suction boundary layer control. A shrouded propeller was used for thrust augmentation at low forward velocities, and beta control on the propeller was successfully used as a drag increment for glide path control.

To date, the XV-11A aircraft has flown 49 flights with a total flight time of 35 hours. The majority of the flight time was involved in aerodynamic research of the shrouded propeller, the distributed suction boundary layer control system and in an evaluation of the general handling characteristics of the aircraft. A minimum of performance data was collected since the primary objective was aerodynamic research. The fiber glass material has demonstrated the excellent possibilities of this type of construction when complex, aerodynamically smooth curvatures are desired.

DD FORM 1473 (1 JAN 64)

14. KEY WORDS	LINK A		LINK B		LINK C	
	ROLE	WT	ROLE	WT	ROLE	WT
STOL						
Fiber Glass Construction						
Shrouded Propeller						
Boundary Layer Control						
Variable Camber						

INSTRUCTIONS

1. ORIGINATING ACTIVITY: Enter the name and address of the contractor, subcontractor, grantee, Department of Defense activity or other organization (corporate author) issuing the report.

2a. REPORT SECURITY CLASSIFICATION: Enter the overall security classification of the report. Indicate whether "Restricted Data" is included. Marking is to be in accordance with appropriate security regulations.

2b. GROUP: Automatic downgrading is specified in DoD Directive 5200.10 and Armed Forces Industrial Manual. Enter the group number. Also, when applicable, show that optional markings have been used for Group 3 and Group 4 as authorized.

3. REPORT TITLE: Enter the complete report title in all capital letters. Titles in all cases should be unclassified. If a meaningful title cannot be selected without classification, show title classification in all capitals in parenthesis immediately following the title.

4. DESCRIPTIVE NOTES: If appropriate, enter the type of report, e.g., interim, progress, summary, annual, or final. Give the inclusive dates when a specific reporting period is covered.

5. AUTHOR(S): Enter the name(s) of author(s) as shown on or in the report. Enter last name, first name, middle initial. If military, show rank and branch of service. The name of the principal author is an absolute minimum requirement.

6. REPORT DATE: Enter the date of the report as day, month, year; or month, year. If more than one date appears on the report, use date of publication.

7a. TOTAL NUMBER OF PAGES: The total page count should follow normal pagination procedures, i.e., enter the number of pages containing information.

7b. NUMBER OF REFERENCES: Enter the total number of references cited in the report.

8a. CONTRACT OR GRANT NUMBER: If appropriate, enter the applicable number of the contract or grant under which the report was written.

8b, 8c, & 8d. PROJECT NUMBER: Enter the appropriate military department identification, such as project number, subproject number, system numbers, task number, etc.

9a. ORIGINATOR'S REPORT NUMBER(S): Enter the official report number by which the document will be identified and controlled by the originating activity. This number must be unique to this report.

9b. OTHER REPORT NUMBER(S): If the report has been assigned any other report numbers (either by the originator or by the sponsor), also enter this number(s).

10. AVAILABILITY/LIMITATION NOTICES: Enter any limitations on further dissemination of the report, other than those imposed by security classification, using standard statements such as:

(1) "Qualified requesters may obtain copies of this report from DDC."

(2) "Foreign announcement and dissemination of this report by DDC is not authorized."

(3) "U. S. Government agencies may obtain copies of this report directly from DDC. Other qualified DDC users shall request through
_____."

(4) "U. S. military agencies may obtain copies of this report directly from DDC. Other qualified users shall request through
_____."

(5) "All distribution of this report is controlled. Qualified DDC users shall request through
_____."

If the report has been furnished to the Office of Technical Services, Department of Commerce, for sale to the public, indicate this fact and enter the price, if known.

11. SUPPLEMENTARY NOTES: Use for additional explanatory notes.

12. SPONSORING MILITARY ACTIVITY: Enter the name of the departmental project office or laboratory sponsoring (paying for) the research and development. Include address.

13. ABSTRACT: Enter an abstract giving a brief and factual summary of the document indicative of the report, even though it may also appear elsewhere in the body of the technical report. If additional space is required, a continuation sheet shall be attached.

It is highly desirable that the abstract of classified reports be unclassified. Each paragraph of the abstract shall end with an indication of the military security classification of the information in the paragraph, represented as (TS), (S), (C), or (U).

There is no limitation on the length of the abstract. However, the suggested length is from 150 to 225 words.

14. KEY WORDS: Key words are technically meaningful terms or short phrases that characterize a report and may be used as index entries for cataloging the report. Key words must be selected so that no security classification is required. Identifiers, such as equipment model designation, trade name, military project code name, geographic location, may be used as key words but will be followed by an indication of technical context. The assignment of links, rules, and weights is optional.